The relationship between ice sheets and submarine mass movements in the Nordic Seas during the Quaternary

Ed L. Pope[1*], Peter J. Talling[2], Colm Ó Cofaigh[1]

[1]*Department of Geography, Durham University, Science Laboratories, South Road, Durham, DH1 3LE, UK.*

[2]*Departments of Earth Science and Geography, Durham University, Science Laboratories, South Road, Durham, DH1 3LE, UK.*

Abstract

Quaternary evolution of high-latitude margins has, to a large degree been shaped by the advance and retreat of ice sheets. Our understanding of these margins and the role of ice sheets is predominantly derived from the polar North Atlantic during the Late Weichselian. This region has formed the basis for conceptual models of how glaciated margins work and evolve through time with particular focus on trough-mouth fans, submarine landslides and channel systems. Here, by reviewing the current state of knowledge of the margins of the Nordic Seas during the Quaternary we provide a new set of models for different types of glaciated margin and their deposits. This is achieved by tracking the growth and decay of the Greenland, Barents Sea and Scandinavian Ice Sheets over the last 2.58 Ma and how these ice sheets have influenced sedimentation along their margins. The reconstructed histories show 1) the completeness of records along each ice sheet margin is highly variable. 2) Climatic deterioration and the adoption of 100 kyr cyclicity has had progressive impacts on each ice sheet and the resulting sedimentation and evolution of its related margin. These reconstructions and records on other margins worldwide enable us to identify first order controls on sediment delivery at ice sheet scales, propose new conceptual models for trough-mouth fans and glaciated margin development. We are also able to show how the relationship between large submarine landslide occurrence and ice sheet histories changes on different types of margin.

Keywords: Glacial history, glaciated continental margins, Nordic Seas, glacimarine sedimentary processes, trough-mouth fans, submarine landslides; ice sheets; Greenland Ice Sheet; Barents Sea Ice Sheet; Scandinavian Ice Sheet

*Corresponding author: Edward.Pope@durham.ac.uk

1. Introduction

Sediment is transported across our planet most efficiently by ice sheets and submarine mass movements (Boulton, 1978; Hallet et al., 1996; Dowdeswell et al., 2010b; Talling et al., 2014). Rates of erosion by ice sheets and the subsequent transport and deposition of the eroded material in marine settings can be an order of magnitude greater than river catchments with larger areas (Milliman and Meade, 1983; Elverhøi et al., 1998). Once deposited this material is then often reworked by submarine gravity-flow processes. For example large submarine landslides, such as the Storegga Slide that occurred 8.2 ka offshore Norway, can contain several thousand cubic kilometres of predominantly glacigenic sediments (Haflidason et al., 2005). A clear relationship therefore exists between ice sheet processes, submarine mass movements and the sedimentary architecture of glaciated continental margins (Heezen and Ewing, 1952; Kuvaas and Kristoffersen, 1996; Vorren et al., 1998; Ó Cofaigh et al., 2003). Understanding the links between the two phenomena is therefore crucial to reconstructing ice sheet histories from the sedimentary record, and understanding the evolution of glaciated margins.

Delivery of sediment to the marine environment by ice sheets is characterised by the sporadic nature and the exceptional volumes involved. The rate of sediment delivery by ice sheets is a function of the frequency of glaciation and its intensity, internal dynamics and the geology over which the ice is moving, i.e. local lithology and permeability. Over long timescales, the growth and decay of ice sheets is controlled by orbital forcing (Jansen and Sjøholm, 1991; Raymo and Ruddiman, 1992; Thiede et al., 1998; Jansen et al., 2000; Ehlers and Gibbard, 2004). At shorter timescales ice sheets can also be affected by sub-orbital forcing, such as reduced thermohaline circulation (Broecker and Denton, 1990; Bond et al., 1999), or the switch on/off of ice streams draining the ice sheet interior (Bennett, 2003; Catania et al., 2006; Dowdeswell et al., 2006b; Christoffersen et al., 2010). Spatially, ice sheet sedimentation also varies according to the position of fast and slow flowing ice (Ottesen et al., 2005), the drift tracks of icebergs (Mugford and Dowdeswell, 2010), the

location of meltwater discharge from the ice front (Dowdeswell et al., 2015) and the type of substrate. This temporal and spatial variability should be reflected in the sedimentary history of glaciated margins and therefore provide insights for ice sheet reconstructions. However, to assess this, accurate ice sheet and sedimentation histories need to be reconstructed and diagnostic facies need to be identified.

1.1. Why is it important to understand the links between ice sheet and sedimentation histories?

The geological record of high-latitude continental margins contains key information on former ice sheets (Dowdeswell et al., 2016b). Specific landforms and sedimentary sequences have been used to provide information on the extent of palaeo-ice sheets as well as the direction and nature of past ice flow and dynamics (Clark, 1993; Ottesen et al., 2005; Ottesen and Dowdeswell, 2006; Ó Cofaigh et al., 2013a; Jakobsson et al., 2014; Hogan et al., 2016). Multiple sequences of alternating till and pro-/deltaic muds have been used to infer short-term advance and retreat cycles (Funder and Hansen, 1996). Eskers and tunnel valleys have been used as indicators of the geometry of past subglacial hydrological systems (Stewart et al., 2013; Greenwood et al., 2016). Trough-mouth fans, covering areas of $10^3 – 10^5$ km^2 with volumes of $10^4 – 10^5$ km^3, are thought to be indicative of the delivery of large volumes of sediment by fast-flowing ice streams present at the shelf edge (Dowdeswell et al., 1997; Vorren and Laberg, 1997; Canals et al., 2003; Ó Cofaigh et al., 2003; Sejrup et al., 2005). These landform interpretations can subsequently by used to constrain/validate ice sheet models, which in turn can be used to model possible future ice sheet changes (Kleman et al., 1997; Greenwood and Clark, 2009).

From an applied perspective, understanding the history of ice sheets and sedimentation along a glaciated margin is important for assessing marine resource potential. Changes in geostatic loading associated with ice sheet growth and decay can lead to the displacement of water or hydrocarbons from low-permeability beds into horizons with superior reservoir properties (Trofimuk et al., 1977;

Kjemperud and Fjeldskaar, 1992; Doré and Jensen, 1996). Alternatively ice sheet induced fluid displacement can result in partial failure of oil and gas reservoirs or the displacement of these hydrocarbons into sediments marginal to the ice sheet (Tasianas et al., 2016; Zieba and Grøver, 2016). Exhumation of sediments can also adversely impact resource potential as the probability of trapping or sealing hydrocarbons is generally reduced (Doré et al., 2002; Fjeldskaar and Amantov, 2017). Upward migration, particularly of free gas, also represents a hazard to resource extraction in terms of drilling and can act as a potential trigger for submarine landslides (Maslin et al., 1998; Pickrill et al., 2001; Chand et al., 2012; Vadakkepuliyambatta et al., 2013).

1.1.1. Ice sheets, climate and sedimentation histories

Interpretations of landforms and sedimentary sequences are based on a combination of observations from contemporary glacial environments and interpretations of the environmental conditions that existed under full-glacial conditions. At the most fundamental level these interpretations reflect our understanding of the relationship between glacier dynamics and climate (Hallam, 1989). To first order, glacial sediment delivery and thus landform genesis is often linked to temperature. It is hypothesised that colder climates result in lower basal temperatures in glaciers and ice sheets (Cuffey and Paterson, 2010). These temperatures reduce meltwater production which in turn impacts upon glacial sliding, erosion and therefore sediment transfer (Herman et al., 2011; Egholm et al., 2012; Koppes et al., 2015). At a process scale, processes dominating glacier-influenced delivery of sediment to marine environments are also linked to temperature. Modern/Quaternary interglacial glacial delivery of sediment to marine environments is conceptualised as a continuum between meltwater-dominated (e.g. Southern Alaska) to iceberg-dominated (e.g. West/East Antarctica) environments (Fig. 1a; Dowdeswell et al., 1998). Under full-glacial conditions, the position of each system and thus the dominance of a given mechanism for sediment delivery, shifts its position on the continuum (Fig. 1b; Dowdeswell et al., 2016b).

105 The evolution and history of sedimentation on continental margins should not, however, be
106 conceptualised simply as glacial vs. interglacial conditions. The length and severity of glacial periods
107 has varied throughout the Quaternary (Thiede et al., 1989; Raymo and Nisancioglu, 2003; Ehlers and
108 Gibbard, 2004). At the simplest level, glacial periods can be divided into those which occurred when
109 climate was dominated by 41 kyr cyclicity and those that occurred under 100 kyr cyclicity (Raymo
110 and Nisancioglu, 2003; Tziperman and Gildor, 2003). In terms of erosion and sediment delivery to
111 the continental margin, it has been proposed that the adoption of the 100 kyr climate cycle led to an
112 intensification of glacial erosion and sediment transport (Faleide et al., 2002; Gulick et al., 2015).
113 However, this assertion, linked to the severity and intensity of the 100 kyr cycles is at odds with the
114 understanding of temperature/climate controlling the rate of glacier driven sedimentation. Long-
115 term marine sedimentary records provide one of the few means through which these relationships
116 can be tested over multiple glacial cycles and thus allow us to reconstruct ice sheets and ice sheet
117 processes and their response to variable climatic forcing.

118

119 **1.1.2. Geohazard assessment**

120 Understanding the links between ice sheets and sedimentary processes on continental margins is
121 also critical for hazard assessment. Since the 1929 Grand Banks submarine landslide, increasing
122 numbers of slide scars and deposits have been mapped on previously glaciated margins (Heezen and
123 Ewing, 1952; Bugge, 1983; 1987; Piper and Aksu, 1987; Dowdeswell et al., 1996; Vorren et al., 1998;
124 Hogan et al., 2013). Considered to be one of the main morphological features of glaciated margins,
125 these events have the potential to generate damaging tsunami and damage local subsea
126 infrastructure (Heezen and Ewing, 1952; Bondevik et al., 1997; 2003; Grauert et al., 2001; Pope et
127 al., 2017a). The Storegga Slide is known to have generated a tsunami with wave run-up heights >20
128 m (Bondevik et al., 2003) while the Grand Banks Slide caused 23 telegraph cable breaks (Piper et al.,
129 1999). The locations of the slides, specifically their often close association with trough-mouth fans,

has led to the hypothesis that rapid rates of ice sheet driven sedimentation is a critical factor in the triggering of these slides (Bryn et al., 2003; 2005; Haflidason et al., 2004; Owen et al., 2007). Understanding the timing and emplacement mechanisms of these slides over multiple glacial cycles relative to changing ice sheet dynamics is therefore crucial to quantifying the potential risk associated with these hazards.

1.2. Previous models linking ice sheet with sedimentation processes and continental margin morphology

Conceived in the mid-1990s, an original model (Fig. 2; Dowdeswell et al., 1996) for large-scale sedimentation on glaciated margins was based on a combination of GLORIA imagery, seismic data and models of former ice sheet behaviour. This model linked the sedimentary architecture seen on the margins of the Nordic Seas (i.e. submarine channels, glacigenic debris-flows, etc.) to the extent/velocity of ice delivering sediment to the shelf break (Dowdeswell et al., 1996; Dowdeswell and Siegert, 1999). Low velocity ice associated with low sediment delivery or ice terminating inshore of the shelf edge was hypothesised to be associated with submarine channel systems. Fast flowing ice streams delivering large amounts of sediment were associated with glacigenic debris-flows, submarine landslides and the build-up of trough-mouth fans (Dowdeswell et al., 1996).

With the available data this model effectively identified where specific sedimentary features and processes were likely to occur and how they related to palaeo-ice sheets. However, since the inception of this model a number of key advances have been made. First, studies have been able to identify how sedimentation has changed over time on specific sections of a margin (e.g. Solheim et al., 1998; Nygård et al., 2005). This implies that a static model of ice sheet driven sedimentary processes is perhaps not appropriate. Second, there has been growing recognition of the importance of specific processes, such as meltwater delivery of sediment, on glaciated margins (Lekens et al., 2005; Lucchi et al., 2013). These processes therefore may have to be incorporated within a model of glacial margin sedimentation. Third, our understanding of other glaciated margins around the world

has improved (Escutia et al., 2000; Ó Cofaigh et al., 2008; 2013; Montelli et al., 2017b). This enables us to analyse whether models of glaciated margins based on observations around the Nordic Seas are applicable to other margins. For these reasons, it is timely to re-evaluate our current models of glaciated margin sedimentation and evolution.

1.3. Why focus on the Nordic Sea?

This study of ice sheet and submarine mass movement histories is focussed initially on their relationship in the Nordic Seas (Fig. 3). We chose to focus on this region for a number of reasons. First, the Nordic Seas and their surrounding margins have been subject to multiple glaciations during the Quaternary. During the Quaternary four major ice sheets, the Greenland, Barents Sea, Scandinavian and the British-Irish ice sheets have grown and decayed on the continents surrounding the Nordic Seas (Ehlers and Gibbard, 2004; Hibbert et al., 2010; Funder et al., 2011; Patton et al., 2015). Each of these ice sheets has different climatic, topographic and geological settings which can affect the processes of ice movement, advance and retreat, and the delivery of sediment (Patton et al., 2016). These contrasts allow us to assess how variable histories of sedimentation are across and between glaciated margins through different glacial cycles.

Second, the Nordic Seas and their surrounding land masses are one of the best studied glaciated margins. The economic resources found here, combined with multiple long-running scientific consortia projects (e.g. PONAM and QUEEN) have resulted in regional scale mapping of the surface and sub-surface of the continental shelf and slope (Faleide et al., 1996; Solheim et al., 1998; Svendsen et al., 2004a). Combined with sedimentological studies, this has resulted in one of the most complete records of ice sheet change and the associated history of sedimentation during the Quaternary (Mangerud et al., 1998; Eidvin et al., 2000; Jansen et al., 2000; Svendsen et al., 2004a; and references therein). It is therefore appropriate that any attempt to understand the evolution of glaciated margins should include a detailed study of the margins of the Nordic Seas. The

transferability of models based on the Nordic Sea margins to other glaciated margins can subsequently be assessed.

1.4. Aims

The purpose of this study is to draw together various records from around the Nordic Seas to achieve the following aims.

1) We aim to reconstruct the growth and decay histories of the Greenland, Barents Sea and Scandinavian ice sheets on the margins of the Nordic Seas and outline the history of sedimentation associated with these ice sheets.

2) We compare sedimentary records on different glaciated margins to those from the Nordic Seas in order to understand the appropriateness of models derived from the Nordic Seas for understanding other glaciated margins.

3) From these records, we derive a set of general models for ice sheet driven sedimentary processes and landform formation on the continental shelf and slope. These general models for different types of system provide a basis for understanding the evolution of glaciated margins.

4) By compiling records of large submarine landslides on glaciated margins, we aim to provide explanations for their spatial distribution and provide conceptual models for understanding their preconditioning and triggering mechanisms.

2. Ice sheet and submarine mass movement histories

The following section will first outline the Late Pliocene history for the Greenland Ice Sheet, Barents Sea Ice Sheet and Scandinavian Ice Sheet. It will then analyse the evolution of each ice sheet during the Quaternary and the associated sedimentation record. First, we focus on the Greenland Ice Sheet; second, the Barents Sea Ice Sheet and last the Scandinavian Ice Sheet.

2.1. Ice sheet histories in the Late Pliocene

The Pliocene spans the period from 5.333 – 2.588 Ma. This period was characterised by significant cooling of high latitude regions (Fronval and Jansen, 1996; Kleiven et al., 2002). The climatic deterioration that occurred during this period led to the expansion of ice sheets around the Nordic Seas (Solheim et al., 1998; Forsberg et al., 1999) and the adoption of orbitally-forced climatic cyclicity (Kleiven et al., 2002). The progression of ice sheet development can be seen in the Ice-Rafted Debris (IRD) histories of ODP sites from around the Nordic Seas (Fig. 3).

Sedimentary records show that the Greenland Ice Sheet was the earliest to expand and was the most expansive ice sheet in the region during this period. The earliest and largest IRD peaks (before 3 Ma) are recorded at ODP Sites 987 and 907. Located on the Scoresby Sund Trough-Mouth Fan and on the Iceland Plateau (Fig. 4), the IRD records from these cores and the lack of comparable records from sites elsewhere around the Nordic Seas suggest that the Greenland Ice Sheet was producing the largest volumes of IRD during this period (Jansen et al., 1988; 2000; Channell et al., 1999).

With the exception of an ice advance ~2.7 Ma (Böse et al., 2012), there is little evidence of ice sheet activity on the Northern European Margin during the Pliocene comparable to the expansion proposed for the Greenland Ice Sheet (Stoker et al., 1994; Böse et al., 2012; Thierens et al., 2012). IRD records on the Yermak Plateau (Sites 910 and 911; Fig. 3) indicate glacial ice growth on the northern, sub-aerially exposed Barents Sea between 3.5 and 2.6 Ma (Rasmussen and Fjeldskaar, 1996; Butt et al., 2002). However, IRD records from the Fram Strait indicate that this growth was fairly limited (Knies et al., 2009). Further south, along the Norwegian continental margin, ODP Sites (644 and 642) on the Vøring Plateau indicate growth of Scandinavian glaciers at this time (Spiegler and Jansen, 1989; Jansen and Sjøholm, 1991). However, the IRD flux is two to three orders of magnitude smaller than Quaternary IRD fluxes indicating far less extensive glaciations before 2.58 Ma (Jansen and Sjøholm, 1991).

2.1.1. Sedimentary records of ice sheet and submarine mass movement histories: Late Pliocene

The impact of ice sheets on the continental shelves of the Nordic Seas varies according to local ice sheet history. The continental shelf of Greenland underwent significant changes during the Late Pliocene. Evidence for repeated glaciation of the shelf comes primarily from IRD records around Greenland (Larsen, 1990; Jansen and Sjøholm, 1991; Larsen et al., 1994). However, this period is also marked by an erosional unconformity across the East Greenland continental shelf, thought to represent a glacial erosion surface and marking the most pronounced depositional change within the geological record of this region (Vanneste et al., 1995; Fig. 5). Correlation of seismic and core records from the Scoresby Sund Trough-Mouth Fan also indicate the presence of glacigenic debris-flow deposits from this period (Larsen, 1990; Vanneste et al., 1995; Solheim et al., 1998; Butt et al., 2001a). The presence of debris-flow deposits is inferred to be indicative of fast flowing ice reaching the shelf edge and depositing large volumes of sediment. The increased delivery of sediment to the fan during the Late Pliocene is hypothesised to mark the start of the main construction phase of the fan in conjunction with widespread progradation of the continental shelf (Larsen, 1990; Jansen and Raymo, 1996; Solheim et al., 1998).

With the exception of a correlatable regional till layer produced by ice sheet advance at ~2.7 Ma, there is no evidence identified as yet of significant Late Pliocene ice sheet influence on the sedimentary evolution of the Scandinavian or Svalbard/Barents Sea continental margins (Sejrup et al., 1996, 2005; Jansen et al., 2000; Lee et al., 2012). There is also no evidence of any link between ice sheet activity and submarine mass movement occurrence at this time.

3. Greenland Ice Sheet

The following section focuses on the evolution of the Greenland Ice Sheet. Specifically it will focus on the sectors of the ice sheet that border the Nordic Seas.

3.1. 2.58 – 1.3 Ma

The Greenland Ice Sheet was the largest ice sheet around the Nordic Seas and advanced the furthest onto the shelf during the Early Quaternary. This is suggested by both IRD records close to the Greenland continental shelf and records further out into the Nordic Seas (Thiede et al., 1998; Jansen et al., 2000; Helmke et al., 2003b) as well as erosional unconformities on the continental shelf (Fig. 4). These records show the 41 kyr periodicity of Greenland Ice Sheet expansion and contraction and a dominant contribution of IRD into the Nordic Seas compared to other surrounding ice masses (Jansen and Sjøholm, 1991; Jansen et al., 2000; Helmke et al., 2003b).

IRD records imply the two largest advances occurred at the start of the Early Quaternary from 2.5 – 2.4 Ma and ~2.1 Ma. Subsequent IRD peaks are smaller, suggesting later advances were not as spatially or temporally as extensive or did not produce similar numbers of icebergs (Jansen and Sjøholm, 1991). It appears that the ice sheet did not undergo widespread collapses that characterised the Laurentide and northern European ice sheets in the Late Quaternary (see Fig. 6 for possible margin extent). This is inferred from the amplitude of $\delta^{18}O$ variations (Lisiecki and Raymo, 2007) and the continuous presence of IRD beyond the shelf edge (Jansen et al., 2000).

3.1.1. Sedimentary records of ice sheet and submarine mass movement histories

The initial 2.5 – 2.4 Ma advance left the largest sedimentary signature during the Early Quaternary. This advance is marked by reflector R6 in Fig. 5c which identifies the base of the glacial units in the Scoresby Sund area (Vanneste et al., 1995). This advance was characterised by the emplacement of glacigenic debris-flow deposits on the Scoresby Sund Trough-Mouth Fan implying a high rate of sediment delivery during this period (Solheim et al., 1998; Channell et al., 1999). Subsequent sedimentation during the period from 2.4 – 1.3 Ma was characterised by silty clays containing variable amounts of IRD, turbidites ranging in thickness from 5 to 60 cm and lower volume glacigenic debris-flows emplaced on the upper parts of Scoresby Sund Trough-Mouth Fan (Solheim et al., 1998; Wilken and Mienert, 2006). The change in depositional character may be a consequence of lower rates of sediment transport to the shelf edge by continental ice and storage on the shelf. This

hypothesis is supported by limited progradation of the shelf edge of only 5 km during the Early Quaternary (Vanneste et al., 1995; Lykke-Andersen, 1998); a rate of progradation 16 times lower than would occur from 1.3 – 0.7 Ma. Alternatively, deposition of sediment by meltwater processes may have led to enhanced turbidity current activity and the transportation of sediment to the deep ocean.

3.2. 1.3 – 0.7 Ma

Compared with the northern European ice sheets, the Greenland Ice Sheet underwent comparatively little change between 1.3 and 0.7 Ma. The ice sheet underwent advance and retreat cycles consistent with climatic forcing. However, the extent of these advances is contentious.

Early analysis of the Greenland Ice Sheet during this time period concluded that the ice sheet was relatively stable (Fig. 6b). Neither its advances, nor its retreats were particularly extensive; the ice sheet remaining on or near to the continental shelf (Solheim et al., 1998; Butt et al., 2001a). This scenario was supported by the continuous supply of IRD provided by the Greenland Ice Sheet to sites both within and outside of the Nordic Seas (Larsen, 1990; Larsen et al., 1994; St. John and Krissek, 2002; Helmke et al., 2003a). Large IRD peaks that might indicate widespread collapse/retreat of an extensive ice sheet are also less common (Jansen et al., 2000).

Subsequent analysis of offshore records has challenged the view of a ‘stable’ restricted ice sheet (Fig. 6b). Glacigenic debris-flows on the Scoresby Sund Trough-Mouth Fan (Fig. 5d) suggest the ice sheet may in fact have advanced sufficiently during this period to reach the shelf edge. The exact timing of advances to the shelf edge are uncertain (Laberg et al., 2013), but is suggestive of a more dynamic glacial regime, more akin to reconstructions of the Late Quaternary Greenland Ice Sheet (Håkansson et al., 2009; Winkelmann et al., 2010).

3.2.1. Sedimentary records of ice sheet and submarine mass movement histories

298 Contrasting sedimentary processes are invoked to be associated with the Greenland Ice Sheet
299 between 1.3 and 0.7 Ma. First, glacigenic debris-flow deposits on the central and southern sides of
300 the Scoresby Sund Trough-Mouth Fan suggest direct input of sediment by an ice stream active at the
301 shelf edge (Laberg et al., 2013; Laberg and Dowdeswell, 2016). Second, the dominant ice sheet
302 driven process responsible for the majority of margin evolution is meltwater delivery of sediment.
303 From 1.3 – 0.6 Ma the East Greenland shelf margin moved seawards by 38 km (Vanneste et al.,
304 1995). This progradation has been attributed to glacimarine deposition through meltwater plumes
305 and turbidity currents (Solheim et al., 1998; Wilken and Mienert, 2006). The delivery of sediment
306 through these processes is also thought to be responsible for vertical aggradation of the shelf by 130
307 m (Vanneste et al., 1995). The predominance of sediment delivery through meltwater processes and
308 the triggering of turbidity currents is also thought to have led to submarine channel formation along
309 the East Greenland Margin during this period (Ó Cofaigh et al., 2004; Wilken and Mienert, 2006;
310 Laberg et al., 2013).

311 The enhanced shelf progradation and aggradation from 1.2 to 0.6 Ma is thought to be a
312 consequence of a period when the Greenland Ice Sheet was particularly erosive (Vanneste et al.,
313 1995; Solheim et al., 1998). The presence of warm-based ice with greater erosive potential is also
314 suggested by margin sedimentation being dominated by meltwater processes.

315 **3.3.0.7 – 0.13 Ma**

316 Repeated glaciations of the Greenland continental shelf are inferred from 0.7 – 0.13 Ma from IRD
317 records but the extent of these advances remains unclear (Solheim et al., 1998; Thiede et al., 1998;
318 Jansen et al., 2000). Between 0.7 – 0.13 Ma background levels of IRD are greater than they were
319 during earlier periods, although IRD pulses are less common (St. John and Krissek, 2002). This could
320 be a consequence of either a larger and more stable ice sheet or a function of greater sea ice
321 coverage preventing IRD reaching the continental shelf (Funder et al., 2011). One exception to this is
322 the Saalian glaciation (Fig. 6c). Terminating at ~130 ka, terrestrial and continental shelf records

suggest that the Saalian Greenland Ice Sheet may represent the maximum ice cover achieved during the Late Quaternary (Stein et al., 1996; Funder et al., 1998; Nam and Stein, 1999; Adrielsson and Alexanderson, 2005; Håkansson et al., 2009).

3.3.1. Sedimentary records of ice sheet and submarine mass movement histories

The Late Quaternary is primarily associated with aggradation of sediment on the continental shelf (Fig. 5b; sequence 10 and 11). From 0.7 – 0.13 Ma the continental shelf aggradated over 260 m, whereas progradation is reduced to less than 5 km (Vanneste et al., 1995). This is attributed to the reduced erosional capabilities of successive advancing ice sheets and the increased distance to the shelf edge (ten Brink et al., 1995; Vanneste et al., 1995; Solheim et al., 1998). As a consequence there is limited evidence for submarine mass movement occurrence on or beyond the continental shelf, although this may be a consequence of subsequent erosion by the Saalian and Weichselian ice sheets.

The shelf edge Saalian advance led to a phase of intense sediment remobilisation. Glacigenic debris-flows occurred on the southern part of the Scoresby Sund Trough-Mouth Fan (Fig. 5; Dowdeswell et al., 1997; Laberg et al., 2013). However, the volumes of these debris-flows was far smaller than those seen on the Bear Island or North Sea Trough-Mouth Fans during similar periods (Dowdeswell et al., 1997). The shift in location of glacigenic debris-flows on the fan is a consequence of a cross-shelf trough migration. The change of drainage path direction is reflected by a lack of mass movement deposits and the lower sedimentation rate after about 0.78 Ma at ODP Site 987 (Nam et al., 1995; Funder et al., 2011; Laberg et al., 2013).

Ice also reached the shelf edge along the section of the Greenland Basin where submarine channels had previously formed between 1.3 and 0.7 Ma (Wilken and Mienert, 2006). The continental margin in this sector was also characterised by limited glacigenic debris-flow emplacement during the Saalian advance. However, unlike earlier advances or indeed the subsequent Weichselian advances,

evidence suggests that this submarine channel system was not active and was in fact overridden by glacigenic debris-flows (Wilken and Mienert, 2006). From this we infer that turbidity currents played a far less pivotal role in sediment transport during the Saalian compared to previous and later glacial advances in this area possibly as a consequence of reduced meltwater input (Wilken and Mienert, 2006).

3.4.0.13 – 0 Ma (Weichselian – Present)

Greenland Ice Sheet history during the Weichselian is the best constrained of any period during the Quaternary. Our understanding of the ice sheet is, however, based primarily on a number of key sites and thus reconstructions involve a large amount of interpolation (Funder et al., 1994; 2011). Along the East Greenland Margin, reconstructions are based primarily on sites around Scoresby Sund and Jameson Land (Fig. 4; Funder et al., 2011). The consequence of this is that we are unable to build precise advance and retreat chronologies with the same level of detail that we are able to for the Barents Sea and Scandinavian Ice Sheets (Fig. 6d).

Five glacial advances are envisaged in East Greenland. The earliest advances are attributed to Marine Isotope Stage (MIS) 5d and 5b, and are dated using the stratigraphical setting and luminescence dates from glaciolacustrine sediments overlying till beds (Funder et al., 1994; Landvik, 1994; Tveranger et al., 1994). During the MIS 5d, glaciers are believed to have advanced at least onto the inner shelf (Ingólfsson et al., 1994; Landvik et al., 1994; Tveranger et al., 1994). IRD records also suggest an advance during MIS 4 followed by a limited retreat between MIS 4 and 3 (Funder et al., 1998; 2011). In the Scoresby Sund area, the extent of the MIS 4 ice sheet around 60 ka Before Present (BP) has been suggested to be close to the limit of the MIS 2 ice sheet using OSL dating of fluvial and deltaic sediments and IRD on the continental slope (Hansen et al., 1999). IRD peaks during MIS 3 which coincide with heavy and light $\delta^{18}O$ values are inferred to represent small advance and retreat cycles (Nam et al., 1995; Stein et al., 1996). However, they may also represent fluctuations in

371 sea ice cover along the East Greenland Coast (Gard and Backman, 1990; Nam et al., 1995; Stein et
372 al., 1996).

373 The last glacial advance occurred in MIS 2. IRD records indicate that glaciers in East Greenland
374 reached their maximum extent from 21 – 16 ka BP (Stein et al., 1996). Changes to glacier margin
375 positions may also be indicated by pulses of IRD at ~32.7, ~30.9 – ~29.7, ~27 – ~25.9, ~24.8 –
376 ~23.6, ~21.3 – ~20, ~17.8 – ~16,4 ka cal BP (Funder et al., 1998). However, the extent and style of
377 glaciation of the MIS 2 advance is uncertain. Basal till, streamlined subglacial bedforms and terminal
378 moraines identified from the south east and south west sectors of the Greenland Ice Sheet show
379 that glaciers expanded to the shelf edge (Jennings et al., 2002; 2006; Andrews, 2008; Dowdeswell et
380 al., 2010a; Funder et al., 2011). In contrast, seismic records of the central East Greenland continental
381 shelf show no seismically resolvable layers associated with this advance (Solheim et al., 1998). Two
382 scenarios have been suggested to explain this; (1) glaciers reached the coast and fjord mouths but
383 did not expand greatly onto the continental shelf (Solheim et al., 1998); or (2) glaciers were cold-
384 based with restricted flow and sediment transfer (Funder et al., 1998). However, more recent
385 cosmogenic dating in the Scoresby Sund region has suggested that ice may have reached the outer
386 shelf (Håkansson et al., 2007; 2009). In the northeast sector of the Greenland Ice Sheet, submarine
387 landforms (mega-scale glacial lineations and elongate bedforms) indicate that the MIS 2 ice sheet
388 expanded to at least the middle-outer continental shelf (Evans et al., 2009). Contrary to the
389 suggested restricted flow pattern in the central eastern sector, bathymetric cross-shelf troughs in
390 this sector were filled by warm-based, fast flowing ice. There is also evidence of elongate bedforms
391 to suggest active ice flow across shallow intra-trough regions (Evans et al., 2009).

392 The exact timing of the initial retreat from the MIS 2 maximum is equally contentious. Funder and
393 Hansen (1996) suggested that the ice margin began retreating from the outer part of fjord basins at
394 ca. 17.8 cal ka BP in the central East Greenland sector. The timing is coincident with a marked
395 decrease in IRD in continental slope records (Nam et al., 1995). An alternative scenario proposes

396 that deglaciation occurred shortly before 10 ka BP (Björck et al., 1994a; 1994b). In the northeast
397 sector, glacier retreat is envisaged to occur after 19.5 cal ka BP, marked by an increase in IRD on the
398 continental slope (Nothold, 1998; Evans et al., 2009).

399 **3.4.1. Sedimentary records of ice sheet and submarine mass movement histories**

400 The sedimentary signature of the Weichselian glaciation along the East Greenland Margin is
401 extremely varied but beyond the shelf break is associated with widespread submarine mass
402 movement occurrence. In more proximal settings, the multiple cycles of ice marginal expansion and
403 contraction can be identified within fjord settings by sedimentary successions. Advances are
404 characterised by tills and overridden/glacially thrust sediments (Tveranger et al., 1994; Funder et al.,
405 1998). Retreats are indicated by pro- and deltaic mud and sand sequences (Funder et al., 1994;
406 1996). Additional sequences include thick laminated fine-grained sediments likely resulting from
407 glacier proximal sediment plumes (Stein et al., 1993; Funder et al., 2011).

408 Beyond the continental shelf, submarine mass movement processes vary by sector. In the Scoresby
409 Sund sector, glacigenic debris-flows occurred on the southern side of the Scoresby Sund Trough-
410 Mouth Fan (Nam et al., 1995; Dowdeswell et al., 1997). The previously active northern side does not
411 appear to have experienced any mass wasting processes during the Weichselian (Laberg et al.,
412 2013). The number and volume of glacigenic debris-flows in the Weichselian continued to be far
413 smaller than those seen on other trough-mouth fans around the Nordic Seas indicating a continued
414 reduction in the volume of sediment delivered compared to the period from 1.2 – 0.5 Ma (Vanneste
415 et al., 1995; Dowdeswell et al., 1997).

416 North of the Scoresby Sund Trough-Mouth Fan, glacigenic debris-flows, turbidity current deposits
417 and extensive channel systems have been identified beyond the shelf break (Fig. 7; Ó Cofaigh et al.,
418 2004; Wilken and Mienert, 2006). Associated with cross-shelf troughs, glacigenic debris-flow lobes
419 are found on the upper and mid- continental slope. Below 2000 m water depth turbidites are the

420 dominant sedimentary facies (Ó Cofaigh et al., 2004). The glacigenic debris-flows are dated >22.8 ka
421 BP (Wilken and Mienert, 2006). Turbidity current activity ceased by 13 ka BP (Fig. 7; Ó Cofaigh et al.,
422 2004). Prior to the cessation of turbidity current activity, deposition on this part of the margin was
423 characterised by laminated silt and mud layers associated with deglaciation. Sedimentation rates
424 peaked between 51 – 79 cm kyr^{-1} between 15 and 13 ka BP before falling to <4 cm kyr^{-1} after 13 ka
425 BP (Ó Cofaigh et al., 2004; Wilken and Mienert, 2006). An extensive submarine channel network is
426 also found along this part of the margin. The channels cross-cut the glacigenic debris-flow deposits
427 on the upper and mid-slope implying their formation post-dates the emplacement of these deposits
428 (Ó Cofaigh et al., 2004). The direct link between ice sheet delivery of meltwater and sediment, the
429 occurrence of turbidity currents and the cessation of activity within any of the channels following
430 the withdrawal of the ice sheet illustrates the role of the Greenland Ice Sheet in the sedimentary
431 evolution of the margin.

432 The northeast sector of the Greenland continental shelf is characterised by multiple mass wasting
433 processes during the Weichselian. Here, as in the previous sector, the upper and mid- continental
434 slopes are characterised by glacigenic debris-flows (Fig. 8; Evans et al., 2009). The lower continental
435 slope is characterised by turbidite deposition. These turbidites are inferred to be the result either of
436 downslope evolution of debris-flows sourced from higher up the slope or the triggering of turbidity
437 currents by other mass-wasting events (Dowdeswell et al., 1997; Evans et al., 2009). Swath
438 bathymetry showing prominent scarps also indicates that submarine landslides have occurred along
439 this part of the East Greenland Margin (Fig. 8c and 8d; Evans et al., 2009). There is little evidence of
440 submarine landslide occurrence along any other part of the East Greenland Margin.

441 The history of the Greenland Ice Sheet and the related sedimentation processes are summarised in
442 Table 1 and Fig. 9a.

443 **4. Barents Sea Ice Sheet**

The following section focusses on the evolution of the Barents Sea Ice Sheet and the Svalbard/south west margin of the Barents Sea (Fig. 10). Compared to the East Greenland Margin, the Svalbard/Barents Sea Margin has been much more intensively studied and this is shown by the comparatively better understanding of this margin during the Quaternary.

4.1.2.58 – 1.6 Ma

The initial part of this period was characterised by the retreat of an extensive ice sheet based on Svalbard and the northern Barents Sea (Myhre et al., 1995; Solheim et al., 1998; Knies et al., 2009). The retreat is inferred from a substantial reduction in IRD at ODP sites on the Yermak Plateau (Wolf-Welling et al., 1996; Winkler et al., 2002), and the presence of a regional seismic reflector (R7 in Fig. 11) on the continental shelf and slope that marks a distinctive change in sedimentation regime (Faleide et al., 1996).

Following the initial ice sheet retreat, the period from 2.5 – 1.6 Ma was characterised by limited advance and retreat of glaciers on Svalbard and in the northern Barents Sea (Fig. 12a; Sejrup et al., 2005). The presence of ice in the northern Barents Sea is indicated by the reduction of specific clay mineral groups (smectite) at ODP sites on the Yermak Plateau and the Fram Strait. Smectite in these areas was previously sourced from the Mesozoic Siberian trap basalts on the Putorana Plateau and transported by the Yenisey and Khatanga rivers and subsequently transported across the northern Barents Sea (Vogt and Knies, 2008). A reduction in the amount of smectite is thought to be indicative of ice blocking the transport path (Knies et al., 2009). The limited extent of ice expansion is inferred from the lack of IRD at the same ODP sites and is thought to indicate that glaciers were too small to calve large numbers of icebergs (Knies et al., 2009).

4.1.1. Sedimentary records of ice sheet and submarine mass movement histories

The average sedimentation rate on the continental shelf offshore Svalbard and in the southwest Barents Sea from 2.5 – 1.6 Ma was higher than during the majority of the Pliocene (Solheim et al.,

1996). Using seismic data from the Storfjorden and Bear Island Trough-Mouth Fans, the average sedimentation rate increased from 3.2 cm/kyr and 2.2 cm/kyr from 55 – 2.3 Ma to 62.5 cm/kyr and 37 cm/kyr respectively (Faleide et al., 1996; Fiedler and Faleide, 1996; Hjelstuen et al., 1996). However, the limited nature of glacier expansion means that sediment was likely transported by meltwater, either through fluvial action or in sediment-laden plumes and deposited in fluvial/glacimarine sequences. These interpretations are supported by numerical modelling which suggests that the continental shelf of the Barents Sea was still subaerial at this time (Butt et al., 2002), and the presence of incised palaeo-channels in the stratigraphy of the present-day trough-mouth fans which are filled with sand and gravel implying a strong meltwater influence (Sættem et al., 1992; 1994; Vorren and Laberg, 1997; Vorren et al., 2011).

Beyond the shelf break offshore Svalbard, this period is also characterised by alternating deposition of hemipelagite and emplacement of submarine mass movement deposits (Fig. 11). The submarine mass movement deposits are characterised as massive, sandy units with soft sediment deformation structures containing contorted and/or variably inclined beds (Jansen, 1996; Forsberg et al., 1999). These deposits are not, however, characteristic of glacigenic debris-flows. It is possible that the hemipelagic sediments possibly acted as glide planes along which the mass movements occurred as a consequence of the increased sedimentation rate. Glaciofluvial and submarine gravity flow deposit emplacement during this period resulted in gradual aggradation and progradation of sedimentary wedges at the continental shelf (Faleide et al., 1996; Hjelstuen et al., 1996; Dahlgren et al., 2005).

4.2.1.6 – 1.3 Ma

The period between 1.6 and 1.3 Ma, is characterised by greater expansion of the Barents Sea Ice Sheet (Fig. 12b). Expansion is indicated by higher rates of IRD accumulation (Knies et al., 2009). Stratigraphically, this expansion is marked regionally by the R6 seismic reflector (Fig. 11; Faleide et al., 1996; Forsberg et al., 1999). During this period, glaciers sourced from Svalbard expanded sufficiently to reach the shelf edge (Faleide et al., 1996; Solheim et al., 1998). Ice masses present in

493 the northern Barents Sea also expanded. However, their expansion southwards was relatively
494 limited. There is no evidence that the ice sheet expanded sufficiently in this sector to reach the shelf
495 edge, and thus the south western margin of the Barents Sea, i.e. the Bear Island Trough, remained
496 unglaciated during this period (Sættem et al., 1992; 1994; Solheim et al., 1998).

497 **4.2.1. Sedimentary records of ice sheet and submarine mass movement histories**

498 From 1.6 – 1.3 Ma the sedimentary processes along the Svalbard/Barents Sea margin can be divided
499 into two sectors. The southwestern margin of the Barents Sea continued to be dominated by
500 glaciofluvial and glacimarine processes (Fig. 11; Sættem et al., 1994; Faleide et al., 1996; Hjelstuen et
501 al., 1996; Solheim et al., 1998). Around Svalbard, reflecting greater glacial expansion, continental
502 slope deposits are characterised by the onset of a period of major glacigenic debris-flow
503 emplacement and the acceleration of sedimentary wedge progradation (Solheim et al., 1998;
504 Dahlgren et al., 2005). These deposits are both thicker and seismically distinct from those associated
505 with the glaciofluvial/glaciomarine period of deposition from 2.5 – 1.6 Ma indicating the enhanced
506 efficiency of glacial sediment transportation and the contrasting character of submarine mass
507 movement deposit emplacement.

508 **4.3.1.3 – 0.7 Ma**

509 The largest change from 1.3 – 0.7 Ma in the Svalbard/Barents Sea sector was the greater expansion
510 of the Barents Sea Ice Sheet (Fig. 12c; Kristoffersen et al., 2004; Vorren et al., 2011). On the Svalbard
511 margin, glaciers originating on the archipelago continued to advance to, and retreat from, the shelf
512 edge (Solheim et al., 1996). Further south, the Barents Sea Ice Sheet expanded sufficiently to reach
513 the shelf edge along the southwestern margin of the Barents Sea for the first time (Andreassen et
514 al., 2004; 2007). Moreover, fast flowing ice has been inferred to have been present in the Bear Island
515 Trough from the presence of buried megascale glacial lineations (Andreassen et al., 2007; Vorren et
516 al., 2011). Further evidence of intensified glacial activity in the Barents Sea during this time comes

517 from IRD records at Site 908 and 909 which show large increases in accumulation during this period
518 (Knies et al., 2009).

519 **4.3.1. Sedimentary records of ice sheet and submarine mass movement histories**

520 The record of sedimentary processes along the Svalbard/Barents Sea Margin from 1.3 – 0.7 Ma is
521 best examined in two parts; the Svalbard and southwest Barents Sea margins. Continued glacial
522 sediment delivery from 1.3 – 0.7 Ma to the Svalbard continental shelf edge led to sustained
523 progradation of glacigenic-wedges through glacigenic debris-flow emplacement (Faleide et al., 1996;
524 Solheim et al., 1998; Dahlgren et al., 2005). Between 1.0 and 0.78 Ma seismic stratigraphy also
525 indicates the presence of small scale slumps on a number of trough-mouth fans, e.g. Isfjorden
526 (Andersen et al., 1994). Although the volumes of these failures appears to be relatively limited, it is
527 important to note this is the first evidence of trough-mouth fan instability in this region beyond
528 those associated with the occurrence of glacigenic debris-flows. The occurrence of these slumps is
529 likely a consequence of either the enhanced sedimentation rate or increased seismicity resulting
530 from isostatic adjustment related to the presence of a larger Barents Sea Ice Sheet.

531 In contrast to the Svalbard margin, the expansion of the Barents Sea Ice Sheet to the shelf edge
532 along the southwestern sector of the margin resulted in a significant change of deposition style
533 marked by regional seismic reflector R5 (Fig. 11; Faleide et al., 1996; Fiedler and Faleide, 1996;
534 Hjelstuen et al., 1996; Solheim et al., 1998; Vorren et al., 2011). Ice sheet expansion to the shelf
535 edge increased the rate of sedimentation to 130 cm/kyr across the Bear Island Trough-Mouth Fan
536 from 1.3 – 1.0 Ma resulting in glacigenic debris-flow emplacement (Fig. 13; Hjelstuen et al., 2007).
537 This rate of sedimentation is nearly double that seen from 2.5 – 1.3 Ma and is attributed to ice sheet
538 expansion over readily erodible sediments on the continental shelf previously deposited by
539 glacimarine and fluvial processes (Fiedler and Faleide, 1996). From 1.0 – 0.78 Ma the rate of
540 sedimentation at the shelf edge of the Bear Island Trough halved to ~70 cm/kyr (Hjelstuen et al.,
541 2007). The reduced rate of sedimentation is thought to result from the drowning of the Barents Sea

and the transition from a subaerial ice sheet to a marine-based ice sheet (Butt et al., 2002). These changing rates of erosion and deposition were also seen on the Storfjorden Trough-Mouth Fan (Hjelstuen et al., 1996; Solheim et al., 1998; Butt et al., 2001b).

In addition to glacigenic debris-flow emplacement, this time period was also witness to submarine landslide occurrence on the Storfjorden and Bear Island Trough-Mouth Fans. Submarine landslides have affected the Storfjorden Trough-Mouth Fan between 1.0 and 0.8 Ma, with volumes up to ~45 km^3 (Hjelstuen et al., 1996; Rebesco et al., 2012; Llopart et al., 2015). They are attributed to instabilities resulting from increasing volumes of deposited sediment (Hjelstuen et al., 1996) being delivered to the fan. On the Bear Island Trough-Mouth Fan seismic stratigraphy suggests that a large submarine landslide occurred between 1.0 and 0.78 Ma (Fig. 13; Hjelstuen et al., 2007). The slide is estimated to have mobilised in excess of 25,000 km^3 of material and is the largest yet found on the planet, nearly 10 times larger than Storegga (Table 2; Kuvaas and Kristoffersen, 1996; Hjelstuen et al., 2007). The occurrence of this slide after 1.0 Ma suggests that its occurrence is related to the increased delivery of sediment associated with glacial intensification associated with the Mid-Pleistocene Transition (Fiedler and Faleide, 1996; Solheim et al., 1998). The expansion of the Barents Sea Ice Sheet would also have led to an increase in regional seismicity as a consequence of isostatic adjustment (Stewart et al., 2000). Increases to the rate of sedimentation and local levels of seismicity would both increase the likelihood of slope failure (Masson et al., 2006; ten Brink et al., 2009). The imprecise dating (Slide BFSC I has an age range of 0.21 Myr; Hjelstuen et al., 2007) makes identification of a specific trigger difficult. However, it is interesting that the slide in fact occurred after the average rate of sedimentation decreased implying that the earlier period of greatest sedimentation was insufficient to reach a threshold whereby slope failure was triggered.

4.4.0.7 – 0.13 Ma

The adoption of the 100 kyr climate cycles was associated with regular expansion of the Barents Sea Ice Sheet to the shelf edge along the Svalbard/Barents Sea Margin of the Barents Sea (Solheim et al.,

1996; Solheim et al., 1998). The ice sheet is interpreted to have reached the shelf edge during MIS 16 (676 – 621 ka BP), 12 (478 – 423 ka BP), 10 (374 – 337), 8 (303 – 245 ka BP) and 6 (186 – 128 ka BP) (Laberg and Vorren, 1996; Vorren and Laberg, 1997; Sejrup et al., 2005; Knies et al., 2009). An advance is also inferred to have occurred during MIS 14 (565 – 524 ka BP) but its extent is contentious. Evidence for each of these advances is present in stable isotope data from ODP Hole 910A (Knies et al., 2007) and buried mega-scale glacial lineations visible in seismic data (Andreassen et al., 2004). Each isotope stage could contain multiple advances to the shelf edge that are unresolvable in seismic data or in IRD records; five advances is therefore the minimum which occurred from 0.7 – 0.13 Ma (Vorren and Laberg, 1997). From ODP Sites around Svalbard, Knies et al. (2009) suggest ice reached the shelf edge, and interpretation of deposits on the Bear Island Trough-Mouth Fan confirms this (Sættem et al., 1994; Laberg and Vorren, 1996; Vorren and Laberg, 1997). It is, however, possible that the ice sheet reached the shelf edge of the Bear Island Trough but not around Svalbard. Of the identified advances, the Saalian (MIS 6) is interpreted to be of longest duration (Svendsen et al., 2004b; Ingólfsson and Landvik, 2013; Pope et al., 2016).

4.4.1. Sedimentary records of ice sheet and submarine mass movement histories

Here, we discuss sedimentary processes along specific sections of the margin, reflecting the large number of studies undertaken which cover this time period.

4.4.1.1. *Western Svalbard Margin*

Ice regularly reached the shelf edge of western Svalbard between 0.7 and 0.13 Ma (Solheim et al., 1998; Spielhagen et al., 2004; Knies et al., 2007; 2009). Each shelf edge advance was characterised by trough-mouth fan glacigenic debris-flow emplacement (Fig. 11; Andersen et al., 1994; Faleide et al., 1996; Fiedler and Faleide, 1996). During this period there was a shift from net-erosion of the continental shelf to net sediment accumulation on the outer continental shelf. As a consequence debris-flow deposit thickness declined compared with deposits before the onset of 100 kyr cyclicity

591 (Elverhøi et al., 1998; Solheim et al., 1998). The decline in glacigenic debris-flow thickness in
592 association with net sediment accumulation of the continental shelf is similar to the temporal
593 evolution of debris-flow characteristics on the Scoresby Sund Trough-Mouth Fan (see Section 3).

594 ***4.4.1.2.*** *Storfjorden Trough-Mouth Fan*

595 Seven distinct seismic units associated with ice stream advance to the shelf edge in the Storfjorden
596 Trough have been identified (Laberg and Vorren, 1996; Vorren and Laberg, 1997). These equate to
597 advances to the shelf edge during MIS 14, 12, 10, 8 and 6. Glacigenic debris-flows are thought to
598 dominate each unit reflecting direct input by the ice stream at the shelf edge (Solheim and
599 Kristoffersen, 1984; Vorren and Laberg, 1997). However, despite glacigenic debris-flows dominating
600 sedimentation across the fan throughout this period, the rate of sedimentation dramatically
601 decreased after 0.44 Ma (Faleide et al., 1996; Hjelstuen et al., 1996). Between 1.0 and 0.44 Ma, an
602 average of 2400 t $km^{-2}a^{-1}$ was deposited across the fan. This decreased to 420 t $km^{-2}a^{-1}$ between 0.44
603 and 0 Ma (Hjelstuen et al., 1996) showing that the adoption of the 'more' intense 100 kyr glacial
604 cycle does not necessarily increase the sediment supply to the shelf edge. Submarine landslides have
605 also been identified in seismic data during this period with volumes up to ~128 km^3 (Llopart et al.,
606 2015).

607 ***4.4.1.3.*** *Bear Island Trough-Mouth Fan*

608 Ice sheet sedimentary processes dominated the Bear Island Trough-Mouth Fan from 0.7 – 0.13 Ma,
609 each advance being correlated to a specific seismic package (Fig. 14). Each of these units I – VI (Fig.
610 10) is dominated on the upper fan by a chaotic seismic facies (Sættem et al., 1992; 1994; Laberg and
611 Vorren, 1996). On the middle and lower fan they have a mounded geometry (Laberg and Vorren,
612 1996). The facies and their associated bounding seismic reflectors are interpreted to represent
613 glacigenic debris-flow lobes, interbedded with hemipelagic sediments (Vorren et al., 1990; Laberg
614 and Vorren, 1995; Vorren and Laberg, 1997). Distally, these sequences are characterised by fine-

615 grained turbidites, derived from the downslope evolution of glacigenic debris-flows, and hemipelagic
616 sediments (Laberg and Vorren, 1996; Pope et al., 2016).

617 Rates of sediment accumulation and debris-flow emplacement are not constant over either the fan
618 or between the different advances. The MIS 12 advance is estimated to have the delivered the most
619 sediment at the highest rate to the fan. Represented by seismic unit III (Fig. 14b), 17,650 km^3 of
620 sediment is estimated to have accumulated at a rate of 63 cm/ka during this glacial with the
621 depocentre on the central part of the fan (Laberg and Vorren, 1996). During the following two
622 glaciations (MIS 10 and 8) 7,266 km^3 of sediment is estimated to have accumulated at a rate of 14
623 cm/ka with the depocentre situated on the southern end of the fan (Laberg and Vorren, 1996). The
624 MIS 6 advance depocentre was on the northern and southern parts of the fan. An estimated 4061
625 km^3 of sediment accumulated at a rate of 19 cm/ka (Laberg and Vorren, 1996). Sedimentation rates
626 and depocentres could not be calculated for the oldest two units, although accumulation rates of
627 ~14 cm/ka have been hypothesised (Laberg and Vorren, 1996). These variations in depocentre and
628 sediment accumulation rate indicate the frequent nature of flow migration of the Bear Island Ice
629 Stream and possible range of sediment delivery rates (Dowdeswell and Siegert, 1999).

630 Five large submarine landslides are also believed to have affected the fan between 0.7 and 0.13 Ma
631 (see Table 2). These landslides range in size from 1.1 km^3 to 24.5 km^3 (Fig. 13; Hjelstuen et al., 2007).
632 The three oldest slides occurred between 0.78 and 0.5 Ma, indicating a period of large-scale
633 instability on the Bear Island Trough-Mouth Fan. Their age, and the unresolvable Units I and II, in
634 seismic profiles prevent a comparison between depocentres and landslide triggering (Laberg and
635 Vorren, 1996). Nevertheless, these are likely associated with the high sedimentation rates which had
636 occurred during this period and since the Mid-Pleistocene Transition and the intensification of
637 Barents Sea glaciation. The next youngest slide occurred between 0.5 and 0.2 Ma (Hjelstuen et al.,
638 2007). The headwall of this landslide occurred on the northern margin of the depocentre associated
639 with the MIS 10 and 8 advances (Fig. 14; Laberg and Vorren, 1996). The Bjørnøya Slide occurred

between 0.3 – 0.2 Ma, post-dating units IV and V and is located on the southern margin of the depocentre of these units (Fig. 14; Laberg and Vorren, 1996). Better constraint of the dates of these slides will be key to understanding their relationship with periods of enhanced sedimentation, sea level change and earthquakes associated with glacio-isostaic adjustment.

4.5.0.13 – 0 Ma (Weichselian – Present)

Understanding of the Barents Sea Ice Sheet is most complete during the Weichselian period (Fig. 12d). Onshore and offshore records show that the ice sheet underwent multiple advance and retreat cycles during this time (Mangerud et al., 1998; Svendsen et al., 1999; 2004a; 2004b; Patton et al., 2015; Hughes et al., 2016).

The prevailing view of Barents Sea Ice Sheet history during the Weichselian is for four advances. The earliest expansion occurred during MIS 5d from 115 – 105 ka (Patton et al., 2015). This advance is believed to have been limited to Svalbard (Mangerud and Svendsen, 1992) but is envisaged to have reached the shelf edge along the western margin (Knies et al., 1998). Evidence for this on Svalbard comes from the dating of till units (Mangerud and Svendsen, 1992; Mangerud et al., 1996) and offshore IRD records (Knies et al., 2001).

A second expansion is reconstructed from 100 – 70 ka BP (MIS 5b; Mangerud et al., 1998). On Svalbard, this expansion is believed to be shorter (~90 – 80 ka BP) and less extensive, i.e. only reaching the coastline, than in the Barents Sea (Svendsen et al., 1999). Ice sheet expansion in the Barents Sea itself was limited to the eastern Barents and Kara Seas (Svendsen et al., 1999, 2004a, b; Siegert et al., 2001). Evidence for the extent and timing of this glacial advance comes from OSL dates on raised beach sediments from ice-damned lakes (Mangerud et al., 2001; 2004), IRD records (Knies et al., 2000) and till layers in the Barents Sea (Sættem et al., 1992).

During the Middle Weichselian (MIS 4 – 3/70 – 50 ka BP), the Barents Sea Ice Sheet advanced to the shelf edge along the western Svalbard margin and in the southwestern Barents Sea (Mangerud and

Svendsen, 1992; Andersen et al., 1996; Knies et al., 2001). In the Bear Island Trough, ice is envisaged to have been at the shelf edge between 68 – 60 ka BP (Pope et al., 2016). Reconstructions of glacier extent on Svalbard from marine records suggest similar timings for maximum extension to the shelf edge (Mangerud, 1991; Dowdeswell et al., 1995; Andersen et al., 1996; Knies et al., 2001). Evidence for this advance includes dated till layers, IRD and glacigenic debris-flows beyond the shelf edge (Mangerud and Svendsen, 1992; Mangerud et al., 1998; Houmark-Nielsen et al., 2001; Pope et al., 2016).

The last advance to the shelf edge occurred during MIS 2. During this period ice began to build up at ~32 cal ka BP (Andersen et al., 1996; Siegert et al., 2001). West of Svalbard, ice reached the shelf break at ~24 cal ka BP (Elverhøi et al., 1995; Dowdeswell and Elverhøi, 2002; Andreassen et al., 2004; Jessen et al., 2010; Hughes et al., 2016). Along the southwestern Barents Sea margin ice reached the shelf edge at ~26 cal ka BP (Elverhøi et al., 1995; Laberg and Vorren, 1995; Vorren et al., 2011; Pope et al., 2016). Ice retreated from the shelf edge in both areas as early as 20 cal ka BP (see Hughes et al., 2016 for more detail).

In addition to these ice advances, a further advance has also been suggested during MIS 3. Pope et al. (2016) suggest that ice advanced in the Bear Island Trough and was present at or close to the shelf edge between 39.4 and 36 cal ka BP. Evidence for this advance came in the form of distal debris-flow muds that were present on the distal Bear Island Trough-Mouth Fan. An ice advance during this period is contrary to reconstructions made using terrestrial deposits on Svalbard (Mangerud et al., 1998; Svendsen et al., 2004b). It is, however, consistent with offshore IRD records (Dowdeswell et al., 1999; Dreger, 1999; Knies et al., 2001).

4.5.1. Sedimentary records of ice sheet and submarine mass movement histories

4.5.1.1. *Western Svalbard Margin*

687 The detailed offshore record of Svalbard glaciation begins at ~80 ka associated with the inferred
688 beginning of the shelf edge advance during MIS 4 (Mangerud et al., 1998; Svendsen et al., 2004b).
689 This period was characterised by the deposition of turbidites beyond the shelf edge (Andersen et al.,
690 1996) and the deposition of large amounts of IRD, especially following retreat of the ice after 60 ka
691 (Landvik et al., 1992; Dowdeswell et al., 1999).

692 Different sedimentary deposits are found offshore western Svalbard in conjunction with different
693 phases of ice advance during later periods. Ice began to build up ~32 cal ka BP, and reached the
694 shelf edge by ~24 cal ka BP (Elverhøi et al., 1995; Jessen et al., 2010). On Bellsund and Isfjorden
695 Trough-Mouth Fans (Fig. 10), deposition of laminated and massive muds and frequent turbidite
696 emplacement are thought to be reflective of periodic increases of meltwater and sediment delivery
697 associated with ice sheet advance (Andersen et al., 1996; Dowdeswell and Elverhøi, 2002; Landvik et
698 al., 2005). This was followed by the emplacement of glacigenic debris-flow deposits reflecting the
699 arrival and 'switch-on' of ice streams at the shelf edge (Alley et al., 1989; Andersen et al., 1996;
700 Dowdeswell and Siegert, 1999; Dowdeswell and Elverhøi, 2002).

701 Initial retreat ~20 cal ka BP was characterised by a return to hemipelagic sedimentation and higher
702 IRD concentrations (Knies et al., 2001; Rasmussen et al., 2007; Jessen et al., 2010). Unlike other
703 regions (e.g. along the Norwegian slope or Storfjorden) there was no period of rapid sedimentation
704 associated with meltwater deposition. Between 15.7 and 14.65 cal ka BP, a second phase of retreat
705 associated with enhanced iceberg calving resulted in increased concentrations of IRD and
706 sedimentation rates offshore western Svalbard (Elverhøi et al., 1995; Andersen et al., 1996; Vogt et
707 al., 2001). Further accelerated retreat after 14.65 cal ka BP is linked to thick, fine-grained laminated
708 mud deposits on the continental slope indicative of meltwater processes (Elverhøi et al., 1995;
709 Rasmussen et al., 1997; Jessen et al., 2010). Sediment accumulation rates during this period were
710 between one and two orders of magnitude higher than they had been when the ice margin was at
711 the shelf edge (Dowdeswell and Siegert, 1999; Dowdeswell and Elverhøi, 2002; Jessen et al., 2010).

712 The record of Weichselian sedimentation shows that the West Svalbard Margin was dominated
713 primarily by meltwater delivery of sediment and subsequent downslope movement of this sediment
714 by turbidity currents. The emplacement of glacigenic debris-flows only occurred during limited
715 periods associated with an ice sheet grounded at the shelf edge.

716 ***4.5.1.2.*** *Storfjorden Trough-Mouth Fan*

717 Estimates of accumulated sediment volumes on the Storfjorden Trough-Mouth Fan during the
718 Weichselian glacial come from seismic stratigraphy. According to these calculations 422 t km^{-2} yr^{-1}
719 were deposited during the Weichselian (Hjelstuen et al., 1996). This figure is part of an average
720 calculated for the last 440 ka (Hjelstuen et al., 1996). Dating of deposits on the Storfjorden Trough-
721 Mouth Fan associated with each of the Weichselian advances has not yet been achieved. This
722 section will therefore focus on the deposits associated with the Late Weichselian (MIS 2) advance.

723 Three depositional lobes can be seen on the Storfjorden Trough-Mouth Fan associated with the Late
724 Weichselian advance. Each of these lobes in inferred to be associated with different flow elements
725 of the larger Storfjorden palaeo-ice stream and has different depositional characteristics (Pedrosa et
726 al., 2011). The two northernmost lobes are characterised by diamictons and over 50 m of glacigenic
727 debris-flow deposits (Lucchi et al., 2013). Radiocarbon dating suggests that these deposits were
728 emplaced around ~23.8 cal ka BP (Lucchi et al., 2013). On the upper part of the fan these deposits
729 have subsequently been incised by gullies and a thin (2 – 3 m) drape of deglacial and Holocene
730 sediments (Pedrosa et al., 2011; Lucchi et al., 2013). These gullies disappear on the mid-slope.

731 The southern sector of the fan has markedly different sedimentary characteristics. The
732 southernmost lobe is characterised by ~20 m of glacigenic debris-flow deposits and multiple
733 submarine landslides with headwalls on the middle and upper slopes (Lucchi et al., 2012; Rebesco et
734 al., 2012; Llopart et al., 2015). The largest of these landslides covers an area of >1,100 km^2 and
735 displaced a volume of ~47 km^3 (Llopart et al., 2015). Stacked mass transport deposits can also found

736 in the middle and lower slope subsurface (Rebesco et al., 2011; 2012). The nearby Kveithola Trough-
737 Mouth Fan exhibits similar characteristics (Lucchi et al., 2012). As on the northern sections of the
738 fan, gullies are also found on the upper slopes (Pedrosa et al., 2011).

739 The southern sector of the fan is also characterised by interlaminated sequences interbedded with
740 glacigenic debris-flow deposits. These facies are believed to relate to the Middle and Late
741 Weichselian advances and to be the result of subglacial meltwater plume deposition (Lucchi et al.,
742 2013). The thickness of the interlaminated sediments decreases from meter thicknesses on the
743 upper fan to only 15 cm 42 km downslope. Plumite deposits from previous deglaciations and
744 subsequent hemipelagic sediments have been identified as the glide planes along which many of the
745 submarine landslides occur (Pedrosa et al., 2011; Lucchi et al., 2012; 2013; Rebesco et al., 2012;
746 Llopart et al., 2015). The contrasting geotechnical properties of these sediment packages therefore
747 appear to have played a key role in the occurrence of the slope failures, in addition to rapid
748 sedimentation (Llopart et al., 2014; 2015). Submarine landslides are also common in the area
749 between the Storfjorden and Kveithola Trough-Mouth Fans due to the thickness of accumulations of
750 plumite deposits in this location (Llopart et al., 2015).

751 To the south of the Storfjorden and Kveithola Trough-Mouth Fans the continental slope is
752 characterised by a dendritic sediment drainage system comprising a number of canyons which
753 converge to form the INBIS Channel (Fig. 15; Taylor et al., 2002b; Laberg et al., 2010).

754 ***4.5.1.3.*** *Bear Island Trough-Mouth Fan*

755 Based on seismic stratigraphies, the estimated ~2400 km^3 of accumulated sediment (13 cm/ka) on
756 the Bear Island Trough-Mouth Fan during the Weichselian is the lowest of any of the 100 kyr glacial
757 cycles (Laberg and Vorren, 1996). This is perceived to be a consequence of ice being stable at the
758 shelf edge for less time during the Weichselian compared to preceding glacials (Laberg and Vorren,
759 1995, 1996; Vorren et al., 2011; Pope et al., 2016).

760 The Weichselian sedimentary history of the Bear Island Trough-Mouth Fan is dominated by the
761 emplacement of glacigenic debris-flow deposits (Fig. 15; Taylor et al., 2002a; 2002b; Laberg and
762 Dowdeswell, 2016; Pope et al., 2016). Initial studies using side-scan sonar mapping showed the most
763 recently active (MIS 2) part of the fan was at its northern end and covered 125,000 km^2 where
764 debris-flow lobes radiated out from the top of the fan (Sættem et al., 1992; 1994; Taylor et al.,
765 2002a; 2002b; Laberg and Dowdeswell, 2016). These flows were shown to have run-out distances of
766 up to 490 km and contain between 10 and 35 km^3 of sediment (Laberg and Vorren, 1995; Laberg and
767 Dowdeswell, 2016).

768 Dating of more distal deposits on the northern end of the Bear Island Trough-Mouth Fan has
769 subsequently shown that glacigenic debris-flows have been emplaced in four distinct clusters during
770 the Weichselian. Each cluster is proposed to be associated with an ice advance to the shelf edge of
771 the Bear Island Trough (Pope et al., 2016). The number and thickness of deposits also suggests that
772 the largest number of glacigenic debris-flows was in fact associated with advances during MIS 4 and
773 MIS 3 rather than the MIS 2 advance (Pope et al., 2016).

774 In addition to the glacigenic debris-flows, the northern end of the fan is characterised by the
775 presence of gullies (Vorren et al., 1989; Laberg and Vorren, 1995). Gullies are also present on the
776 southern margin of the fan (Bellec et al., 2016). Two hypotheses for gully formation exist. First, cold
777 and turbid dense water related to brine rejection during sea ice formation during the Holocene was
778 able to erode and transport sediment from the shelf and/or generate turbidity currents (Laberg and
779 Vorren, 1995). Second, hyperpycnal flows resulting from meltwater and sediment delivery when ice
780 was at or near to the shelf edge resulted in channel incision (Laberg and Vorren, 1995; Mulder et al.,
781 2003; Dowdeswell et al., 2006a; Bellec et al., 2016). This was, however, concentrated at the margins
782 of the trough-mouth fan.

783 Following retreat of the Bear Island Ice stream from the shelf edge, a relatively thin sequence (<10
784 m) of glacimarine sediments was left in the trough (Vorren et al., 1990). On the upper fan, less than

785 1 m of glacimarine sediments have been recovered above debris-flow deposits (Laberg and Vorren,
786 1995). On the lower part of the fan, no glacimarine sediments have been found (Laberg and Vorren,
787 1995; Pope et al., 2016). This supports the rapid rate of retreat of the Bear Island Ice stream which
788 has been inferred from seafloor geomorphology in the Barents Sea (Winsborrow et al., 2010; 2012).

789 The history of the Barents Sea Ice Sheet and the related sedimentation processes are summarised in
790 Table 3 and Fig. 9b.

791 **5. Scandinavian Ice Sheet**

792 The following section will focus on the evolution of the Scandinavian Ice Sheet (Fig. 16) during the
793 Quaternary.

794 **5.1. 2.58 – 1.1 Ma**

795 Of the three major ice sheets, the Scandinavian Ice Sheet was the least extensive during this period
796 (Fig. 17a; Eidvin et al., 1998; Sejrup et al., 2000; Faleide et al., 2002; Henriksen et al., 2005; Ottesen
797 et al., 2009; Rise et al., 2010). The prevalent belief is that the ice sheet remained at an intermediate
798 size, rarely extending beyond the fjords of western Norway (Jansen and Sjøholm, 1991; Henrich and
799 Baumann, 1994; Dahlgren et al., 2002). Evidence for this comes from the limited IRD delivery to ODP
800 sites on the Vøring Plateau, the Norwegian Basin and cores bordering the Barents Sea as well as
801 seismic stratigraphy of the continental margin of Norway (Jansen et al., 1988; Henrich, 1989;
802 Haflidason et al., 1991; Sejrup et al., 1996; Rise et al., 2010). Further evidence of a limited but
803 sufficiently large ice sheet to calve icebergs on the Norwegian coast as early as ~2 Ma comes from
804 iceberg ploughmarks observed in seismic data (Rise et al., 2006; Dowdeswell and Ottesen, 2013;
805 Newton et al., 2016).

806 An alternative view suggests that ice caps in northern and southern Scandinavia behaved differently
807 from 2.58 – 1.1 Ma (Fig. 17a). According to this interpretation, at latitudes higher than the Vøring
808 Plateau, the ice sheet regularly advanced to the palaeo-shelf edge between 2.7 and 1.1 Ma

809 (Rokoengen et al., 1995; Henriksen and Vorren, 1996). Meanwhile, south of the Vøring Plateau, the
810 ice sheet remained limited in size (Rise et al., 2005). Two hypotheses exist for the contrasting
811 response of the Scandinavian Ice Sheet. First, it may have been a consequence of the greater
812 influence of obliquity forcing at higher latitudes (Mangerud et al., 1996). Second, it may have been a
813 consequence of southern Norway being starved of sufficient moisture to build-up a large ice sheet as
814 a consequence of the presence of a British Irish Ice Sheet influencing atmospheric circulation
815 patterns (Thierens et al., 2012).

816 **5.1.1. Sedimentary records of ice sheet and submarine mass movement histories**

817 There is little direct evidence of Scandinavian Ice Sheet expansion from 2.58 – 1.1 Ma on the
818 continental shelf with the exception of iceberg ploughmarks and IRD records from more distal core
819 sites (Montelli et al., 2017a). There is no evidence of submarine mass movements in any ODP core
820 beyond the shelf break which are related to ice sheet sedimentation (Jansen and Raymo, 1996;
821 Jansen et al., 2000). It is therefore suggested that from 2.58 – 1.1 Ma sea level change and the
822 related continental shelf exposure was the dominant control on sedimentation along the West
823 Norwegian Margin (Eidvin et al., 2000; Faleide et al., 2002). In spite of the lack of rapid
824 sedimentation, a large submarine landslide (Slide W; Fig. 18) is inferred to have occurred in the same
825 area as the Storegga Slide complex between 2.7 and 1.7 Ma remobilising an estimated 24,600 km^3 of
826 sediment (Hjelstuen and Andreassen, 2015). The occurrence of this slide does not appear to be
827 directly related to glacial processes although the imprecise dating makes this conclusion uncertain
828 (Solheim et al., 2005a).

829 The alternative model to explain differences in the development of the Scandinavian Ice Sheet
830 between northern and southern Scandinavia is based primarily on poorly constrained dating of
831 different seismic packages along the margin (Rise et al., 2005). According to this interpretation
832 limited ice advances in the south had little influence on sedimentary processes along this part of the
833 margin (Rise et al., 2005; 2010). However, in the north, ice is envisaged to have reached the shelf

834 edge on numerous occasions and to have contributed significantly to sediment wedge progradation,
835 particularly in the Trænabanken/Trænadjupet area (Fig. 19b; Henriksen and Vorren, 1996; Rise et al.,
836 2005; Ottesen et al., 2012; Montelli et al., 2017a).

837 **5.2.1.1 – 0.7 Ma**

838 Large scale intensification of glaciation in the Northern Hemisphere is believed to have started after
839 1.1 Ma (Fig. 17b; Mudelsee and Schulz, 1997; Mudelsee and Stattegger, 1997). The initial climate
840 step towards a longer glacial/interglacial periodicity is marked by the first definitive expansion of the
841 Scandinavian Ice Sheet to the shelf edge along the entire continental margin (Haflidason et al., 1991;
842 Sejrup et al., 1995; 2000; 2005). The extent of this advance is shown by dated till layers (Haflidason
843 et al., 1991) and IRD records on the Vøring Plateau and in the Norwegian Sea (Baumann and Huber,
844 1999; Helmke et al., 2003a; 2005). Following deglaciation the Scandinavian Ice Sheet appears to
845 have reverted to its relatively restricted dimensions exhibited from 2.58 – 1.1 Ma until the abrupt
846 adoption of the 100 kyr climatic cycles (Mudelsee and Schulz, 1997; Mudelsee and Stattegger, 1997).

847 **5.2.1. Sedimentary records of ice sheet and submarine mass movement histories**

848 The extent of the 1.1 Ma Scandinavian Ice Sheet advance is marked by the presence of a nearly
849 continuous till layer across the continental shelf (Sejrup et al., 2004). On the mid-Norwegian shelf
850 the rate of sedimentation increased by ~60% compared to the period from 2.58 – 1.1 Ma as a
851 consequence of the increased glacial influence (Montelli et al., 2017a). The shelf break also migrated
852 seaward by ~50 km from 1.3 – 0.8 Ma although the age of the top surface of this seismic unit is
853 uncertain (Montelli et al., 2017a).

854 On the southern margin of the Scandinavian Ice Sheet analysis of glacial tills in the Troll borehole
855 using amino acid, micropalaeontological and palaeomagnetic analysis has suggested that the 1.1 Ma
856 advance represents initiation of the Norwegian Channel Ice Stream (Haflidason et al., 1991; Sejrup et
857 al., 1995; Berg et al., 2005). The presence of the Norwegian Channel Ice Stream resulted in

858 significant delivery of glacial sediments to the location where the North Sea Trough-Mouth Fan
859 would develop (Fig. 19c; King et al., 1996). However, despite progradation of the proximal fan and
860 the inferred rapid delivery of glacigenic sediment, there are no recognisable debris-flow lobes
861 associated with this advance in the seismic stratigraphy (King et al., 1996; Faleide et al., 2002).
862 Moreover, the chronological control on the initiation of the Norwegian Channel Ice Stream has been
863 challenged, suggesting it may have initiated no earlier than ~0.5 Ma (Ottesen et al., 2014).

864 Despite uncertainty over the initiation of the Norwegian Channel Ice Stream, the presence of
865 Cretaceous chalk IRD at Site MD992277 (Fig. 3) associated with the 1.1 Ma advance indicates the
866 extension of the Scandinavian and British-Irish ice sheets into the North Sea (Helmke et al., 2005).
867 The nearest source of chalk extends from the Britain across the North Sea (Ziegler, 1990), thereby
868 implying a large number of icebergs originated from the North Sea region at this time (Helmke et al.,
869 2003b).

870 Marine sedimentation returned along the continental margin following the retreat of the ice sheet
871 from its maximum extent (Jansen et al., 1988; Haflidason et al., 1991). The marine sediment package
872 is 40 m thick in the Norwegian Channel above the 1.1 Ma till (Sejrup et al., 1996). During subsequent
873 glaciations between 1.1 and 0.7 Ma, it does not appear that the Scandinavian Ice Sheet expanded
874 out onto the continental shelf and thus had little impact on sedimentary processes. Moreover, the
875 sporadic amount of IRD found in marine sequences from this period has been thought to suggest
876 that the ice sheet barely reached the coast (Sejrup et al., 2004; 2005).

877 **5.3.0.7 – 0.13 Ma**

878 The Scandinavian Ice Sheet remained restricted to alpine settings until ~600 ka (Sejrup et al., 2000;
879 Nygård et al., 2005) although there is evidence to suggest an eastward expansion during MIS 16
880 (Velichko et al., 2005; Gozhik et al., 2012; Šeirienė et al., 2015). IRD records from ODP Sites 643 and

644 show major increases in the amplitude of IRD peaks associated with the adoption of the 100 kyr climatic cycle after ~600 ka (Henrich and Baumann, 1994; Mudelsee and Schulz, 1997).

From 0.7 – 0.13 Ma, 5 major advances are envisaged. Of these, four reached the shelf edge (Fig. 17c), while one is thought to have been restricted to the inner shelf (Dahlgren et al., 2002). The four shelf-edge advances are attributed to MIS 14, MIS 12, MIS 10 and MIS 6. Disagreements exist as to the extent of the MIS 8 advance. Some studies suggest that the ice sheet reached the shelf break across most of the continental shelf (Sejrup et al., 2000; Berg et al., 2005; Nygård et al., 2005; Rise et al., 2005; Montelli et al., 2017a). Others suggest that it only reached the mid-shelf (Dahlgren et al., 2002).

The extent of retreat from these glacial maximum positions is equally varied. Reconstructions suggest that Scandinavia was completely deglaciated during MIS 13 (524 – 478 ka BP), MIS 11 (423 – 362 ka BP) and MIS 5e (128 – 115 ka BP) (Henrich and Baumann, 1994; Hjelstuen et al., 2005; Sejrup et al., 2005). This was a consequence of these interglacials being particularly warm (Helmke and Bauch, 2003; Helmke et al., 2003a). In contrast, during MIS 9 (339 – 303 ka BP) and 7 (245 – 186 ka BP) the Scandinavian Ice Sheet only retreated to fjord and alpine settings (Sejrup et al., 2000) as a consequence of these interglacials being significantly cooler than other interglacials from 0.7 Ma to the present (Helmke and Bauch, 2003). These interpretations have been based primarily on IRD, stable isotope records and ocean temperature record reconstructions (Helmke and Bauch, 2003; Helmke et al., 2003a; Kandiano and Bauch, 2003; 2007).

5.3.1. Sedimentary records of ice sheet and submarine mass movement histories

The six advances of the Scandinavian Ice Sheet from 0.7 – 0.13 Ma are reflected in the stratigraphic record of the Norwegian continental shelf and its slope deposits (Figs 19 - 21; Dahlgren et al., 2002; 2005). Until the MIS 14 advance, the continental shelf and slope were dominated by deposition of interbedded hemipelagic and glacimarine sediments reflecting the more restricted position of the

ice sheet at this time (Sejrup et al., 1989, 2004; King et al., 1996; Nygård et al., 2005). From MIS 14 onwards, continental shelf and slope deposition were dominated by glacigenic sediment delivery (Dahlgren et al., 2005; Newton et al., 2016; Montelli et al., 2017a). The change in ice sheet extent at this time is also reflected in the IRD records from the Vøring Plateau and in the Norwegian Basin; larger amounts of IRD from the Scandinavian Ice Sheet penetrating further westward (Krissek, 1989; Helmke et al., 2003b).

As far south as the Møre Shelf (Fig. 16), the MIS 14 advance is marked by the presence of a structureless diamicton along the outer shelf (Fig. 20a; Dahlgren et al., 2002). Beyond the shelf edge, seismic stratigraphy and ODP core records indicate that glacigenic debris-flows were the dominant process by which sediment was re-worked (Talwani et al., 1976; Dahlgren et al., 2002). In contrast, there is no evidence of an ice advance onto the continental shelf in southwestern Norway at this time (Helmke et al., 2003a; Hjelstuen et al., 2005). This may be a consequence of later reworking of sediment. However, it is unlikely that an advance in this area during MIS 14 was as significant for sediment delivery as later advances.

The more extensive MIS 12 advance is marked by a diamicton on the shelf along most of the Norwegian Margin (Fig. 20; Sejrup et al., 2000; Nygård et al., 2005). Beyond the continental shelf, the sedimentation history is more varied. The outer Møre shelf and the continental slope beyond is characterised by marine/glacimarine deposition (Fig 20; STRATAGEM, 2002; Nygård et al., 2005). In the Møre shelf region, seismic stratigraphy suggests that this unit has primarily infilled the areas between the MIS 14 advance depositional lobes and that the volume of deposited MIS 12 glacimarine sediment may have been greater than that deposited during MIS 14 (Dahlgren et al., 2002). Further south, the North Sea Trough-Mouth Fan underwent a major constructional phase (Fig. 21). It is estimated that the Norwegian Channel Ice Stream delivered as much as 3000 km^3 of sediment during this glacial, the majority of which was remobilised as glacigenic debris-flows (King et al., 1996; Nygård et al., 2005). However, following deglaciation the Møre Submarine Landslide (400 –

930 380 ka BP) is estimated to have reworked 1200 km^3 of this sediment (Figs 20b and 21; King et al.,
931 1996; Nygård et al., 2005; Hjelstuen et al., 2007). The coincidence of high sedimentation rates on the
932 North Sea Trough-Mouth Fan and the occurrence of the Møre Slide strongly implicates high
933 sedimentation as having a role in the triggering of the slide. Crucially, it has also been suggested that
934 the preceding period was dominated by meltwater and contourite deposition in the area of the fan
935 (Batchelor et al., 2017) thus allowing for the development of weak layers previously suggested to
936 have been responsible for mass failures on the Storfjorden Trough-Mouth Fan (Rebesco et al., 2012;
937 Lucchi et al., 2013; Llopart et al., 2015).

938 On the mid-Norwegian shelf MIS 10 and MIS 8 are characterised by diamicton on the shelf (Fig. 17a;
939 Rise et al., 2005). Beyond the shelf edge seismic data reveals large stacked glacigenic debris-flow
940 lobes and stacked glacigenic debris-flow lenses, related to strong glacial erosion of the shelf (Nygård
941 et al., 2003; Rise et al., 2005; Ottesen et al., 2009; Rydningen et al., 2016). As a consequence of
942 poorly constrained dating of different seismic facies, it is not clear what thickness of sediment is
943 related to the MIS 10 advance and what thickness is related to the MIS 8 advance (Dahlgren et al.,
944 2002; Rise et al., 2005).

945 In contrast to the mid-Norwegian shelf, MIS 10 and 8 can be clearly differentiated on the
946 southwestern part of the margin. Two distinct glacigenic till units were deposited on the South
947 Vøring Margin and North Sea Margin associated with these two glacials (Figs 20, 21b-d; King et al.,
948 1996; Haflidason et al., 1998). The MIS 10 and 8 advances are estimated to have delivered
949 approximately 2600 and 3500 km^3 of sediment to the North Sea Trough-Mouth Fan respectively
950 (Nygård et al., 2005). Once deposited by the ice at the shelf edge the MIS 10 glacigenic sediment was
951 remobilised and emplaced down the fan by glacigenic debris-flows (King et al., 1996; Sejrup et al.,
952 2004; 2005; Solheim et al., 2005a). In contrast, the initial phase of MIS 8 deposition (~2100 km^3) was
953 characterised by a combination of glacimarine, marine and gravity-flow processes as a consequence
954 of ice terminating inshore of the shelf edge (Dahlgren et al., 2002; Sejrup et al., 2004). The second

phase of deposition (~1400 km^3) was dominated by glacigenic debris-flow emplacement and is thought to represent the period when ice was at the shelf edge of the Norwegian Channel (Sejrup et al., 2004; Nygård et al., 2005).

Two large submarine landslides also occurred during MIS 8. On the South Vøring Margin, the Sklinnadjupet Landslide (Fig. 18) is inferred to have occurred ~300 ka BP, the headwall of the slide being based at the mouth of the Sklinnadjupet Trough (Dahlgren et al., 2002; Solheim et al., 2005a; Hjelstuen et al., 2007). Further to the south at the mouth of Frøyabankhola Trough, the R Landslide is also inferred to have occurred ~300 ka BP (Sejrup et al., 2005). The probable role of high sediment delivery by ice streams in the triggering of large submarine landslides is shown by the close association of the Sklinnadjupet and R Slides with cross-shelf troughs.

The sedimentary deposits from the mid-Norwegian shelf suggests that the Saalian ice sheet (MIS 6) did not reach the shelf edge (Fig. 22b; Rokoengen et al., 1995; Rise et al., 2005). Glacigenic sediments composed of laterally stacked 'till tongues', up to 200 m thick, were deposited on the outer part of the shelf and are inferred to be the result of ice streams flowing out between Haltenbanken and Trænabanken (Fig. 22b; Rise et al., 2005). Further south, the Saalian ice sheet did reach the shelf edge. An extensive till layer is found from the South Vøring Margin to the northern North Sea Margin (Fig. 20; Sejrup et al., 2004; 2005). Sediment deposited at the shelf edge along these margins has been predominantly reworked by glacigenic debris-flows (Sejrup et al., 2004; Batchelor et al., 2017). During this glacial, it is estimated that 2600 km^3 of sediment was deposited on the North Sea Trough-Mouth Fan, the majority being reworked by glacigenic debris-flows (King et al., 1996; Nygård et al., 2005). Large amounts of material were also supplied to the area where the Storegga Slide subsequently occurred (Rise et al., 2005). Estimating the volume of sediment delivered to this margin by the Saalian ice sheet is, however, problematic. This is a consequence of the Tampen and Storegga Slides evacuating large volumes of material into the Norwegian Basin (Haflidason et al., 2005; Paull et al., 2007). The Tampen Slide was originally thought to have occurred

on the North Sea Trough-Mouth Fan at ~130 ka BP, after the retreat of the Saalian ice sheet (Bryn et al., 2003; Bryn et al., 2005; Solheim et al., 2005a), but this date has large uncertainties.

The ice sheet chronology and the associated sedimentary processes that have been described in this section portray a simple pattern of advance, deposition and reworking of sediment, followed by retreat of the ice sheet. This is, however, likely to be a simplification of the actual chronology. Reconstructions of ice sheet histories in the Weichselian (see following section) show the ice sheet to have undergone multiple advances and retreats during a single glaciation. It is therefore likely that diamict and glacigenic debris-flow units which encompass a single glacial cycle could in the future be subdivided to reflect multiple ice sheet fluctuations within one glacial (Dahlgren et al., 2002). This will require higher resolution seismic stratigraphies of the continental shelf and slope combined with higher resolution dating of marine sediments.

5.4.0.13 – 0 Ma (Weichselian – Present)

As was demonstrated for the Svalbard/Barents Sea region, the higher temporal resolution and more complete records allow us to identify multiple advance and retreat cycles of the Scandinavian Ice Sheet during the Weichselian (Sejrup et al., 2000; Svendsen et al., 2004a; Hughes et al., 2016).

Two advances are proposed during the Early Weichselian. Increased rates of IRD deposition around the Norwegian Sea show the earliest advance to have occurred during MIS 5d (Baumann et al., 1995; Fronval and Jansen, 1997; Rasmussen et al., 2003). From marine sediment records glacial ice is believed to have expanded sufficiently to reach the coast and its fjords during this period (Sejrup et al., 2004; Lekens et al., 2009). Ice retreated inland during MIS 5c before expanding to reach the outer coastline during MIS 5b. Ice again retreated inland during MIS 5a (Hjelstuen et al., 2005).

The first ice sheet expansion to the shelf edge occurred during MIS 4. During this period ice is hypothesised to have reached the shelf edge between 70 and 60 ka BP (Mangerud, 1991). MIS 3 was predominantly characterised by ice sheet retreat into western Norwegian fjords (Baumann et al.,

1004 1995). A minor readvance, the Jæren-Skjonghelleren has been proposed at ~42 cal ka BP (Mangerud
1005 et al., 2003; Sejrup et al., 2003; Lambeck et al., 2010). This advance is tentatively proposed to have
1006 extended beyond the western Norwegian coastline before retreating by 37 cal ka BP (Sejrup et al.,
1007 2000). The exact extent of this retreat along the margin is uncertain; however, the minimum retreat
1008 scenario suggests that the ice sheet receded to the heads of the Norwegian fjords (Mangerud, 1991,
1009 2004; Svendsen et al., 2004a).

1010 Records of the MIS 2 Scandinavian Ice Sheet vary depending on location (Fig. 17d). In northern
1011 Norway, in the Andfjorden area, the ice sheet is hypothesised to have expanded from 34 cal ka BP
1012 (Vorren and Plassen, 2002), reaching the shelf edge from 24 – 23 cal ka BP. A retreat of up to 100 km
1013 occurred between 22 and 20 cal ka BP (Vorren and Plassen, 2002). It then readvanced and was
1014 present at the shelf edge from 16 – 14 cal ka BP before retreating. The remainder of the Late
1015 Weichselian was characterised by retreat, stillstands and minor readvances (Vorren and Plassen,
1016 2002; Dahlgren and Vorren, 2003).

1017 In mid-Norway reconstruction of the Late Weichselian ice sheet is highly dependent on the type of
1018 record used. Solely based on terrestrial data, the main expansion to the shelf edge is interpreted to
1019 have begun at ~24 cal ka BP, ice reaching the shelf edge at 23.5 cal ka BP (Olsen et al., 2001a;
1020 2001b). Limited advances had occurred previously between 34 – 32 and 30 – 28 cal ka BP (Olsen et
1021 al., 2001b). Terrestrial records suggest the ice retreated from the shelf edge after 23 cal ka BP, which
1022 was followed by a short re-advance after 18 cal ka BP until 16 cal ka BP (Olsen et al., 2001a; Dahlgren
1023 and Vorren, 2003). Using marine records (IRD and continental slope deposits) the ice sheet in mid-
1024 Norway is interpreted to have advanced to, and retreated from, the shelf edge four times between
1025 21 – 16 cal ka BP (Dahlgren and Vorren, 2003); a retreat occurring, on average, every 2 ka. The
1026 marine records suggest that the ice retreated from the shelf edge for the last time at ~16 cal ka BP
1027 (Dahlgren and Vorren, 2003).

The glacial history of the Late Weichselian Scandinavian Ice Sheet in southwest Scandinavia is the best constrained in terms of chronology due to the numerous studies focussing on the Storegga Slide (Sejrup et al., 1996; 2000; Bryn et al., 2003; Haflidason et al., 2005; Hjelstuen et al., 2005). The ice sheet is interpreted to have expanded from 30 ka BP in this sector and to have reached its first glacial maximum as early as 29 – 27 ka BP (Larsen et al., 2009; Svendsen et al., 2015), remaining on the shelf edge until 23 cal ka BP (Sejrup et al., 1994). Following a retreat from the shelf edge, the ice sheet subsequently readvanced to the shelf edge along the south western Norwegian margin from ~19 – ~15 ka BP after which it retreated. The ice sheet did not, however, advance to the shelf edge of the Norwegian Channel and thus the Norwegian Channel Ice Stream was not present at the shelf edge at this time (Sejrup et al., 2000; Sejrup et al., 2003; Hjelstuen et al., 2005; Svendsen et al., 2015). A more detailed history of the retreat is available from Hughes et al. (2016).

5.4.1. Sedimentary records of ice sheet and submarine mass movement histories

The record of associated ice sheet sedimentary processes is highly variable along the continental margin of Scandinavia. The completeness of the record and the precision with which it has been dated increases from north to south.

5.4.1.1. North Norwegian continental shelf

The record of Weichselian sedimentary deposits is least well understood along the northern margin (Lofoten – Vesterålen) of Norway and only extends back to MIS 3 (Fig. 16). Here, seismic and swath bathymetric mapping of the continental shelf and slope reveal mega-scale glacial lineations indicating the presence of former areas of fast flowing ice (Ottesen et al., 2005). However, the thickness of glacigenic sediment deposited on the shelf and upper continental slope is limited (Brendryen et al., 2015; Rydningen et al., 2016). This is thought to be a consequence of relatively small ice stream catchment areas limiting sediment transport volumes (Brendryen et al., 2015; Rydningen et al., 2016) and effective downslope transport of sediment via gullies and canyons on

1052 the continental slope (Baeten et al., 2013; Rise et al., 2013). The number and size of submarine
1053 canyons in this sector is unique along the Norwegian Margin (Rise et al., 2012; 2013). Moreover, the
1054 Andøya Canyon and Lofoten Channel are the only canyon and channel systems of comparable size to
1055 the Greenland Submarine Channel system (Ó Cofaigh et al., 2006).

1056 The earliest dated sedimentary deposits on the Lofoten – Vesterålen margin correspond to the
1057 hypothesised 34 cal ka BP ice sheet expansion (Vorren and Plassen, 2002). Glacigenic debris-flow
1058 deposits and a plumite deposit (dated to 29.3 ± 0.095 cal ka BP) characterise this advance on the
1059 continental slope (Brendryen et al., 2015). The combination of these deposits suggest that the ice
1060 sheet was present at the shelf edge prior to 29.3 ± 0.095 cal ka BP before undergoing a major
1061 retreat. Subsequent glacigenic debris-flow deposits, indicative of ice at the shelf edge, are dated to
1062 18.5, 23 and between 25 and 25.7 cal ka BP (Baeten et al., 2014; Brendryen et al., 2015). Between
1063 these deposits, several laminated units interpreted as plumites were deposited (Brendryen et al.,
1064 2015). On top of the last glacigenic debris-flow deposits, finely-laminated units and finely-laminated
1065 dropstone muds were deposited; the former interpreted to be a plumite (Vorren and Plassen, 2002),
1066 the later, deposits beneath an ice shelf (Brendryen et al., 2015).

1067 Beyond the shelf edge, submarine landslide headscars are also visible on bathymetry. The largest is
1068 the Andøya Slide headwall. Located to the north of the Andøya Canyon, the Andøya Slide covers
1069 ~9,700 km^2 with a run-out distance of ~190 km (Laberg et al., 2000). Further south, slide scars from
1070 landslides containing between 0.061 and 8.7 km^3 of sediment have also been mapped (Baeten et al.,
1071 2013). These landslides are interpreted to be of Holocene age due to a lack of sediment drape and
1072 rugged seafloor relief (Laberg et al., 2000; Baeten et al., 2013). However, more accurate dates are
1073 yet to be obtained. Baeten et al. (2013; 2014) postulate that earthquakes were the likely cause of
1074 these failures.

1075 *Mid-Norwegian Shelf*

Studies of the mid-Norwegian Shelf and slope have identified two types of deposits associated with the Weichselian glacial. The MIS 5 and 4 advances are associated with two sets of laminated seismic facies on the continental slope (Henrich and Baumann, 1994; Dahlgren and Vorren, 2003). The MIS 5 sediment package is thickest on the lower to mid-slope and is ~30 m thick (Dahlgren and Vorren, 2003). The MIS 4 deposits are up to 70 m thick and thickest on the southern side of the Sklinnadjupet Slide scar (Dahlgren et al., 2002; Dahlgren and Vorren, 2003). Both deposits are thought to have been emplaced within 10 ka and correspond to marine and glacimarine deposition reflecting a more withdrawn ice sheet position.

In contrast to earlier advances, the MIS 2 ice sheet is thought to have extended to the shelf edge along the entire mid-Norwegian Shelf (Ottesen et al., 2001; Taylor et al., 2002b). Two continental shelf till units can be recognised. These structureless grey diamictons terminate in sediment wedges at the shelf edge (Dahlgren and Vorren, 2003). According to conservative age estimates of ice sheet activity along this margin the till layers were deposited from 25.9 – 19.4 cal ka BP (Olsen et al., 2001b; Dahlgren and Vorren, 2003). This advance is associated with glacigenic debris-flow emplacement on the continental slope (Dahlgren et al., 2002). It has, however, been suggested from IRD records that these till layers may in fact represent up to four advances to the shelf edge between ~27 ± 0.1 cal ka BP and ~18.8 ± 0.04 cal ka BP (Dokken and Jansen, 1999; Dahlgren and Vorren, 2003). In contrast to other parts of the Norwegian Margin, ice sheet retreat is not associated with plumite deposition (Hjelstuen et al., 2004; 2005).

The preservation of these till layers and glacigenic debris-flows varies from north to south. In the north these sediments have been removed by successive submarine landslides (Fig. 22c; Laberg and Vorren, 2000; Laberg et al., 2003). Two large submarine landslides have been identified beyond the mouth of the Trænadjupet Trough. The Nyk Slide affects an area of 4,000 – 6,000 km^2 and contained an estimated 400 – 720 km^3 of material (Lindberg et al., 2004; Allin et al., in review). The slide is dated from 21.8 – 19.3 cal ka BP (Allin et al., in review). The Trænadjupet Slide affected an area of

4,000 – 5,000 km^2 and contained an estimated 500 – 700 km^3 of material (Laberg and Vorren, 2000; Laberg et al., 2002a). The Trænadjupet Slide is dated from 3.5 – 2.8 cal ka BP (Allin et al., in review). The relationship between the timing of these slides and the local sedimentation patterns is significantly different. The Nyk Slide occurred after a period of glacigenic debris-flow emplacement on the continental slope beyond the Trænadjupet Trough when sedimentation rates were as high as 4 m/ka showing the possible role that high sedimentation rates had in triggering the landslide (Baeten et al., 2014; Brendryen et al., 2015). The Trænadjupet Slide occurred ~10 ka after ice retreat from the shelf edge when sedimentation rates were reduced to only a few cm/ka (Baeten et al., 2014). Thus if high sedimentation rates had a role in triggering the Trænadjupet Slide, failure occurred after a substantial delay; eventual slope failure probably resulting from an additional triggering mechanism.

South Vøring Margin

Little evidence has yet been found that ice reached the shelf break along the South Vøring Margin before the MIS 2 glaciation (Hjelstuen et al., 2005; Hughes et al., 2016). Instead sedimentation is dominated by marine and glacimarine processes (King et al., 1996; Nygård et al., 2005). Three separate glacigenic units, envisaged to be glacigenic debris-flows, have been identified from MIS 2 (Solheim et al., 2005a). These units are interpreted to have been deposited at ~24.8 ± 0.07, 19 ± 0.05, 18.6 ± 0.06 cal ka BP (Hjelstuen et al., 2005). They are separated by laminated sequences reflecting a more restricted extent of the ice sheet.

Thin and restricted to the uppermost continental slope, till and debris-flow units on the South Vøring Margin suggest slow rates of sediment delivery during MIS 2. In contrast, the rate of hemipelagic and glacimarine sedimentation which covered the limited glacial deposits was extremely rapid (Hjelstuen et al., 2005). Three periods of plumite deposition are hypothesised; 21.5 – 19.7 cal ka BP, 18.6 – 18.3 cal ka BP and a less northerly extensive period from 18.3 – 18.0 cal ka BP (Fig. 23; Lekens et al., 2005; 2009). During the deposition of these deposits it has been calculated that the sedimentation rate

over this part of the margin was 1250 cm/ka and was as much as 1750 cm/ka (Lekens et al., 2005). The source of these sediments is inferred to be the Norwegian Channel Ice Stream (Hjelstuen et al., 2004). The greater rate of sediment accumulation in the Storegga Slide area and the South Vøring Margin is hypothesised to be related to slope parallel currents moving suspended sediment northwards from the North Sea Margin.

North Sea Margin

Weichselian sedimentation along the North Sea Margin is dominated by emplacement of diamict layers on the continental shelf and glacigenic debris-flow deposits beyond the shelf edge (Sejrup et al., 2003; Hjelstuen et al., 2005). With the exception of the MIS 2 advance of the Scandinavian Ice Sheet, there is a large amount of uncertainty concerning the extent of the earlier advances. Some authors suggest that there is little/no evidence of an ice advance to the shelf edge in the Norwegian Channel before 28 ka BP (Hjelstuen et al., 2005; Nygård et al., 2005; 2007). According to this interpretation sedimentation up until 28 ka BP was dominated by marine and glacimarine processes. Other studies have suggested that multiple till units exist and are linked to advances during the Karmøy Stadial (~85 to 70 ka BP) and the Skjonghelleren Stadial (~50 to 36 ka BP) (Sejrup et al., 1995; 2003; 2004). These till layers can be traced beyond the shelf break in the form of glacigenic debris-flow deposits on the upper slope (Sejrup et al., 2003).

If it is assumed that ice only reached the shelf edge during MIS 2, 4 oscillations of the ice front are envisaged, although the Norwegian Channel Ice Stream was only present at the shelf edge during the earliest advance from after 30 cal ka BP to 23 cal ka BP (Sejrup et al., 1994; Nygård et al., 2005). Three sequences of glacigenic debris-flow deposits are associated with this advance on the North Sea Trough-Mouth Fan (Fig. 20). Each debris-flow sequence is separated by a phase of hemipelagic deposition (Lekens et al., 2009). Individual debris-flows from this period can be mapped out as far as 500 km from the shelf edge (King et al., 1998). The volume of sediment accumulated on the fan

during this period is estimated to be up to ~5,300 km^3 (Nygård et al., 2005) out of a total of ~5,800 km^3 deposited during the entire Weichselian (Nygård et al., 2005).

Following the retreat of the Norwegian Channel Ice Stream at ~23 cal ka BP, the North Sea Trough-Mouth Fan was dominated by marine and glacimarine deposition (Fig. 23; Lekens et al., 2005). However, sedimentation rates were an order of magnitude lower compared to the Storegga and South Vøring areas. From 19 – 18 cal ka BP, plumite sedimentation rates were ~60 cm/ka. From 18 – 17 cal ka BP, plumite sedimentation rates were ~30 cm/ka. This rose to ~40 cm/ka until 14.5 cal ka BP before returning to normal sedimentation rates of <10 cm/ka (Sejrup et al., 2000; Lekens et al., 2005; 2009).

During the Weichselian two large submarine landslides are known to have occurred in this region (Fig. 18). The earlier slide, the Tampen Slide, has been dated to ~130 ka BP (Nygard et al., 2005), but this date is uncertain as it uses sedimentation rates. The headwall of this slide is found on the North Sea Trough-Mouth Fan (Figs 20b and 21j). The timing of this slide relative to Norwegian Channel Ice Stream activity is uncertain. If the ice stream is assumed to have reached the shelf edge repeatedly during the Weichselian then the slide occurred after the ice stream retreated from the shelf edge at the end of MIS 4. If correct a large volume of material was likely advected to the shelf edge and subsequently remobilised with large volumes of North Sea Trough-Mouth Fan Saalian deposits as part of this slide. If the ice stream is assumed not to have reached the shelf edge until MIS 2/3 then the slide occurred as a consequence of relatively little deposition of material on the trough-mouth fan. In this scenario, the majority of evacuated sediments were derived from the Saalian glaciation.

The Storegga Slide occurred north of the North Sea Trough-Mouth Fan ~8,200 BP (Haflidason et al., 2005). The slide evacuated an estimated 3,000 km^3 of sediment and affected an area of 95,000 km^2 (Haflidason et al., 2004). The Storegga Slide occurred significantly (6 ka) after the period of high sedimentation had finished. Within the Storegga Slide escarpment additional slides have been identified and dated to 5.7 cal ka BP and 2.8 – 2.2 cal ka BP (Haflidason et al., 2005; Lekens et al.,

2009). The Storegga Slide is thought to have been triggered by the sediment load from the preceding glaciation and an earthquake resulting from glacio-isostatic rebound initiating failure of marine clays (the Brygge Formation) (Bryn et al., 2005). Following this initial failure, the toe support for sediments further up the continental slope was removed resulting in a retrogressive failure propagating towards the continental shelf along the glide plane provided by marine clay layers (Bryn et al., 2003; 2005; Haflidason et al., 2003; 2004; Kvalstad et al., 2005).

The history of the Scandinavian Ice Sheet and the related sedimentation processes are summarised in Table 4 and Fig. 9c.

6. How do the continental margins of the Nordic Seas compare with other glaciated margins?

The previous sections outlined the evolution of the continental margins of the Nordic Seas with respect to the histories of three ice sheets. The following section will discuss observed similarities and differences of processes observed on a range of other glaciated continental margins. The margins we have chosen to include in this comparison reflect the range of environments outlined in the continuum of glacier-influenced settings in Fig. 1.

6.1. Antarctic continental margin

The continental margins of Antarctica have the coldest climate and should therefore be the least influenced by meltwater processes. Many of the morphological features identified on the margins of the Nordic Seas are also present on the Antarctic continental margin. Bathymetric, seismic and sedimentological studies have all identified the presence of trough-mouth fans, submarine channels, gullies and landslides (Kuvaas and Leitchenkov, 1992; Dowdeswell et al., 2008; Amblas and Canals, 2016; Canals et al., 2016; Gales et al., 2016; and references therein). However, there are significant differences in the morphologies of these features, their relative numbers and the relative timescales over which different sedimentation processes operate.

6.1.1. Antarctic trough-mouth fans

1199 Antarctica has been glaciated for ~34 Ma (Zachos et al., 2001). However, despite the extended
1200 period over which glacial processes have operated compared with other regions and the number of
1201 cross-shelf troughs that have been identified there are relatively few trough-mouth fans (Ó Cofaigh
1202 et al., 2003). Nonetheless, three large trough-mouth fans have been recognised; the Crary Trough-
1203 Mouth Fan in the Weddell Sea (Kuvaas and Kristoffersen, 1991), the Prydz Bay Trough-Mouth Fan
1204 offshore of the Lambert-Amery glacial system in East Antarctica (Kuvaas and Leitchenkov, 1992), and
1205 the Belgica Trough-Mouth Fan in the Bellingshausen Sea (Dowdeswell et al., 2008).

1206 Of these trough-mouth fans, the morphology and inferred processes of the Belgica Trough-Mouth
1207 Fan most clearly resemble those outlined on Nordic Sea trough-mouth fans (Fig. 24a). It covers an
1208 estimated area of at least 22,000 km^2 and contains ~60,000 km^3 of sediment that has accumulated
1209 over the past 5.3 Ma (Scheuer et al., 2006; Dowdeswell et al., 2008). Compared to the Nordic Sea
1210 trough-mouth fans it therefore falls between Storfjorden and Scoresby Sund (115,000 and 15,000
1211 km^3 respectively) in terms of volume despite having a palaeo-drainage basin under full-glacial
1212 conditions an order of magnitude greater (200,000 km^2 vs 60,000 km^2) than either of the Nordic Sea
1213 systems (Vorren et al., 1998; Ó Cofaigh et al., 2005; Håkansson et al., 2007). As seen in the Nordic
1214 Seas, seismic stratigraphic analysis of the Belgica Trough-Mouth Fan reveals semi-transparent lenses
1215 interpreted to be glacigenic debris-flow deposits (Ó Cofaigh et al., 2005; Hillenbrand et al., 2010).
1216 Gully and channel systems have been cut into the emplaced deposits (Fig. 24a; Dowdeswell et al.,
1217 2008). As seen on some trough-mouth fans in the Nordic Seas the density of these features is
1218 highest at the margins of the Belgica Trough-Mouth Fan. However, the depth of incision, downslope
1219 extent beyond the lower slope and presence across the entire width of the fan contrasts strongly
1220 with systems in the Nordic Seas whose gully systems are much less well developed and generally
1221 confined to the upper slopes (Dowdeswell et al., 2008; Pedrosa et al., 2011; Lucchi et al., 2013;
1222 Llopart et al., 2015). This may be a consequence of more sustained periods of brine rejection and
1223 cold water cascading off of the continental shelf (Ivanov et al., 2004). Also unlike the largest fans in
1224 the Nordic Seas, there is no evidence of major slides or other mass wasting (Nitsche et al., 1997;

1225 Dowdeswell et al., 2008). Unfortunately, no chronologic information is available to date the timing
1226 of debris-flow emplacement and channel incision.

1227 The Prydz Bay Trough-Mouth Fan is the best understood of the Antarctic trough-mouth fans (Fig.
1228 24c). Its development can be divided into three phases. Phase 1 lasted from the Late Miocene (ca. 7
1229 Ma) until 1.1 Ma. During this period the Lambert Glacier advanced to the shelf edge, depositing
1230 diamictons which were subsequently reworked by glacigenic debris-flows (Kuvaas and Leitchenkov,
1231 1992; O'brien and Harris, 1996; Passchier et al., 2003; O'Brien et al., 2007). The volumes of these
1232 flows were much lower than those seen on the Bear Island and North Sea Trough-Mouth Fans
1233 (O'brien and Harris, 1996). These deposits were interbedded with contouritic sediments and
1234 turbidites (Passchier et al., 2003). During Phase 2 (1.1 – 0.78 Ma), glacial sediment input decreased
1235 leading to a reduction in the number and thickness of glacigenic debris-flows (O'Brien et al., 2007).
1236 Phase 3 (0.78 Ma – present), coinciding with the adoption of 100 kyr climate cyclicity, was
1237 characterised by a cessation of debris-flow activity and a growing dominance of glacimarine
1238 deposition as the Lambert Glacier failed to reach the shelf edge (Passchier et al., 2003). No evidence
1239 has yet been found for large scale mass failures (Kuvaas and Leitchenkov, 1992). The volume of
1240 sediment which accumulated during the construction of the Prydz Bay Trough-Mouth Fan is
1241 comparatively small (27,740 km^3) when the drainage area (3.5 x 10^5 km^2) of the Lambert Glacier
1242 under full glacial conditions is considered (Denton and Hughes, 2002).

1243 The Crary-Weddell Sea Fan system of which the Crary Tough-Mouth Fan is part covers an estimated
1244 area of 750,000 km^2 (Anderson et al., 1986). Initiation of the fan began ~34 Ma but unlike other
1245 trough-mouth fans has been dominated by the presence of large channel-levee complexes (Kuvaas
1246 and Kristoffersen, 1991). Three channel-levee complexes have existed during the last 34 Ma (Fig.
1247 24b). They are hypothesised as being a result of brine rejection eroding channels during interglacials
1248 and depositing winnowed fine sediments from the upper slope and shelf on the levees (Kuvaas and
1249 Kristoffersen, 1991). During glacials, glacial meltwater transport of sediment, turbidity currents and

downslope evolving submarine slumps and debris-flows result in enhanced channel-levee activity and fan progradation (Kuvaas and Kristoffersen, 1991; Melles and Kuhn, 1993). Dating of material from the levee complexes supports this hypothesis; deposition on the levees in water depths of 2000 – 3000 m ranged from 100 – 200 cm/kyr during the last glacial and has only been a few cm/kyr during the Holocene (Weber et al., 1994). Glacigenic debris-flows and submarine landslides have also been identified (Melles and Kuhn, 1993; Gales et al., 2016). Larger submarine landslides have also been suggested to have occurred on the Crary Trough-Mouth Fan during the Early Pleistocene during the drawdown of East Antarctica (Bart et al., 1999).

6.1.2. Antarctic gullies and submarine channels

A large proportion of the mapped Antarctic Margin is dominated by gullies and channel systems and therefore bears a greater similarity to the East Greenland Margin than the Norwegian Margin. The Antarctic gullies and channels are, however, more numerous and permanent features.

Gullies have been found incised into trough-mouth fans (e.g. the Crary Trough-Mouth Fan) and the continental slope in front and between cross-shelf troughs (Ó Cofaigh et al., 2003; Dowdeswell et al., 2004; 2006a; Heroy and Anderson, 2005; Wellner et al., 2006; Gales et al., 2013; 2014). Depending on their location, gully formation has been linked to different processes. Along parts of the Antarctic Margin, gully formation is hypothesised to be a consequence of cold-dense water cascading down the continental slope through brine rejection (Noormets et al., 2009). Many, however, are hypothesised to be a consequence of turbidity current activity, sediment-laden subglacial meltwater discharge or small-scale mass failures (Dowdeswell et al., 2006a; Gales et al., 2016). In many cases gullies feed channel systems or coalesce to form channels themselves further down the continental slope.

Extensive channel networks have been found offshore of the continental shelf around most of the Antarctic Margin (Rebesco et al., 1996; 2002; De Santis et al., 2003; Dowdeswell et al., 2006a;

Hillenbrand et al., 2008). Offshore of the Antarctic Peninsula, dendritic canyon-channel systems are found at the mouths of cross-shelf troughs (Amblas et al., 2006; Amblas and Canals, 2016). These systems are a consequence of intense turbidity current activity which occurs due to ice at the shelf edge delivering large amounts of sediment and, subglacial meltwater, as well as the relatively steep continental slope favouring turbidity current formation (Pudsey and Camerlenghi, 1998; Dowdeswell et al., 2004). Sediment mounds are found between these channels as a consequence of bottom current reworking and deposition of sediment (Amblas et al., 2006).

Other extensive channel/submarine canyon and related submarine fan systems have been found on the Wilkes Land Margin (130 – 145°E) and Queen Maud Land (12 – 18°W) (Escutia et al., 2000; Busetti et al., 2003; De Santis et al., 2003; Ó Cofaigh et al., 2003). The presence and morphology of these systems are thought to be the result of multiple factors and reflect the dynamic evolution of the Antarctic Ice Sheet with changing climate in this sector (Donda et al., 2007). During the Early – Late Miocene (23.03 – 5.333 Ma), the meltwater derived from a highly dynamic temperate Antarctic Ice Sheet delivered large amounts of sediment to the shelf edge. The high sedimentation rate led to the triggering of submarine mass movements (probably turbidity currents) which led in turn to the development of high-relief channel-levee complexes (Donda et al., 2007). Since the end of the Miocene, climatic deterioration has led to a less dynamic ice sheet (Rebesco and Camerlenghi, 2008). As a result the ice streams feeding these systems are relatively small, frequently migrate and deliver insufficient volumes of sediment when at the shelf edge to build a trough-mouth fan (Cooper et al., 1991; Escutia et al., 2000; 2005). The proportionally larger volumes of coarse sediment delivered to the top of these systems by ice streams is also thought to be partially responsible for their steep upper and mid- slopes when compared to similar fluvial systems (Escutia et al., 2000; 2003).

6.1.3. Antarctic submarine landslides

When compared to the margins of the Nordic Seas, the Antarctic continental margin is notable for its lack of submarine landslides. Exceptions exist, the Gebra Slide on the Antarctic Peninsula margin contains ~21 km^3 of sediment (Imbo et al., 2003; Canals et al., 2004; 2016) and slides have been identified on the Crary Trough-Mouth Fan (Gales et al., 2014; 2016). The Gebra Slide and the recurrence of large mass movements in this area are thought to result from enhanced sediment delivery associated with the onset of 100 kyr climate cyclicity and the extension of the Laclavere, Mott Snowfield and D'Urville ice streams to the shelf edge (García et al., 2008; 2009). The failure of deposited glacial sediments is thought to result from a strong earthquake associated with tectonic activity of a half-graben and related structures, or volcanic activity and changes in the slope profile related to the opening of the Central Bransfield Basin (Casas et al., 2013). It is thought that interglacial sediments, muddy turbidites and hemipelagites, acted as weak layers and glide planes (García et al., 2011; Casas et al., 2013). The Crary Trough-Mouth Fan slides are also thought to be a consequence of the presence of weak layers which are susceptible to liquefaction under loading (Long et al., 2003). These layers are thought to result from dense bottom water formation on the Southern Weddell Sea Shelf which deposits winnowed fines on the continental slope as it forms cascading bottom flows (Melles and Kuhn, 1993; Weber et al., 2011). Actual slope failure may result from rapid sedimentation or an earthquake.

There is as yet little evidence of frequent mass wasting events around Antarctica with volumes comparable to the Storegga or Trænadjupet Slides, despite the clear contrasts in sediment package characteristics that would be deposited by glacial and contouritic processes that operate around Antarctica (Kuvaas et al., 2005; Gales et al., 2014).

6.2. East Canadian Margin

The continental margin of East Canada was the location of the furthest eastern extension of the Laurentide Ice Sheet (Fig. 25). Running from ~40 – 76°N, the East Canadian Margin has features similar to those seen on other glaciated margins but also exhibits features indicative of greater

meltwater influence. This could be a consequence of either the lower latitude of the southern part of the margin or of the internal dynamics of the Laurentide Ice Sheet (Bond et al., 1992; Piper, 2005).

6.2.1. East Canadian trough-mouth fans

Trough-mouth fans have been identified along the entire East Canadian Margin (Aksu and Hiscott, 1989; Piper, 2005; Tripsanas and Piper, 2008a; Li et al., 2011). However, their morphology changes with latitude. At the northern end of the East Canadian Margin, trough-mouth fans have similar architectures and sedimentation regimes to those described on the Svalbard/Barents Sea continental margin. For example, the depositional systems operating on Lancaster Sound and Trinity Trough-Mouth Fan are dominated by the emplacement of glacigenic debris-flow units (Fig. 26; Piper and McCall, 2003; Tripsanas and Piper, 2008a; Li et al., 2011). Originating from till wedges higher on the continental slope, glacigenic debris-flow emplacement is responsible for the majority of progradation of these fans during glacial periods (Piper, 2005).

Further south, the Laurentian and Northeast Trough-Mouth Fans have very different morphologies and thus different sedimentation histories (Mosher et al., 2017). Both trough-mouth fans are dominated by large channel-levee systems (Hughes Clarke et al., 1992; Piper et al., 2016). Seismic profiles across both fans shows that similar channel systems have previously existed on these fans throughout the Quaternary (Campbell and Mosher, 2014; Piper et al., 2016). These channel systems and the growth of these fans is hypothesised to have been the result of exceptionally large discharges of sediment-laden meltwater to the slope from the Laurentide Ice Sheet leading to the formation of hyperpycnal flows or turbidity currents which re-work the rapidly deposited plume deposits (Hughes Clarke et al., 1990; Piper et al., 2007; Clare et al., 2016b). Submarine slump and debris avalanche reworking of deposited material is also thought to play a role in the sedimentation history of these fans (Piper et al., 2012). Critically, there is little evidence of glacigenic debris-flows being important to the development of these trough-mouth fans.

6.2.2. East Canadian gullies and submarine channels

Much of the East Canadian Margin is characterised by alternating regions of high and low density gullies and channels (Hesse et al., 1999; Mosher et al., 2004; Jenner et al., 2007; Campbell and Mosher, 2014). Where cross-shelf troughs are found, sedimentation is dominated by glacigenic debris-flow emplacement (Hesse et al., 2001; Piper, 2005). Gullies and channels have, however, been incised into the emplaced debris-flow units by sediment-laden meltwater being discharged from the ice margin and the downslope evolution of glacigenic debris-flows into turbidity currents (Piper, 2005; Dowdeswell et al., 2016a; 2016c; Piper et al., 2016). Between the cross-shelf troughs, meltwater processes dominate resulting in the formation of dendritic gully and canyon systems. These systems are hypothesised to be a consequence of hyperpycnal and hypopycnal flow formation (Piper and Hundert, 2002; Piper and Normark, 2009), the re-working of sediment by turbidity currents which has settled out from meltwater plumes that have been entrained southward by the Labrador Current and mass-wasting processes (Fig. 26; Hesse et al., 1997; 2001; 2004; Ó Cofaigh et al., 2003). Many of the channel and canyon systems subsequently coalesce to feed deep-sea channels such as the North Atlantic Mid-Ocean Channel (Piper, 2005).

6.2.3. East Canadian submarine landslides

The first identified submarine landslide was the Grand Banks Slide in 1929 (Heezen and Ewing, 1952; Piper and Aksu, 1987). Like the Storegga region, these events appear to be relatively common along the East Canadian Margin. Landslide headscarps have been identified on the upper continental slope, in gullies, on canyon flanks, and at the base of the continental slope (Mosher et al., 1994; 2004; Piper, 2005; Dowdeswell et al., 2016a). These landslides are therefore likely to play an important role in the maintenance and morphology of the channel and gully systems which exist along much of the margin (Piper, 2005; Dowdeswell et al., 2016a; 2016c).

1370 The majority of the landslides within the gully and channel systems north of Orphan Basin have been
1371 interpreted to have contained relatively small volumes of sediment. As a consequence these
1372 landslides are unlikely to have the geohazard potential of the large submarine landslides seen during
1373 the Holocene in the Nordic Seas. They do, however, still represent a significant hazard to offshore
1374 infrastructure development (Pickrill et al., 2001). In contrast, the south eastern part of the Canadian
1375 Margin from the Flemish Cap to Georges Banks has experienced large numbers of large mass failures
1376 during the Quaternary (Piper et al., 2003; Piper, 2005; Bennett et al., 2014). Here, failures with
1377 volumes up to ~800 km^3 have been identified (Piper and Ingram, 2003). 10 Quaternary landslides
1378 with volumes >10 km^3 have been identified on this part of the margin suggesting a mean recurrence
1379 interval of 0.25 Ma (Piper and Ingram, 2003; Piper et al., 2003). However, the recurrence times vary
1380 between individual basins (Piper et al., 2003) and there are large dating uncertainties on most
1381 landslides. The recurrence of smaller, but still >1 km^3, landslides is shorter. For example, 9 turbidite
1382 deposits, interpreted to originate from landslides on the Flemish Cap occurred during the last 150 ka
1383 (Huppertz and Piper, 2009).

1384 The identified large submarine landslides on the south eastern part of the Canadian Margin are
1385 thought to be directly linked to glaciation of the continental slope and delivery of large volumes of
1386 glacigenic sediment. Glacial and pro-glacial sediment packages have been shown to fail
1387 retrogressively along their bedding plane on this section of the margin (Piper et al., 1999; Mosher et
1388 al., 2004). Moreover, the most recent failures identified on the Scotian Slope and Grand Banks
1389 occurred at or immediately after the Laurentide Ice Sheet reached its local maximum extent during
1390 the last glaciation of the shelf (Piper and Campbell, 2005). Extrapolating further back into the
1391 Quaternary, the Laurentide Ice Sheet is interpreted to have reached the shelf edge in this area
1392 repeatedly from MIS 12 (0.45 Ma) onwards (Piper et al., 1994). However, the poorly constrained
1393 dating of the large mass transport deposits which pre- and post- date MIS 12 prevents any further
1394 understanding of the influence that shelf edge glaciations have had on the frequency of large
1395 submarine landslides. Based on the distribution of failures (Piper et al., 1985) and sediment strength

estimates (Baltzer et al., 1994; Mosher et al., 1994; 2004) the majority of slope failures identified are thought to result from large passive margin earthquakes, the frequency of which are increased as a consequence of glacial loading and unloading associated with Laurentide Ice Sheet growth and decay (Stewart et al., 2000).

7. Glaciated margin systems – a new conceptual model

In the following section we develop a new conceptual model of sedimentation on glaciated margins based on the ice sheet histories around the Nordic Seas outlined in Sections 2 – 5 and the comparisons made in Section 6 with other margins.

7.1. How has ice sheet history and sedimentation changed with climate?

We first address the influence that climate has had in the Nordic Seas on ice sheet and sedimentation histories in reference to the variables outlined in Section 1.1 and in Figs. 1 and 2. Two key questions have to be addressed. First, do cooler climates result in increased glacial sediment delivery to the continental margin? Second, has the transition between the 41 and 100 kyr climate cycles enhanced glacial delivery of sediment?

If the history of ice sheets and sedimentation around the Nordic Seas is considered as a whole then no clear relationship exists between climate and delivery of glacigenic sediment. For example, a fundamental contrast exists between the East Greenland and southern Norwegian margins. The delivery of sediment by the Greenland Ice Sheet appears to increase as climate cools until the adoption of the 100 kyr climate cycles at which point it decreases (Table 1). In contrast, glacial sedimentation dramatically increases on the southern Norwegian Margin as climate cools and the 100 kyr climatic cycles are adopted (Table 4). It is therefore prudent to instead consider the evolution of ice sheet sediment delivery on individual margins of the Nordic Seas related to their climatic setting.

The Nordic Seas margins can be considered to exist within a climatic range. The southern Norwegian section of the margin is the warmest and wettest (Patton et al., 2016). Both the temperature and volume of precipitation are believed to reduce with increasing latitude along this margin; Svalbard therefore having the coolest and driest climate (Patton et al., 2016). The Greenland Margin is the coolest of the margins (Fig. 1). For each of these margins the climatic deterioration seen during the Quaternary therefore represents a shift towards a cooler climate (Fronval and Jansen, 1996; Thiede et al., 1998; Jansen et al., 2000). Assuming that this is correct, it therefore appears that a threshold exists, at which point continued cooling of the climate serves to reduce the efficiency of ice sheet sedimentation. This threshold is likely controlled by the comparative areas of cold-based ice and the extent and area of fast flowing ice streams. The sedimentation history offshore Svalbard most clearly illustrates such a relationship (Table 3). As climate deteriorated from 2.8 Ma to 1.0 Ma, ice sheet driven sedimentation through glacimarine processes and glacigenic debris-flow emplacement on the continental shelf increased. However, since 1.0 Ma the rate of sedimentation and the thickness of glacigenic debris-flow deposits have decreased (Sættem et al., 1994; Solheim et al., 1998; Knies et al., 2009). Despite the extent and drainage area of the ice sheet being similar it therefore appears that the efficiency of glacial sedimentation decreased following a cooling of the climate and adoption of the 100 kyr climate cycles. Further support for this suggestion is found on the Norwegian Margin where the location of maximum volume of deposited sediment has progressively moved southwards as climate has cooled (Fig. 19; Rise et al., 2005).

Analysis of the history of sedimentation offshore Antarctica (Section 6.1) supports the idea of a tipping point in glacigenic sediment delivery across a continental margin. Since the inception of the Antarctic Ice Sheet, glacigenic sedimentation has occurred on the continental margin (Kuvaas and Kristoffersen, 1991). Dating of sediment packages beyond the continental shelf has, however, shown the volume of sediment transported to have decreased in line with cooling climates. For example, sedimentation on the Prydz Bay Trough-Mouth Fan from the Late Miocene to 1.1 Ma was dominated by glacigenic debris-flows (Passchier et al., 2003). As climate continued to cool, the temperature of

the East Antarctic interior and precipitation received there were reduced. This led to a hypothesised reduction in the area of fast flowing warm-based ice (Passchier et al., 2003; O'Brien et al., 2004). The reduced sediment transport manifest itself in reduced numbers and thickness of glacigenic debris-flow deposits; emplacement of these deposits eventually ceasing after 0.78 Ma with the adoption of 100 kyr climate cycles.

7.2. Trough-mouth fans

The largest sedimentary features on glaciated margins are trough-mouth fans which are of comparable size to deep-sea fans formed offshore the World's largest rivers. They form preferentially in front of cross-shelf troughs as a consequence of fast-flowing ice streams delivering large volumes of sediment to the shelf edge over repeated glacial cycles (Ó Cofaigh et al., 2003; Dowdeswell et al., 2010b). The classical trough-mouth fan model was developed from observations in the Nordic Seas (Laberg and Vorren, 1995; Dowdeswell et al., 1996; Vorren and Laberg, 1997). This model was further developed by Ó Cofaigh et al. (2003) recognising the importance of slope setting and hypothetical cases of low sedimentation. Here, we attempt to improve the model of trough-mouth fan processes using the observations outlined in previous sections.

7.2.1. Characterisation of trough-mouth fans

Our analysis of trough-mouth fans around the Nordic Seas and on other continental margins identifies four variants of trough-mouth fan depending on the dominant sediment/meltwater environment present in each location (Fig. 27). Type 1 trough-mouth fans are dominated almost entirely by glacigenic debris-flow emplacement. During full-glacial conditions, the rate of sediment delivery to the shelf edge is sufficient to trigger multiple glacigenic debris-flows which dominate the upper slope (Vorren and Laberg, 1997; Laberg and Dowdeswell, 2016). Sufficient numbers of flows can occur, that form an apron radiating out from the top of the fan to the mid/lower slope (Fig. 27; King et al., 1998; Taylor et al., 2002a). The lower slope is dominated by interbedded hemipelagic

sediments and distal debris-flow muds and turbidites from the downslope evolution of glacigenic debris-flows (Laberg and Vorren, 1995). The volume and rate of sediment delivery to type 1 trough-mouth fans by ice streams is sufficiently large to dampen any influence that meltwater sedimentation may have on trough-mouth fan evolution. The Bear Island Trough-Mouth Fan represents a type 1 trough-mouth fan. During full-glacial conditions, sedimentation has been dominated by the emplacement of glacigenic debris-flow deposits on the upper and mid-fan, and on the lower fan by distal debris-flow muds, turbidites and hemipelagic sediments (Vorren et al., 1989; Sættem et al., 1994; Laberg and Vorren, 1996; Vorren et al., 1998; Pope et al., 2016). No large submarine landslide is thought to have originated from the Bear Island Trough-Mouth Fan for >200 ka, a period which includes two full glacial cycles. However, prior to that seismic data suggests that the fan may have experienced 'relatively' frequent large submarine landslides (Figs 13 and 14) and would therefore have been categorised differently during these periods. A further example of a type 1 trough-mouth fan can be found in the Gulf of Alaska. Here, sedimentation dominated by glacigenic debris-flow emplacement has resulted in the construction of the Bering Trough-Mouth Fan (Montelli et al., 2017b).

Type 2 trough-mouth fans are dominated by a range of submarine mass movement processes (Fig. 27). In the Nordic Seas, the North Sea and Storfjorden Trough-Mouth Fans are the type examples of type 2 trough-mouth fans. As on type 1 trough-mouth fans, these fans are dominated by the emplacement of glacigenic debris-flow deposits. Where these fans differ to type 1 fans is that the rate of sedimentation and the emplacement of the debris-flow apron leads to further instabilities within the trough-mouth fan. These instabilities can culminate in submarine slumping and large submarine landslides. Although other processes may play a role in the evolution of these trough-mouth fans (e.g. gully formation, plumite or contourite deposition which are key to landslide occurrence), their sedimentary architecture is dominated by different types of submarine mass movement deposit.

Type 3 trough-mouth fans are characterised by medium rates of sediment delivery but meltwater processes also have a greater influence (Fig. 27). Kveithola is an example of a type 3 trough-mouth fan. As was the case for type 1 and type 2 trough-mouth fans, a significant volume of a type 3 trough-mouth fan may still be made up of glacigenic-debris flow deposits which are emplaced when ice is at the shelf edge. However, the number and volume of these deposits is limited compared to type 1 and type 2 trough-mouth fans. Instead the defining characteristic of these fans is the presence of gullies, channel systems and plumites deposits. Gully incision in the upper slope has been hypothesised as a consequence of sediment-laden subglacial meltwater flow (Lowe and Anderson, 2002; Noormets et al., 2009; Bellec et al., 2016; Ó Cofaigh et al., in review). Alternatively they may be the result of dense water formation related to sea ice production on the shelf which subsequently cascades down the face of the trough-mouth fan. Although relatively rare, in some settings, e.g. Laurentian, Northeast and Crary Trough-Mouth Fans (Fig. 24b), channel-levee complexes have also been observed (Aksu and Piper, 1987; Piper, 1988; Kuvaas and Kristoffersen, 1991). It is interesting to note the contrasting latitudes where these trough-mouth fans are found; the channel-levee systems perhaps being initiated by different processes. Channel formation is thought to be characteristic of warm-based ice at the shelf edge delivering large amounts of meltwater and sediment. Where sufficient meltwater and sediment is present, turbidity currents and hyperpycnal flows are able to produce channel systems (Aksu and Piper, 1987; Piper and Normark, 2009). It has also been speculated that some of these systems may be associated with catastrophic meltwater discharge; in some cases from subglacial lake drainage. Plumites meanwhile are deposited as a consequence of sediment-laden meltwater plumes (Lucchi et al., 2013). The extent and influence of these processes may, however, be controlled by the rate of retreat of the ice stream from the trough-mouth fan during deglaciation.

Type 4 trough-mouth fans are characterised by low rates of sedimentation (Fig. 27). Scoresby Sund and Prydz Bay Trough-Mouth Fan represent type 4 trough-mouth fans. These fans are comparatively sediment starved, even during full-glacials. This reflects a number of factors, either individually or in

combination. It can be a consequence of ice delivering little sediment to the fan due to it rarely extending to the shelf edge or to be being present at the shelf edge for only a limited period of time, or to supplying relatively little sediment. Importantly, meltwater processes associated with ice stream advance and retreat also deliver little sediment to the shelf edge. The lack of sediment delivery means that glacigenic debris-flows are infrequent with small volumes and do not produce the apron of deposits seen on type 1 and 2 trough-mouth fans (Dowdeswell et al., 1997). It is perhaps unlikely that a trough-mouth fan would form under type 4 conditions alone. These systems therefore probably reflect rates of sediment delivery associated with glacial maxima where different ice sheet regimes existed or where margins have evolved and which no longer favour progradation of the trough-mouth fan.

7.2.1.1. Can trough-mouth fan characteristics change?

To understand glaciated continental margin evolution it is important to understand whether trough-mouth fans can switch their type characteristics. Fundamental to this question is whether location, e.g. continental shelf geology and catchment area, or climate/ice sheet characteristics control the type of trough-mouth fan which develops. It is clear from the compilation of sedimentary records from the Nordic Seas that location can play a significant role in the type of trough-mouth fan which develops or whether a trough-mouth fan is able to develop at all (Wellner et al., 2001; Ó Cofaigh et al., 2003). For example, there is a clear contrast between the East Greenland and Svalbard/Barents Sea margin trough-mouth fans as a consequence of ice streams overriding sediments and bedrock with contrasting erodibilities (Solheim et al., 1996; 1998; Ó Cofaigh et al., 2003). The position and flow of ice streams is not, however, static. Analysis of buried mega-scale glacial lineations has shown that ice streams frequently migrate between glaciations (Dowdeswell et al., 2006b; Graham et al., 2009). Flow migration may result in the ice stream flowing over a substrate with contrasting properties and thus changing the input of sediment to a trough-mouth fan. Flow migration of the Lambert-Amery Ice Stream, from an area of readily erodible sediment to hard bedrock, has been

cited as one of the main contributing factors for the initial reduction in sediment transport to the Prydz Bay Trough-Mouth Fan (Passchier et al., 2003; O'Brien et al., 2007).

The compilation of ice sheet and sedimentation histories does, however, suggest that climate and its associated impacts on ice sheet characteristics may have a larger impact on controlling temporal switches between trough-mouth fan types. Climatic deterioration can clearly be seen as a driving factor behind the transition of the Scoresby Sund Trough-Mouth Fan from a type 1 to a type 4 fan. It is also responsible for the cessation of sediment supply to the Prydz Bay Trough-Mouth Fan after the adoption of 100 kyr climatic cyclicity. Further evidence can also be found in the changing sedimentation regimes seen on trough-mouth fans on the Svalbard margin (Table 3) and the transition in fan type associated with latitudinal change along the east Canadian margin. Interestingly, it could also be suggested that the Bear Island Trough-Mouth Fan has transitioned between type characteristics. Between 1.3 and 0.2 Ma the Bear Island Trough-Mouth Fan was dominated by glacigenic debris-flow emplacement and large submarine landslide occurrence (i.e. a type 2 trough-mouth fan). However, since at least 0.2 Ma (a consequence of poor age constraints), there is no evidence of large submarine landslide occurrence on the fan itself (Fig. 14). It is therefore possible that the Bear Island Trough-Mouth Fan has transitioned to type 1, characterised predominantly by glacigenic debris-flow emplacement. A possible explanation for this is the continued subsidence of the Barents Sea continental shelf and deepening of the Bear Island Trough which may have reduced the sediment supply (see Fig. 14). It may also have led to a reduction in the volume of glacimarine sediment deposition on the fan as the Bear Island Ice stream became more susceptible to rapid retreat due to its deeper water setting. This may have reduced the volume of contrasting sediment packages on the fan hypothesised to be required for large submarine landslide occurrence (Bryn et al., 2005).

7.2.1.2. Do trough-mouth fans have characteristic depositional sequences?

The sedimentary sequence of the Late Weichselian advance and retreat has been described on a number of trough-mouth fans around the Nordic Seas, e.g. Isfjorden (Elverhøi et al., 1995; Dowdeswell and Elverhøi, 2002). However, the setting of, and sedimentary processes operating on trough-mouth fans are highly variable. For example, depositional characteristics vary across and between the Storfjorden and Bear Island trough-mouth fans during the Late Weichselian (Laberg and Vorren, 1995; Pedrosa et al., 2011; Lucchi et al., 2013). It is therefore difficult if not problematic to describe a characteristic depositional sequence for a trough-mouth fan type.

7.2.2. How can we better understand controls on trough-mouth fans?

Understanding the controls on trough-mouth fan morphologies and processes remains challenging. Fundamentally this stems from there being very few/no direct observations of sediment transport by ice streams and submarine mass movements on trough-mouth fans and thus estimating sediment accumulation across a single trough-mouth fan during a full glacial period is very difficult. This is the case even when using the sedimentary record; there are very few studies which have been able to produce estimates of sediment accumulation (Laberg and Vorren, 1996; Nygård et al., 2005). Crucially, the precise timing of sediment delivery is usually uncertain in these studies. Fewer studies still have been able to model the delivery of sediment by ice streams to trough-mouth fans (Dowdeswell et al., 1999; Dowdeswell et al., 2010b). Future efforts to understand trough-mouth fans should therefore follow two separate lines. First, understanding of ice stream transfer of sediment needs to be improved and how this can be impacted by meltwater drainage system evolution. Achieving this will likely require observations from currently deforming glacier beds and proglacial environments in marine settings (e.g., Hart et al., 2011; Dowdeswell et al., 2015). Second, additional high resolution seismic and sedimentary records are needed on trough-mouth fans in order to precisely constrain the timing and volume of sediment delivery by ice streams.

7.3. Glaciated continental margins

In addition to the multiple types of trough-mouth fan that have been identified, our records also indicate that there are multiple types of glaciated margins (Fig. 28). We recognise three characteristic margin types. The first is characterised by high sediment inputs by ice streams and by the formation of trough-mouth fans (Dowdeswell et al., 1996). Along these margins, ice stream sedimentation is sufficiently high or has been sufficiently high in the past to allow trough-mouth fans to form even when conditions appear unfavourable such as seismically active or steep margins, e.g. the Bering Trough-Mouth Fan formation over the Aleutian Trench (Montelli et al., 2017b).

The second margin type is characterised by high sediment inputs but which are insufficient to lead to the formation of trough-mouth fans. Along these margins, large volumes of sediment are delivered by a range of mechanisms. First, ice sheet flow delivers sediment at an enhanced rate compared to rates of interglacial sedimentation (Dowdeswell and Elverhøi, 2002). Second, ice streams may still be present and deliver large volumes of sediment. Third, sediment is delivered by glacial meltwater in addition to glacigenic debris-flows (Lekens et al., 2005; 2006). Fourth, ocean currents may deposit significant contourite deposits. The interbedding of the multiple types of sediment and the contrasting properties of these packages can lead to instabilities within the sediment stack (Baeten et al., 2013; 2014). As a consequence these margin types are often characterised by the occurrence of submarine slumps and landslides. The Storegga region is the type example for this margin type.

The third margin type is characterised by low sediment input (Dowdeswell et al., 1996; Ó Cofaigh et al., 2003). Here, ice may not always reach the shelf edge during full glacials and thus direct delivery of sediment by ice is temporally limited. Alternatively, where ice regularly reaches the shelf edge, it may not transport large volumes of sediment. As a consequence the number and extent of glacigenic debris-flows is limited, as is the progradation of glacigenic structures. The development of these features will be further hindered if the continental slope is steep or the margin is tectonically active. The continental shelf and slope are, thus dominated by glacimarine and marine processes. As a

result the dominant sediment transport process which dominates margin characteristics is turbidity currents which often result in the formation of channels.

8. Submarine mass movements on glaciated margins: geohazard assessment

Submarine mass movements are a common feature of glaciated margins and are considered significant geohazards. Poleward migration of human activity as a consequence of climate change increases exposure to these hazards necessitating hazard mitigation (Øverland, 2010; Boswell and Collett, 2011; Bennett, 2016). Hazard assessment requires us to understand the impact of past events, likely triggering mechanisms and their frequency. In the following section we discuss; (1) the potential hazard associated with these events using historical examples; (2) the potential triggers for submarine mass movements on glaciated margins; (3) the history of submarine landslides, their connection to ice sheet histories and conceptual models of flow preconditioning and triggering.

8.1. Submarine mass movements and societal impacts

Submarine mass movements have the potential to generate very damaging and far travelling tsunami and damage seafloor infrastructure and they can therefore have significant societal impacts. The following section will briefly outline the geohazard potential based on two events; the Storegga Slide and the Grand Banks Slide.

8.1.1. Landslide-generated tsunami

The Storegga Slide (>3000 km^3) and the Grand Banks Slide (~200 km^3) both triggered tsunamis which impacted surrounding coastlines. The 1929 Grand Banks generated tsunami had runup heights of 13 m along the Burin Peninsula, Canada, killing 27 people and leaving >1000 homeless (Fine et al., 2005). The 8.2 ka Storegga Slide generated a tsunami which impacted the coastlines of Greenland, Norway, the Shetland Islands, the Faroe Islands, Scotland, Eastern England and Doggerland with runup heights in excess of 20 m (see Fig. 29; Dawson et al., 1988; Long et al., 1989; Bondevik et al., 1997; 2003; 2005; 2012; Grauert et al., 2001; Bondevik et al., 2003; Smith et al., 2004; Fruergaard et

al., 2015). In addition to fatalities directly caused by the tsunami, the Storegga tsunami is also thought to have had significant impacts on Mesolithic societies. Occurring contemporaneously with climatic deterioration associated with the 8.2 ka neoglacial, the tsunami is thought to have had significant long term impacts on Mesolithic populations around the coasts of the North Sea due to the combined stress caused by multiple hazards (Wicks and Mithen, 2014; Ballin, 2017; Waddington and Wicks, 2017). In addition, archaeological evidence has also suggested shifting settlement patterns following the tsunami with the abandonment of sites affected by the tsunami (Bondevik, 2003; Weninger et al., 2008; Waddington and Wicks, 2017). Recurrence of an event of this scale today would also have significant impacts due to the increase in population inhabiting areas affected by the Storegga tsunami and the location of critical infrastructure on these coastlines such as power stations.

Despite clear evidence of tsunami generation by large submarine landslides, there is evidence to suggest that not all large submarine landslides generate damaging tsunami. The Trænadjupet Slide contained 500 – 700 km^3 of material, at least double that of the Grand Banks Slide, but no significant tsunami deposit has yet been linked with the slide (Løvholt et al., 2017). Landslide-tsunami generation is dependent on; (1) landslide volume, whether it is emplaced in one or multiple stages; (2) initial acceleration and speed of the mass movement; (3) the length and thickness of the slide and; (4) the water depth (Geist, 2000; Tappin et al., 2001; Waythomas and Watts, 2003; Harbitz et al., 2006; Masson et al., 2006; Waythomas et al., 2006; Hunt et al., 2011; Hunt et al., 2013; Harbitz et al., 2014; Løvholt et al., 2016). If the mass movement is of sufficient volume and accelerates quickly enough, it can generate a tsunami. The clear contrasts between the tsunami generated by the Storegga Slide and the Trænadjupet Slide shows that further work is needed in order to understand the likelihood of different potential failure mechanisms for submarine landslides around these margins.

8.1.2. Damage to seafloor infrastructure

Submarine mass movement damage to seafloor infrastructure has the potential to cause significant environmental and economic impacts. They represent a threat to seafloor infrastructure used for seafloor resource extraction which can be worth many millions of dollars including infrastructure used by the hydrocarbon industry (Thomas et al., 2010). For example, the Ormen Lange gas field, which currently supplies ~20% of the UK's supply of natural gas is located directly below the headwall of the Storegga Slide (Talling et al., 2014). They can also break seafloor telecommunications cables which currently carry >99% of intercontinental data traffic, including the internet and financial markets (Carter et al., 2014). Damage to cables at pinch points, i.e. areas where multiple cables transfer extremely high proportions of data traffic between specific regions, by turbidity currents has been shown to have significant impacts on local and regional economies (Rauscher, 2010; Carter et al., 2012; Gavey et al., 2017). The Grand Banks represents one such pinch point (Clare et al., 2016a). The 1929 slide and its associated turbidity current broke 11 telegraph cables (Heezen and Ewing, 1952). Today, >20 submarine fibre optic cables exist in the same area (Clare et al., 2016a). A similar event could therefore have a significant impact on the global economy.

8.2. Submarine mass movement triggers on glaciated margins

This section serves to summarise the processes that precondition and trigger submarine mass movements on glaciated margins. Numerous mechanisms by which submarine mass movements can be triggered have been proposed. On non-glaciated margins individual triggers have been identified using submarine cable breaks (Heezen and Ewing, 1952; 1955; Heezen et al., 1964; El-Robrini et al., 1985; Piper et al., 1999; Hsu et al., 2008; Carter et al., 2012; 2014; Cattaneo et al., 2012; Pope et al., 2017a; 2017b), repeat bathymetric surveys (Clare et al., 2016b), acoustic Doppler current profilers (Shepard et al., 1979; Ikehara, 2012; Liu et al., 2012; Azpiroz-Zabala et al., 2017) and damage to marine platforms (Prior et al., 1982; Bea et al., 1983; Alvarado, 2006). However, on glaciated margins, evidence for most submarine mass movements comes from their deposits. It is therefore

1691 often difficult to definitively link a specific flow deposit to a specific triggering mechanism. It must
1692 also be recognised that many individual triggering mechanisms, such as rapid sedimentation, can
1693 also act as preconditioning factors; the actual failure resulting from a subsequent trigger.

1694 **8.2.1. Earthquakes**

1695 Submarine mass movements on all margins are commonly attributed to earthquakes (ten Brink et
1696 al., 2009; Stigall and Dugan, 2010; Masson et al., 2011). In addition to earthquakes related to plate
1697 tectonics, glaciated margins are also subject to pronounced increases in seismic activity associated
1698 with glacio-isostatic adjustment (Fjeldskaar et al., 2000; Stewart et al., 2000; Bryn et al., 2003;
1699 Bungum et al., 2005; Steffen and Wu, 2011). Establishing a direct causal link between a mass
1700 movement and an earthquake from the geological record alone is challenging. Previous attempts
1701 include the use of contemporaneous mass movement deposits to infer periods of enhanced
1702 seismicity or large regional earthquakes (Goldfinger, 2011; Goldfinger et al., 2012; Bellwald et al.,
1703 2016). Alternatively, isostatic rebound models have been used to assess peaks in earthquake
1704 numbers and magnitudes related to glacio-isostatic adjustment (see Steffen and Wu, 2011 for full
1705 details), the outputs of which are then compared to known dated mass movement deposits (Bryn et
1706 al., 2003; 2005). Most submarine landslides are suggested to have an earthquake trigger, however,
1707 the Grand Banks Slide is known to have been triggered by a M_w 7.2 earthquake (Heezen and Ewing,
1708 1952), whilst a strong earthquake is believed to have played some role in triggering the Storegga
1709 Slide (Bryn et al., 2005). Both earthquakes are thought to be the result of isostatic adjustment.

1710 Earthquakes mainly trigger submarine mass movements in two ways. First, acceleration-induced
1711 sliding occurs when strong seismic motions subject sediments to horizontal and vertical
1712 accelerations that exceed their yield strength (Owen et al., 2007; 2008). Second, liquefaction-
1713 induced sliding can occur as a consequence of reduced sediment strength due to accumulated
1714 deformation from cyclic shearing. Cyclic loading can also result in the generation of excess pore
1715 pressures due to the upward migration of pore fluid. The migration of this fluid can generate

instability if the migrating fluid encounters a sediment layer or region with a lower dissipation rate thereby allowing pore pressures to build up and eventually cause a failure to occur (Biscontin et al., 2004; Biscontin and Pestana, 2006; Özener et al., 2009; L'Heureux et al., 2013). The timing of the subsequent slope failure may occur several months after the seismic event that has triggered it as the time required to reach critical conditions for different sediment profiles ranges from minutes to months according to consolidation profiles, sediment types and dissipation rates (Biscontin and Pestana, 2006; Leynaud et al., 2009).

8.2.2. High sedimentation rates

The importance of high sedimentation rates for triggering submarine mass movements on glaciated margins has been emphasised throughout this review. Extension of a grounded ice sheet to the shelf edge has commonly been shown to be associated with enhanced rates of deposition and the occurrence of greater numbers of mass movements. High sedimentation rates are linked to slope failure in two ways. First, rapid sedimentation can lead to oversteepening of a slope resulting in eventual failure of the sediment (Powell and Domack, 1995; Powell and Alley, 1997; Dugan and Flemings, 2000; Clare et al., 2016b). Second, rapid sediment deposition can lead to progressively increasing pore pressures by preventing dewatering of the deposited sediment (Leynaud et al., 2007; Flemings et al., 2008; Stigall and Dugan, 2010). This can lead to the build-up of excess pore pressure (overpressure) and eventually lead to failure (Dugan and Sheahan, 2012). In addition to these mechanisms, glacigenic debris-flows have been interpreted to have been triggered in a third way. From observations on the Newfoundland continental slope, glacigenic debris-flows have been attributed to the continuous (or near continuous) input of sediment at the shelf break (Aksu and Hiscott, 1989, 1992). When triggered by this mechanism, downslope transport of sediment in glacigenic debris-flows has been likened to a ‘lava flow’ (Vorren and Laberg, 1997).

8.2.3. Hydrate dissociation

Gas hydrate dissociation has been suggested to be a preconditioning or triggering mechanism for submarine mass movements on glaciated margins (Best et al., 2003; Kennett et al., 2003). Seabed and subsurface fluid escape features have been identified along the Norwegian continental shelf, the Barents Sea and other glaciated margins indicating the presence of overpressure and pressure release in continental shelf sediments in these environments (Solheim and Elverhøi, 1985; Mienert et al., 1998; Gravdal et al., 2003; Hovland et al., 2005; Mienert et al., 2005; Chand et al., 2012; Andreassen et al., 2017). Hydrates form where there is a sufficient supply of gas, water at moderate pressure and relatively low temperatures (Berndt, 2005; Mienert et al., 2005). Dissociation of these hydrates can occur as a consequence of changes to pressure or temperature regimes in the substrate (Vanoudheusden et al., 2004; Hornbach et al., 2007; Berndt et al., 2014). Hydrate dissociation can provide overpressure through the expulsion of gas leading to the generation of a potential failure plane as a consequence of the reduction of yield strength. This can either cause failure to occur or increase the susceptibility of sediment to fail as a consequence of a further trigger (Prior et al., 1982; Kayen and Lee, 1991; Mienert et al., 1998; Sultan et al., 2004a). Alternatively submarine mass movements can cause dissociation themselves by exposing new horizons in the headwall and slide scar or by de-weighting deeper sediments (Sultan et al., 2004b). This alternative mechanism for dissociation greatly complicates identifying the exact role that dissociation may have had in triggering a mass movement (Maslin et al., 2004).

8.2.4. Sea level change

Sea level change is commonly invoked as being linked to changes in submarine mass movement frequency on all margins (Vail et al., 1977; Piper and Savoye, 1993; Owen et al., 2007; Lebreiro et al., 2009; Covault and Graham, 2010; Brothers et al., 2013; Smith et al., 2013). Sea level change itself is thought to be capable of causing slope failure as it can alter seafloor stress regimes due to changes in hydrostatic water pressure (Weaver and Kuijpers, 1983; Lee et al., 1996; Urlaub et al., 2012). These pressure changes are thought to also have the potential to cause hydrate dissociation (Maslin

et al., 1998; 2004; Sultan et al., 2004a; Vanoudheusden et al., 2004; Leynaud et al., 2007; Owen et al., 2007). Modelling studies have also suggested that particularly rapid changes in sea level can also lead to increased seismicity (Brothers et al., 2013). However, it is the change to the location and rate of deposition that results from sea level change that is most commonly associated with changes in submarine mass movement frequency (Lee, 2009; Covault and Graham, 2010; Urlaub et al., 2012).

Isolating the direct role of sea level change on submarine mass movement triggering on glaciated margins is challenging. This is a consequence of (1) the difficulty in precisely dating deposits (Urlaub et al., 2014; Pope et al., 2015); (2) needing to constrain local isostatic adjustment resulting from local ice sheet growth/decay (Shennan et al., 2002); (3) precisely dating and quantifying the local effects of rapid sea level change (Clark et al., 2002; Weaver et al., 2003; Brothers et al., 2013; Smith et al., 2013) and; (4) understanding the relative roles of other preconditioning and triggering mechanisms. Nonetheless, slope failures on glaciated margins have been recognised to be associated with rising sea levels and highstand (Owen et al., 2007; Lebreiro et al., 2009; Lee, 2009).

8.2.5. Hyperpycnal and hypopycnal flows

Hyperpycnal and hypopycnal flows are both known to have triggered submarine mass movements on glaciated margins. Hyperpycnal flows occur as a consequence of water discharged into the ocean having a sufficiently high sediment concentration to overcome the density difference between fresh water and sea water (Mulder and Moran, 1995; Parsons et al., 2001; Mulder et al., 2003; Felix et al., 2006). Once sediment-laden water is able to plunge it may then continue downslope under gravity and entrain water and sediments leading to the formation of a turbidity current (Carter et al., 2012). In contrast, hypopycnal flows initially maintain their sediment loads in suspension. Fallout from the plume can then trigger a subsequent submarine mass movement (Parsons et al., 2001; Curran et al., 2004; Zajaczkowski, 2008; Piper and Normark, 2009). Examples of deposits from submarine mass movements triggered by these flows can be found on the East Canadian Margin, dating from the

Weichselian and as during ice sheet retreat (Hesse et al., 2001; Piper and Hundert, 2002; Piper et al., 2007; Tripsanas and Piper, 2008b).

8.3. Submarine landslides on glaciated margins

Submarine landslides are considered to be one of the main morphological features of glaciated margins and a common feature of trough-mouth fans. In the following section we will therefore discuss the connection between ice sheets and landslides and conceptual models of these flows on glaciated margins.

8.3.1. The distribution of large submarine landslides

The global distribution of known large submarine landslides on glaciated margins is very uneven. Where large submarine landslides have been identified, their locations appear to favour recurrent mass-failures of this scale. In other areas they are extremely rare or have yet to be identified as a consequence of globally uneven data coverage. The frequency of these events in two regions standout; they are especially common on the Norwegian/Barents Sea Margin and the South East Canadian Margin (e.g. Hjelstuen et al., 2005; Urlaub et al., 2013). They are conspicuously absent from several other glaciated margins. The following section will discuss the likely causes of this distribution.

8.3.1.1. Sediment supply and the presence of weak layers

Sediment supply appears to be crucial for submarine landslide occurrence on glaciated margins. Models based on the Storegga Slide suggested that ice stream driven rapid sedimentation could generate overpressure or increased pore pressures (Bryn et al., 2003; Haflidason et al., 2003). Sedimentary evidence from this part of the Norwegian Margin suggests that sedimentation rates were as high as 1750 cm/ka during deglaciation (Lekens et al., 2005; 2009). However, slope failure was not caused by the rate of sedimentation alone but by the contrasting strength and porosity profiles of soft marine clays and glacigenic sediments (Bryn et al., 2003; 2005; Kvalstad et al., 2005;

Leynaud et al., 2007). The boundary between the two sediment packages provided the plane along which slope failure occurred. Geotechnical investigations of other sections of the Norwegian margin where submarine landslide are common have revealed similar site characteristics (Lucchi et al., 2013; Baeten et al., 2014; Llopart et al., 2014; Madhusudhan et al., 2017). In the Trænadjupet region, the contrast is provided by glacigenic sediments, contouritic and marine clays (Laberg et al., 2003; Baeten et al., 2014). Failures on the Storfjorden Trough-Mouth Fan are thought to relate to the contrasting properties of glacigenic sediments and water-rich, clayey sediments with low shear strength deposited by meltwater plumes and contour currents (Hjelstuen et al., 1996; Rebesco et al., 2012; Lucchi et al., 2013). The South East Canadian Margin also experiences similarly rapid sedimentation (4 m/ka) from meltwater plumes (Mosher et al., 1989; Piper and Ingram, 2003).

We therefore suggest that the Bryn et al. (2005) model for triggering/preconditioning of large submarine landslides where rapid deposition of sediment by ice sheets onto pre-existing 'weak' layers is applicable to large sections of glaciated continental margins not just the Storegga section of the Norwegian Margin (Fig. 30).

8.3.1.2. Passive vs. active margins

Earthquakes are often cited as the triggering mechanisms for submarine mass movements (see previous section). Indeed, the Grand Banks submarine landslide is evidence that large earthquakes can trigger large submarine landslides on glaciated margins (Heezen and Ewing, 1952; Piper et al., 1999). However, as has been identified on non-glaciated margins there is a significant contrast between submarine landslide occurrence on passive and active margins. The multiple large submarine landslides on the South East Canadian and Norwegian margins are thought to have been triggered by earthquakes related to isostatic adjustment following ice sheet retreat (Laberg and Vorren, 2000; Piper and Ingram, 2003; Bryn et al., 2005; Piper, 2005). The passive nature of both these margins means that sediments deposited by the ice sheets were rarely subject to seismic shaking sufficient to generate large surface motions. Sufficient sediment was therefore able to

accumulate in both regions before failure was triggered by the increased seismicity associated with deglaciation. In contrast, no large submarine landslides have been identified on the South Alaskan Margin during the Quaternary. Here, ice sheet deposited sediments as well as those deposited more recently by rivers are exposed to repeated strong ground-shaking. Observations from large historical earthquakes, i.e. the 1964 Alaskan Earthquake, have shown that smaller scale submarine mass movements regularly remove weaker sediments (Brothers et al., 2016), while subduction zone shaking has been shown to lead to enhanced consolidation and strengthening of seafloor sediment (Sultan et al., 2004a; Völker et al., 2011; Sawyer and DeVore, 2015; Pope et al., 2017a; Sawyer et al., 2017). The combination of enhanced consolidation and the regular removal of weaker sediments therefore likely prevents large submarine landslides occurring on active glaciated margins.

8.3.2. An integrated model of submarine landslides on glaciated margins?

The Bryn et al. (2005) model of large submarine landslide occurrence was used in geohazard assessment for the development of the Ormen Lange gas field (Solheim et al., 2005b) and has since been used to inform tsunami hazard assessment on the margins of the Nordic Seas (e.g. Tsunami risk and strategies for the European Region Project). Hazard assessment for submarine landslides requires the likely triggering mechanisms, failure dynamics and frequency of events to be identified (Talling et al., 2014; Pope et al., 2015). However, our increasing understanding of landslides along the Norwegian Margin has shown significant differences between landslides on different parts of the margins.

In terms of frequency, the Bryn et al. (2005) model suggests that each submarine landslide requires a separate ice stream advance to the shelf edge; each advance delivering sediment to fill the slide scar from the previous event and recharge the slope for failure (Fig. 30). However, dating of other landslides along this margin shows that landslide recurrence does not correlate simply with each ice advance. The Nyk and Trænadjupet Slides were separated by about 14 ka. A short lived glacial advance occurred between the two events but did not reach the shelf edge nor did it result in a large

1863 increase in sedimentation (Olsen et al., 2001b). Even in the Storegga area the recurrence rate for the
1864 three submarine landslides that occurred here (Storegga, R and S) was 200 kyr representing multiple
1865 ice stream advances to the shelf edge (Hjelstuen et al., 2005).

1866 A contrast between the failure dynamics also exists. Analysis of the Storegga Slide deposits has led
1867 to the interpretation that the slide was a retrogressive failure during which the slide mass
1868 disintegrated rapidly forming a large turbidite (Haflidason et al., 2004; Bondevik et al., 2005; Masson
1869 et al., 2006). The initial acceleration of the slide mass was key to the generation of the associated
1870 tsunami (Løvholt et al., 2005; Harbitz et al., 2006). In contrast, detailed analysis of the Trænadjupet
1871 Slide has led to the hypothesis that the Trænadjupet Slide occurred top-down due to the presence of
1872 three progressively deeper headwalls and that the slide mass largely failed to disintegrate as shown
1873 by the presence of large block fields (Laberg et al., 2002b). Progressive subaerial landslides have
1874 been recognised in a number of locations, notably Norway and Quebec (Locat et al., 2008; Quinn et
1875 al., 2012). These landslides are generally a consequence of strain induced loss of structure in clays
1876 resulting in slope failure (Urciuoli et al., 2007). In the submarine environment, top-down slope
1877 failure would likely have been initiated as a consequence of pore pressure build-up along a 'weak'
1878 layer. This is likely to have been a contouritic deposit in the Trænadjupet case (Sultan et al., 2004a;
1879 Baeten et al., 2014). Failure of the initial sediment package and its downslope progression resulted
1880 in the subsequent failure of deeper 'weak' layers due to shearing or rapid increases in overburden
1881 pressure. It is possible that the occurrence of the Nyk Slide played a significant role in the triggering
1882 of the Trænadjupet Slide either through unloading of the seafloor or as a consequence of
1883 deformation of seafloor sediments due to overriding slide material (Fig. 30). The different failure
1884 dynamics means that the tsunamigenic potential of landslides from the two regions is probably
1885 different (Løvholt et al., 2005; 2016; 2017).

1886 Despite the clear similarities identified in terms of preconditioning and triggering mechanisms in the
1887 Storegga and Trænadjupet regions clear differences exist which are important for understanding

landslide processes on glaciated margins. This suggests that a single model of landslide occurrence may not be appropriate. Further work is therefore needed in order to understand whether the close temporal association of the Nyk and Trænadjupet Slides is unique or whether this can be a common feature on these margins.

9. Conclusions

Our understanding of glaciated continental margin processes and evolution has come predominantly from studies of the Nordic Seas during the last glacial period. Using a combination of geophysical and sedimentological records, these studies have produced conceptual models for processes associated with different morphological features, continental slope architecture and the primary drivers (e.g. climate) behind these observations. Here, we have reviewed the current understanding of ice sheet growth and decay around the Nordic Seas and how this is related to the history of sedimentation and margin architecture. These histories have then been compared with other glaciated margins in order to identify unified models of glaciated continental margin evolution. This contribution achieves the following:

1) A comprehensive record of Greenland, Barents Sea and Scandinavian Ice Sheet growth and decay on the margins of the Nordic Seas over the last 2.58 Ma is provided.
2) The record of sedimentation and submarine mass movements which have occurred as a consequence of the growth and decay of the reconstructed ice sheets has been compiled.
3) However, the completeness of ice sheet growth and decay records and the record of sedimentary processes is shown to be temporally and spatially highly variable.
4) From the records of ice sheet growth and decay and the associated sedimentation, we have been able to review the first order controls on sediment delivery to the continental margin at the scale of an ice sheet.
5) We have identified a new conceptual model of trough-mouth fans and glaciated margins worldwide according to the driving factors behind their associated sedimentary processes.

6) We have provided a review of the relationship between ice sheets and large submarine landslides on glaciated margins. We have tested previous models of submarine landslide occurrence on glaciated margins using this information and hence proposed an additional model to explain some large submarine landslides.

Acknowledgements

This contribution is based on the previous work by numerous individuals worldwide whose efforts we greatly appreciate. This research was supported by the UK NERC Arctic Research Programme under the project on whether climate change increases the landslide-tsunami risk to the UK (NE/K00008K/1). E. Pope was supported by grant NE/K00008K/1. We thank the editor Ian Candy, Jonathan Lee and an anonymous reviewer; their comments greatly improved the manuscript.

References

Adrielsson, L., Alexanderson, H., 2005. Interactions between the Greenland Ice Sheet and the Liverpool Land coastal ice cap during the last two glaciation cycles. Journal of Quaternary Science 20, 269-283.

Aksu, A.E., Hiscott, R.N., 1989. Slides and debris flows on the high-latitude continental slopes of Baffin Bay. Geology 17, 885-888.

Aksu, A.E., Hiscott, R.N., 1992. Shingled Quaternary debris flow lenses on the north-east Newfoundland Slope. Sedimentology 39, 193-206.

Aksu, A.E., Piper, D.J.W., 1987. Late Quaternary sedimentation in Baffin Bay. Canadian Journal of Earth Sciences 24, 1833-1846.

Alley, R.B., Blankenship, D.D., Rooney, S.T., Bentley, C.R., 1989. Sedimentation beneath ice shelves—the view from ice stream B. Mar Geol 85, 101-120.

Alvarado, A., 2006. Updates on MMS (Minerals Management Service) regulatory issues for offshore operators. Uniform Resource Locator (URL): http://www.southerngas.org/EVENTS/documents/SGAOGO06Alvarado.pdf (accessed 13 March, 2007).

Amblas, D., Canals, M., 2016. Contourite drifts and canyon-channel systems on the Northern Antarctic Peninsula Pacific margin. Geological Society, London, Memoirs 46, 393-394.

Amblas, D., Urgeles, R., Canals, M., Calafat, A.M., Rebesco, M., Camerlenghi, A., Estrada, F., De Batist, M., Hughes-Clarke, J.E., 2006. Relationship between continental rise development and palaeo-ice sheet dynamics, Northern Antarctic Peninsula Pacific margin. Quaternary Sci Rev 25, 933-944.

Andersen, E.S., Dokken, T.M., Elverhoi, A., Solheim, A., Fossen, I., 1996. Late Quaternary sedimentation and glacial history of the western Svalbard continental margin. Mar Geol 133, 123-156.

Andersen, E.S., Solheim, A., Elverhøi, A., 1994. Development of a high Arctic margin, exemplified by the western margin of Svalbard, International Conference on Arctic Margins, Alaska, pp. 155 - 160.

Anderson, J.B., Wright, R., Andrews, B., 1986. Weddell Fan and associated abyssal plain, Antarctica: morphology, sediment processes, and factors influencing sediment supply. Geo-Mar Lett 6, 121-129.

Andreassen, K., Hubbard, A., Winsborrow, M., Patton, H., Vadakkepuliyambatta, S., Plaza-Faverola, A., Gudlaugsson, E., Serov, P., Deryabin, A., Mattingsdal, R., 2017. Massive blow-out craters formed by hydrate-controlled methane expulsion from the Arctic seafloor. Science 356, 948-953.

Andreassen, K., Nilssen, L.C., Rafaelsen, B., Kuilman, L., 2004. Three-dimensional seismic data from the Barents Sea margin reveal evidence of past ice streams and their dynamics. Geology 32, 729-732.

Andreassen, K., Ødegaard, C.M., Rafaelsen, B., 2007. Imprints of former ice streams, imaged and interpreted using industry three-dimensional seismic data from the south-western Barents Sea. Geological Society, London, Special Publications 277, 151-169.

Andrews, J.T., 2008. The role of the Iceland Ice Sheet in the North Atlantic during the late Quaternary: a review and evidence from Denmark Strait. Journal of Quaternary Science 23, 3-20.

Azpiroz-Zabala, M., Cartigny, M.J.B., Talling, P.J., Parsons, D.R., Sumner, E.J., Clare, M.A., Simmons, S.M., Cooper, C., Pope, E.L., 2017. Newly recognised turbidity current structure can explain prolonged flushing of submarine canyons. Science Advances 3, e1700200.

Baeten, N.J., Laberg, J.S., Forwick, M., Vorren, T.O., Vanneste, M., Forsberg, C.F., Kvalstad, T.J., Ivanov, M., 2013. Morphology and origin of smaller-scale mass movements on the continental slope off northern Norway. Geomorphology 187, 122-134.

Baeten, N.J., Laberg, J.S., Vanneste, M., Forsberg, C.F., Kvalstad, T.J., Forwick, M., Vorren, T.O., Haflidason, H., 2014. Origin of shallow submarine mass movements and their glide planes—Sedimentological and geotechnical analyses from the continental slope off northern Norway. Journal of Geophysical Research: Earth Surface 119, 2335-2360.

Ballin, T.B., 2017. Rising waters and processes of diversification and unification in material culture: the flooding of Doggerland and its effect on north-west European prehistoric populations between ca. 13 000 and 1500 cal BC. Journal of Quaternary Science 32, 329-339.

Baltzer, A., Cochonat, P., Piper, D.J.W., 1994. In situ geotechnical characterization of sediments on the Nova Scotian Slope, eastern Canadian continental margin. Mar Geol 120, 291-308.

Bart, P.J., De Batist, M., Jokat, W., 1999. Interglacial collapse of Crary Trough-mouth fan, Weddell Sea, Antarctica: implications for Antarctic glacial history. Journal of Sedimentary Research 69.

Batchelor, C.L., Ottesen, D., Dowdeswell, J.A., 2017. Quaternary evolution of the northern North Sea margin through glacigenic debris-flow and contourite deposition. Journal of Quaternary Science 32, 416-426.

Baumann, K.-H., Lackschewitz, K.S., Mangerud, J., Spielhagen, R.F., Wolf-Welling, T.C.W., Henrich, R., Kassens, H., 1995. Reflection of Scandinavian ice sheet fluctuations in Norwegian Sea sediments during the past 150,000 years. Quaternary Res 43, 185-197.

Baumann, K.H., Huber, R., 1999. 12. Sea-surface gradients between the North Atlantic and the Norwegian Sea during the last 3.1 MY: Comparison of Sites 982 and 985, Proceedings of the Ocean Drilling Program: Scientific Results. The Program, p. 179.

Bea, R.G., Wright, S.G., Sircar, P., Niedoroda, A.W., 1983. Wave-Induced Slides in South Pass Block 70, Mississippi Delta. J Geotech Eng-Asce 109, 619-644.

Bellec, V.K., Rise, L., Bøe, R., Dowdeswell, J.A., 2016. Glacially related gullies on the upper continental slope, SW Barents Sea margin. Geological Society, London, Memoirs 46, 381-382.

Bellwald, B., Hjelstuen, B.O., Sejrup, H.P., Haflidason, H., 2016. Postglacial Mass Failures in the Inner Hardangerfjorden System, Western Norway, Adv Nat Tech Haz Res. Springer, pp. 73-82.

Bennett, M.M., 2016. Discursive, material, vertical, and extensive dimensions of post-Cold War Arctic resource extraction. Polar Geography 39, 258-273.

Bennett, M.R., 2003. Ice streams as the arteries of an ice sheet: their mechanics, stability and significance. Earth-Sci Rev 61, 309-339.

Bennett, R., Campbell, D.C., Furze, M.F.A., 2014. The shallow stratigraphy and geohazards of the Northeast Baffin Shelf and Lancaster Sound. Bulletin of Canadian Petroleum Geology 62, 217-231.

Berg, K., Solheim, A., Bryn, P., 2005. The Pleistocene to recent geological development of the Ormen Lange area. Mar Petrol Geol 22, 45-56.

Berndt, C., 2005. Focused fluid flow in passive continental margins. Philosophical Transactions of the Royal Society of London A: Mathematical, Physical and Engineering Sciences 363, 2855-2871.

Berndt, C., Feseker, T., Treude, T., Krastel, S., Liebetrau, V., Niemann, H., Bertics, V.J., Dumke, I., Dünnbier, K., Ferré, B., Graves, C., Gross, F., Hissmann, K., Hühnerbach, V., Krause, S., Lieser, K., Schauer, J., Steinle, L., 2014. Temporal Constraints on Hydrate-Controlled Methane Seepage off Svalbard. Science 343, 284-287.

Best, A.I., Clayton, C.R.I., Longva, O., Szuman, M., 2003. The role of free gas in the activation of submarine slides in Finneidfjord, Adv Nat Tech Haz Res. Springer, pp. 491-498.

Biscontin, G., Pestana, J.M., 2006. Factors affecting seismic response of submarine slopes. Natural Hazards and Earth System Science 6, 97-107.

Biscontin, G., Pestana, J.M., Nadim, F., 2004. Seismic triggering of submarine slides in soft cohesive soil deposits. Mar Geol 203, 341-354.

Björck, S., Bennike, O., Ingólfsson, Ó., Barnekow, L., Penney, D.N., 1994a. Lake Boksehandsken's earliest postglacial sediments and their palaeoenvironmental implications, Jameson Land, East Greenland. Boreas 23, 459-472.

Björck, S., Wohlfarth, B., Bennike, O., Hjort, C., Persson, T., 1994b. Revision of the early Holocene lake sediment based chronology and event stratigraphy on Hochstetter Forland, NE Greenland. Boreas 23, 513-523.

Bond, G., Heinrich, H., Broecker, W., Labeyrie, L., McManus, J.F., Andrews, J., Huon, S., Jantschik, R., Clasen, S., Simet, C., 1992. Evidence for massive discharges of icebergs into the North Atlantic ocean during the last glacial period.

Bond, G.C., Showers, W., Elliot, M., Evans, M., Lotti, R., Hajdas, I., Bonani, G., Johnson, S., 1999. The North Atlantic's 1-2 Kyr Climate Rhythm: Relation to Heinrich Events, Dansgaard/Oeschger Cycles and the Little Ice Age. Mechanisms of global climate change at millennial time scales, 35-58.

Bondevik, S., 2003. Storegga tsunami sand in peat below the Tapes beach ridge at Harøy, western Norway, and its possible relation to an early Stone Age settlement. Boreas 32, 476-483.

Bondevik, S., Løvholt, F., Harbitz, C.B., Mangerud, J., Dawson, A., Inge Svendsen, J., 2005. The Storegga Slide tsunami—comparing field observations with numerical simulations. Mar Petrol Geol 22, 195-208.

Bondevik, S., Mangerud, J., Dawson, S., Dawson, A., Lohne, Ø., 2003. Record-breaking height for 8000-year-old tsunami in the North Atlantic. Eos, Transactions American Geophysical Union 84, 289-293.

Bondevik, S., Stormo, S.K., Skjerdal, G., 2012. Green mosses date the Storegga tsunami to the chilliest decades of the 8.2 ka cold event. Quaternary Sci Rev 45, 1-6.

Bondevik, S., Svendsen, J.I., Johnson, G., Mangerud, J., Kaland, P.E., 1997. The Storegga tsunami along the Norwegian coast, its age and run up. Boreas 26, 29-53.

Böse, M., Lüthgens, C., Lee, J.R., Rose, J., 2012. Quaternary glaciations of northern Europe. Quaternary Sci Rev 44, 1-25.

Boswell, R., Collett, T.S., 2011. Current perspectives on gas hydrate resources. Energy & environmental science 4, 1206-1215.

Boulton, G.S., 1978. Boulder shapes and grain-size distributions of debris as indicators of transport paths through a glacier and till genesis. Sedimentology 25, 773-799.

Brendryen, J., Haflidason, H., Rise, L., Chand, S., Vanneste, M., Longva, O., L'Heureux, J.S., Forsberg, C.F., 2015. Ice sheet dynamics on the Lofoten–Vesterålen shelf, north Norway, from Late MIS-3 to Heinrich Stadial 1. Quaternary Sci Rev 119, 136-156.

Broecker, W.S., Denton, G.H., 1990. The role of ocean-atmosphere reorganizations in glacial cycles. Quaternary Sci Rev 9, 305-341.

Brothers, D.S., Haeussler, P.J., Liberty, L., Finlayson, D., Geist, E.L., Labay, K., Byerly, M., 2016. A submarine landslide source for the devastating 1964 Chenega tsunami, southern Alaska. Earth and Planetary Science Letters 438, 112-121.

Brothers, D.S., Luttrell, K.M., Chaytor, J.D., 2013. Sea-level-induced seismicity and submarine landslide occurrence. Geology 41, 979-982.

Bryn, P., Berg, K., Forsberg, C.F., Solheim, A., Kvalstad, T.J., 2005. Explaining the Storegga slide. Mar Petrol Geol 22, 11-19.

Bryn, P., Solheim, A., Berg, K., Lien, R., Forsberg, C.F., Haflidason, H., Ottesen, D., Rise, L., 2003. The Storegga Slide complex; repeated large scale sliding in response to climatic cyclicity, Adv Nat Tech Haz Res. Springer, pp. 215-222.

Bugge, T., 1983. Submarine slides on the Norwegian continental margin, with special emphasis on the Storegga area, vol. 110. Trondheim, Norway: Continental Shelf and Petroleum Technology Research Institute, A/S publication.

Bugge, T., Befring, S., Belderson, R.H., Eidvin, T., Jansen, E., Kenyon, N.H., Holtedahl, H., Sejrup, H.P., 1987. A giant three-stage submarine slide off Norway. Geo-Mar Lett 7, 191-198.

Bungum, H., Lindholm, C., Faleide, J.I., 2005. Postglacial seismicity offshore mid-Norway with emphasis on spatio-temporal–magnitudal variations. Mar Petrol Geol 22, 137-148.

Busetti, M., Caburlotto, A., Armand, L., Damiani, D., Giorgetti, G., Lucchi, R.G., Quilty, P.G., Villa, G., 2003. Plio-Quaternary sedimentation on the Wilkes Land continental rise: preliminary results. Deep Sea Research Part II: Topical Studies in Oceanography 50, 1529-1562.

Butt, F.A., Drange, H., Elverhøi, A., Otterå, O.H., Solheim, A., 2002. Modelling Late Cenozoic isostatic elevation changes in the Barents Sea and their implications for oceanic and climatic regimes: preliminary results. Quaternary Sci Rev 21, 1643-1660.

Butt, F.A., Elverhøi, A., Forsberg, C.F., Solheim, A., 2001a. Evolution of the Scoresby Sund Fan, central East Green land-evidence from ODP Site 987. NORSK GEOLOGISK TIDSSKRIFT 81, 3-15.

Butt, F.A., Elverhøi, A., Hjelstuen, B.O., Dimakis, P., Solheim, A., 2001b. Modelling late Cenozoic isostatic elevation changes in Storfjorden, NW Barents Sea: an indication of varying erosional regimes. Sediment Geol 143, 71-89.

Campbell, D.C., Mosher, D.C., 2014. Detailed geomorphology and surficial geology of the outer Nova Scotia margin. Atlantic Geology 50.

Canals, M., Amblas, D., Casamor, J.L., Lastras, G., 2016. Gebra Slide: glacial and tectonic controls on recurrent submarine landsliding off the northern tip of the Antarctic Peninsula. Geological Society, London, Memoirs 46, 417-418.

Canals, M., Calafat, A., Camerlenghi, A., De Batist, M., Urgeles, R., Farran, M., Geletti, R., Versteeg, W., Amblas, D., Rebesco, M., 2003. Uncovering the footprint of former ice streams off Antarctica. EOS: TRANSACTIONS AMERICAN GEOPHYSICAL UNION 84, 97-103.

Canals, M., Lastras, G., Urgeles, R., Casamor, J.L., Mienert, J., Cattaneo, A., De Batist, M., Haflidason, H., Imbo, Y., Laberg, J.S., Locat, J., Long, D., Longva, O., Masson, D.G., Sultan, N., Trincardi, F., Bryn, P., 2004. Slope failure dynamics and impacts from seafloor and shallow sub-seafloor geophysical data: case studies from the COSTA project. Mar Geol 213, 9-72.

Carter, L., Gavey, R., Talling, P.J., Liu, J.T., 2014. Insights into submarine geohazards from breaks in subsea telecommunication cables. Oceanography 27, 58-67.

Carter, L., Milliman, J.D., Talling, P.J., Gavey, R., Wynn, R.B., 2012. Near-synchronous and delayed initiation of long run-out submarine sediment flows from a record-breaking river flood, offshore Taiwan. Geophys Res Lett 39.

Casas, D., Ercilla, G., García, M., Yenes, M., Estrada, F., 2013. Post-rift sedimentary evolution of the Gebra Debris Valley. A submarine slope failure system in the Central Bransfield Basin (Antarctica). Mar Geol 340, 16-29.

Catania, G.A., Scambos, T.A., Conway, H., Raymond, C.F., 2006. Sequential stagnation of Kamb ice stream, West Antarctica. Geophys Res Lett 33.

Cattaneo, A., Babonneau, N., Ratzov, G., Dan-Unterseh, G., Yelles, K., Bracene, R., De Lepinay, B.M., Boudiaf, A., Déverchere, J., 2012. Searching for the seafloor signature of the 21 May 2003 Boumerdes earthquake offshore central Algeria. Nat Hazard Earth Sys 12, 2159-2172.

Chand, S., Thorsnes, T., Rise, L., Brunstad, H., Stoddart, D., Bøe, R., Lågstad, P., Svolsbru, T., 2012. Multiple episodes of fluid flow in the SW Barents Sea (Loppa High) evidenced by gas flares, pockmarks and gas hydrate accumulation. Earth and Planetary Science Letters 331, 305-314.

Channell, J.E.T., Smelror, M., Jansen, E., Higgins, S.M., Lehman, B., Eidvin, T., Solheim, A., 1999. 10. Age models for glacial fan deposits off East Greenland and Svalbard (Sites 986 and 987), Proceedings of the Ocean Drilling Program: Scientific results. The Program, p. 149.

Christoffersen, P., Tulaczyk, S., Behar, A., 2010. Basal ice sequences in Antarctic ice stream: Exposure of past hydrologic conditions and a principal mode of sediment transfer. Journal of Geophysical Research: Earth Surface (2003–2012) 115.

Clare, M., Pope, E., Talling, P., Hunt, J., Carter, L., 2016a. What threat do turbidity currents and submarine landslides pose to submarine telecommunications cable infrastructure?, EGU General Assembly Conference Abstracts, p. 4347.

Clare, M.A., Hughes Clarke, J.E., Talling, P.J., Cartigny, M.J.B., Pratomo, D.G., 2016b. Preconditioning and triggering of offshore slope failures and turbidity currents revealed by most detailed monitoring yet at a fjord-head delta. Earth and Planetary Science Letters 450, 208-220.

Clark, C.D., 1993. Mega-scale glacial lineations and cross-cutting ice-flow landforms. Earth Surf Proc Land 18, 1-29.

Clark, P.U., Mitrovica, J.X., Milne, G.A., Tamisiea, M.E., 2002. Sea-level fingerprinting as a direct test for the source of global meltwater pulse IA. Science 295, 2438-2441.

Cooper, A.K., Barrett, P.J., Hinz, K., Traube, V., Letichenkov, G., Stagg, H.M.J., 1991. Cenozoic prograding sequences of the Antarctic continental margin: a record of glacio-eustatic and tectonic events. Mar Geol 102, 175-213.

Covault, J.A., Graham, S.A., 2010. Submarine fans at all sea-level stands: Tectono-morphologic and climatic controls on terrigenous sediment delivery to the deep sea. Geology 38, 939-942.

Cuffey, K.M., Paterson, W.S.B., 2010. The physics of glaciers. Academic Press.

Curran, K.J., Hill, P.S., Milligan, T.G., Cowan, E.A., Syvitski, J.P.M., Konings, S.M., 2004. Fine-grained sediment flocculation below the Hubbard Glacier meltwater plume, Disenchantment Bay, Alaska. Mar Geol 203, 83-94.

Dahlgren, K.I.T., Vorren, T.O., 2003. Sedimentary environment and glacial history during the last 40 ka of the Vøring continental margin, mid-Norway. Mar Geol 193, 93-127.

Dahlgren, K.I.T., Vorren, T.O., Laberg, J.S., 2002. Late Quaternary glacial development of the mid-Norwegian margin—65 to 68 N. Mar Petrol Geol 19, 1089-1113.

Dahlgren, K.I.T., Vorren, T.O., Stoker, M.S., Nielsen, T., Nygård, A., Sejrup, H.P., 2005. Late Cenozoic prograding wedges on the NW European continental margin: their formation and relationship to tectonics and climate. Mar Petrol Geol 22, 1089-1110.

Dawson, A., Long, D., Smith, D., 1988. The Storegga slides: evidence from eastern Scotland for a possible tsunami. Mar Geol 82, 271-276.

De Santis, L., Brancolini, G., Donda, F., 2003. Seismo-stratigraphic analysis of the Wilkes Land continental margin (East Antarctica): influence of glacially driven processes on the Cenozoic deposition. Deep Sea Research Part II: Topical Studies in Oceanography 50, 1563-1594.

Denton, G.H., Hughes, T.J., 2002. Reconstructing the Antarctic Ice Sheet at the Last Glacial Maximum. Quaternary Sci Rev 21, 193-202.

Dokken, T.M., Jansen, E., 1999. Rapid changes in the mechanism of ocean convection during the last glacial period. Nature 401, 458-461.

Donda, F., Brancolini, G., O'Brien, P.E., De Santis, L., Escutia, C., 2007. Sedimentary processes in the Wilkes Land margin: a record of the Cenozoic East Antarctic Ice Sheet evolution. Journal of the Geological Society 164, 243-256.

Doré, A.G., Corcoran, D.V., Scotchman, I.C., 2002. Prediction of the hydrocarbon system in exhumed basins, and application to the NW European margin. Geological Society, London, Special Publications 196, 401-429.

Doré, A.G., Jensen, L.N., 1996. The impact of late Cenozoic uplift and erosion on hydrocarbon exploration: offshore Norway and some other uplifted basins. Global and Planetary Change 12, 415-436.

Dowdeswell, E.K., Todd, B.J., Dowdeswell, J.A., 2016a. Canyons and slides on the continental slope seaward of a shallow bank, Labrador margin, eastern Canada. Geological Society, London, Memoirs 46, 405-406.

Dowdeswell, J.A., Canals, M., Jakobsson, M., Todd, B.J., Dowdeswell, E.K., Hogan, K.A., 2016b. Introduction: an Atlas of Submarine Glacial Landforms. Geological Society, London, Memoirs 46, 3-14.

Dowdeswell, J.A., Dowdeswell, E.K., Todd, B.J., Saint-Ange, F., Piper, D.J.W., 2016c. Channels and gullies on the continental slope seaward of a cross-shelf trough, Labrador margin, eastern Canada. Geological Society, London, Memoirs 46, 385-386.

Dowdeswell, J.A., Elverhøi, A., 2002. The timing of initiation of fast-flowing ice streams during a glacial cycle inferred from glacimarine sedimentation. Mar Geol 188, 3-14.

Dowdeswell, J.A., Elverhøi, A., Andrews, J.T., Hebbeln, D., 1999. Asynchronous deposition of ice-rafted layers in the Nordic seas and North Atlantic Ocean. Nature 400, 348-351.

Dowdeswell, J.A., Elverhoi, A., Spielhagen, R., 1998. Glacimarine sedimentary processes and facies on the Polar North Atlantic margins. Quaternary Sci Rev 17, 243-272.

Dowdeswell, J.A., Evans, J., Ó Cofaigh, C., 2010a. Submarine landforms and shallow acoustic stratigraphy of a 400 km-long fjord-shelf-slope transect, Kangerlussuaq margin, East Greenland. Quaternary Sci Rev 29, 3359-3369.

Dowdeswell, J.A., Evans, J., Ó Cofaigh, C., Anderson, J.B., 2006a. Morphology and sedimentary processes on the continental slope off Pine Island Bay, Amundsen Sea, West Antarctica. Geological Society of America Bulletin 118, 606-619.

Dowdeswell, J.A., Hogan, K.A., Arnold, N.S., Mugford, R.I., Wells, M., Hirst, J.P.P., Decalf, C., 2015. Sediment-rich meltwater plumes and ice-proximal fans at the margins of modern and ancient tidewater glaciers: Observations and modelling. Sedimentology 62, 1665-1692.

Dowdeswell, J.A., Kenyon, N.H., Elverhøi, A., Laberg, J.S., Hollender, F.J., Mienert, J., Siegert, M.J., 1996. Large-scale sedimentation on the glacier-influenced polar North Atlantic Margins: Long-range side-scan sonar evidence. Geophys Res Lett 23, 3535-3538.

Dowdeswell, J.A., Kenyon, N.H., Laberg, J.S., 1997. The glacier-influenced Scoresby Sund Fan, East Greenland continental margin: evidence from GLORIA and 3.5 kHz records. Mar Geol 143, 207-221.

Dowdeswell, J.A., Maslin, M.A., Andrews, J.T., McCave, I.N., 1995. Iceberg production, debris rafting, and the extent and thickness of Heinrich layers (H-1, H-2) in North Atlantic sediments. Geology 23, 301-304.

Dowdeswell, J.A., Ó Cofaigh, C., Noormets, R., Larter, R.D., Hillenbrand, C.-D., Benetti, S., Evans, J., Pudsey, C.J., 2008. A major trough-mouth fan on the continental margin of the Bellingshausen Sea, West Antarctica: the Belgica Fan. Mar Geol 252, 129-140.

Dowdeswell, J.A., Ó Cofaigh, C., Pudsey, C.J., 2004. Continental slope morphology and sedimentary processes at the mouth of an Antarctic palaeo-ice stream. Mar Geol 204, 203-214.

Dowdeswell, J.A., Ottesen, D., 2013. Buried iceberg ploughmarks in the early Quaternary sediments of the central North Sea: a two-million year record of glacial influence from 3D seismic data. Mar Geol 344, 1-9.

Dowdeswell, J.A., Ottesen, D., Rise, L., 2006b. Flow switching and large-scale deposition by ice streams draining former ice sheets. Geology 34, 313-316.

Dowdeswell, J.A., Ottesen, D., Rise, L., 2010b. Rates of sediment delivery from the Fennoscandian Ice Sheet through an ice age. Geology 38, 3-6.

Dowdeswell, J.A., Siegert, M.J., 1999. Ice-sheet numerical modeling and marine geophysical measurements of glacier-derived sedimentation on the Eurasian Arctic continental margins. Geological Society of America Bulletin 111, 1080-1097.

Dreger, D., 1999. Decadal to Centennial Scale Sediment Records of Ice Advance on the Barents Shelf and Meltwater Discharge Into the Northeastern Norwegian Sea Over the Last 40 Kyr: Dekadische Bis Jahrhundert-Variabilität Von Eisvorstößen Auf Dem Barentsschelf und Schmelzwasserschüben in Die Nordöstliche Norwegensee Während Der Letzten 40 Ka. Inst. für Geowiss., pp. 1 - 79.

Dugan, B., Flemings, P.B., 2000. Overpressure and fluid flow in the New Jersey continental slope: implications for slope failure and cold seeps. Science 289, 288-291.

Dugan, B., Sheahan, T.C., 2012. Offshore sediment overpressures of passive margins: Mechanisms, measurement, and models. Rev Geophys 50.

Egholm, D.L., Pedersen, V.K., Knudsen, M.F., Larsen, N.K., 2012. Coupling the flow of ice, water, and sediment in a glacial landscape evolution model. Geomorphology 141, 47-66.

Ehlers, J., Gibbard, P.L., 2004. Quaternary Glaciations-Extent and Chronology: Part I: Europe. Elsevier.
Eidvin, T., Brekke, H., Riis, F., Renshaw, D.K., 1998. Cenozoic stratigraphy of the Norwegian Sea continental shelf, 64 N-68 N. Norsk Geologisk Tidsskrift 78, 125-152.

Eidvin, T., Jansen, E., Rundberg, Y., Brekke, H., Grogan, P., 2000. The upper Cainozoic of the Norwegian continental shelf correlated with the deep sea record of the Norwegian Sea and the North Atlantic. Mar Petrol Geol 17, 579-600.

El-Robrini, M., Gennesseaux, M., Mauffret, A., 1985. Consequences of the El-Asnam earthquakes: Turbidity currents and slumps on the Algerian margin (Western Mediterranean). Geo-Mar Lett 5, 171-176.

Elverhøi, A., Andersen, E.S., Dokken, T., Hebbeln, D., Spielhagen, R., Svendsen, J.I., Sorflaten, M., Rornes, A., Hald, M., Forsberg, C.F., 1995. The growth and decay of the late weichselian ice sheet in western Svalbard and adjacent areas based on provenance studies of marine sediments. Quaternary Res 44, 303-316.

Elverhøi, A., Hooke, R.L.B., Solheim, A., 1998. Late Cenozoic erosion and sediment yield from the Svalbard–Barents Sea region: Implications for understanding erosion of glacierized basins. Quaternary Sci Rev 17, 209-241.

Escutia, C., De Santis, L., Donda, F., Dunbar, R.B., Cooper, A.K., Brancolini, G., Eittreim, S.L., 2005. Cenozoic ice sheet history from East Antarctic Wilkes Land continental margin sediments. Global and Planetary Change 45, 51-81.

Escutia, C., Eittreim, S.L., Cooper, A.K., Nelson, C.H., 2000. Morphology and acoustic character of the Antarctic Wilkes Land turbidite systems: ice-sheet-sourced versus river-sourced fans. Journal of Sedimentary Research 70, 84-93.

Escutia, C., Warnke, D., Acton, G.D., Barcena, A., Burckle, L., Canals, M., Frazee, C.S., 2003. Sediment distribution and sedimentary processes across the Antarctic Wilkes Land margin during the Quaternary. Deep Sea Research Part II: Topical Studies in Oceanography 50, 1481-1508.

Evans, J., Ó Cofaigh, C., Dowdeswell, J.A., Wadhams, P., 2009. Marine geophysical evidence for former expansion and flow of the Greenland Ice Sheet across the north-east Greenland continental shelf. Journal of Quaternary Science 24, 279-293.

Faleide, J.I., Kyrkjebø, R., Kjennerud, T., Gabrielsen, R.H., Jordt, H., Fanavoll, S., Bjerke, M.D., 2002. Tectonic impact on sedimentary processes during Cenozoic evolution of the northern North Sea and surrounding areas. Geological Society, London, Special Publications 196, 235-269.

Faleide, J.I., Solheim, A., Fiedler, A., Hjelstuen, B.O., Andersen, E.S., Vanneste, K., 1996. Late Cenozoic evolution of the western Barents Sea-Svalbard continental margin. Global and Planetary Change 12, 53-74.

Felix, M., Peakall, J., McCaffrey, W.D., 2006. Relative importance of processes that govern the generation of particulate hyperpycnal flows. Journal of Sedimentary Research 76, 382-387.

Fiedler, A., Faleide, J.I., 1996. Cenozoic sedimentation along the southwestern Barents Sea margin in relation to uplift and erosion of the shelf. Global and Planetary Change 12, 75-93.

Fine, I.V., Rabinovich, A.B., Bornhold, B.D., Thomson, R.E., Kulikov, E.A., 2005. The Grand Banks landslide-generated tsunami of November 18, 1929: preliminary analysis and numerical modeling. Mar Geol 215, 45-57.

Fjeldskaar, W., Amantov, A., 2017. Effects of glaciations on sedimentary basins. J Geodyn.

Fjeldskaar, W., Lindholm, C., Dehls, J.F., Fjeldskaar, I., 2000. Postglacial uplift, neotectonics and seismicity in Fennoscandia. Quaternary Sci Rev 19, 1413-1422.

Flemings, P.B., Long, H., Dugan, B., Germaine, J., John, C.M., Behrmann, J.H., Sawyer, D., Scientists, I.E., 2008. Erratum to "Pore pressure penetrometers document high overpressure near the seafloor where multiple submarine landslides have occurred on the continental slope, offshore Louisiana, Gulf of Mexico" (vol 269, pg 309, 2008). Earth and Planetary Science Letters 274, 269-283.

Forsberg, C.F., Solheim, A., Elverhøi, A., Jansen, E., Channell, J.E.T., Andersen, E.S., 1999. 17. The depositional environment of the Western Svalbard margin during the Late Pliocene and the Pleistocene: Sedimentary facies changes at Site 986, Proceedings of the Ocean Drilling Program: Scientific results. The Program, p. 233.

Fronval, T., Jansen, E., 1996. Late Neogene paleoclimates and paleoceanography in the Iceland-Norwegian Sea: evidence from the Iceland and Vøring Plateaus, Proceedings of the Ocean Drilling Program. Scientific Results. Ocean Drilling Program, pp. 455-468.

Fronval, T., Jansen, E., 1997. Eemian and early Weichselian (140–60 ka) paleoceanography and paleoclimate in the Nordic seas with comparisons to Holocene conditions. Paleoceanography 12, 443-462.

Fruergaard, M., Piasecki, S., Johannessen, P.N., Noe-Nygaard, N., Andersen, T.J., Pejrup, M., Nielsen, L.H., 2015. Tsunami propagation over a wide, shallow continental shelf caused by the Storegga slide, southeastern North Sea, Denmark. Geology 43, 1047-1050.

Funder, S., Hansen, L., 1996. The Greenland ice sheet-a model for its culmination and decay during and after the last glacial maximum. Geological Society of Denmark.

Funder, S., Hjort, C., Landvik, J.Y., 1994. The last glacial cycles in East Greenland, an overview. Boreas 23, 283-293.

Funder, S., Hjort, C., Landvik, J.Y., Nam, S.-I., Reeh, N., Stein, R., 1998. History of a stable ice margin—East Greenland during the middle and upper Pleistocene. Quaternary Sci Rev 17, 77-123.

Funder, S., Kjeldsen, K.K., Kjær, K.H., Ó Cofaigh, C., 2011. The Greenland Ice Sheet during the past 300,000 years: A review. Developments in Quaternary Science 15, 699-713.

Gales, J.A., Forwick, M., Laberg, J.S., Vorren, T.O., Larter, R.D., Graham, A.G.C., Baeten, N.J., Amundsen, H.B., 2013. Arctic and Antarctic submarine gullies—A comparison of high latitude continental margins. Geomorphology 201, 449-461.

Gales, J.A., Larter, R.D., Leat, P.T., Jokat, W., 2016. Components of an Antarctic trough-mouth fan: examples from the Crary Fan, Weddell Sea. Geological Society, London, Memoirs 46, 377-378.

Gales, J.A., Leat, P.T., Larter, R.D., Kuhn, G., Hillenbrand, C.-D., Graham, A.G.C., Mitchell, N.C., Tate, A.J., Buys, G.B., Jokat, W., 2014. Large-scale submarine landslides, channel and gully systems on the southern Weddell Sea margin, Antarctica. Mar Geol 348, 73-87.

García, M., Ercilla, G., Alonso, B., 2009. Morphology and sedimentary systems in the Central Bransfield Basin, Antarctic Peninsula: sedimentary dynamics from shelf to basin. Basin Research 21, 295-314.

García, M., Ercilla, G., Alonso, B., Casas, D., Dowdeswell, J.A., 2011. Sediment lithofacies, processes and sedimentary models in the Central Bransfield Basin, Antarctic Peninsula, since the Last Glacial Maximum. Mar Geol 290, 1-16.

García, M., Ercilla, G., Anderson, J.B., Alonso, B., 2008. New insights on the post-rift seismic stratigraphic architecture and sedimentary evolution of the Antarctic Peninsula margin (Central Bransfield Basin). Mar Geol 251, 167-182.

Gard, G., Backman, J., 1990. Synthesis of Arctic and Sub-Arctic Coccolith Biochronology and History of North Atlantic Drift Water Influx during the Last 500.000 Years, in: Bleil, U., Thiede, J. (Eds.), Geological History of the Polar Oceans: Arctic versus Antarctic. Springer Netherlands, Dordrecht, pp. 417-436.

Gavey, R., Carter, L., Liu, J.T., Talling, P.J., Hsu, R.T., Pope, E.L., Evans, G., 2017. Frequent sediment density flows during 2006 to 2015, triggered by competing seismic and weather events: Observations from subsea cable breaks off southern Tawain. Mar Geol 384, 147-158.

Geist, E.L., 2000. Origin of the 17 July 1998 Papua New Guinea tsunami: earthquake or landslide. Seismological Research Letters 71, 344-351.

Goldfinger, C., 2011. Submarine Paleoseismology Based on Turbidite Records. Annu Rev Mar Sci 3, 35-66.

Goldfinger, C., Nelson, C.H., Morey, A.E., Johnson, J.E., Patton, J.R., Karabanov, E., Gutierrez-Pastor, J., Eriksson, A.T., Gracia, E., Dunhill, G., 2012. Turbidite event history: Methods and implications for Holocene paleoseismicity of the Cascadia subduction zone. US Department of the Interior, US Geological Survey.

Gozhik, P., Lindner, L., Marks, L., 2012. Late Early and early Middle Pleistocene limits of Scandinavian glaciations in Poland and Ukraine. Quatern Int 271, 31-37.

Graham, A.G.C., Larter, R.D., Gohl, K., Hillenbrand, C.-D., Smith, J.A., Kuhn, G., 2009. Bedform signature of a West Antarctic palaeo-ice stream reveals a multi-temporal record of flow and substrate control. Quaternary Sci Rev 28, 2774-2793.

Grauert, M., BJÖRCK, S., Bondevik, S., 2001. Storegga tsunami deposits in a coastal lake on Suouroy, the Faroe Islands. Boreas 30, 263-271.

Gravdal, A., Haflidason, H., Evans, D., 2003. Seabed and subsurface features on the southern Vøring Plateau and northern Storegga slide escarpment, in: Mienert, J., Weaver, P.E. (Eds.), European Margin Sediment Dynamics: Side-Scan Sonar and Seismic Images. Springer, Berlin, pp. 111-117.

Greenwood, S.L., Clark, C.D., 2009. Reconstructing the last Irish Ice Sheet 1: changing flow geometries and ice flow dynamics deciphered from the glacial landform record. Quaternary Sci Rev 28, 3085-3100.

Greenwood, S.L., Clason, C.C., Jakobsson, M., 2016. Ice-flow and meltwater landform assemblages in the Gulf of Bothnia, in: Dowdeswell, J.A., Canals, M., Jakobsson, M., Todd, B.J., Dowdeswell, E.K., Hogan, K.A. (Eds.), Geological Society, London, Memoirs. Geological Society, London, pp. 321-324.

Gulick, S.P.S., Jaeger, J.M., Mix, A.C., Asahi, H., Bahlburg, H., Belanger, C.L., Berbel, G.B.B., Childress, L., Cowan, E., Drab, L., Forwick, M., Fukumura, A., Ge, S., Gupta, S., Kioka, A., Konno, S., LeVay, L.J., März, C., Matsuzaki, K.M., McClymont, E.L., Moy, C., Müller, J., Nakamura, A., Ojima, T., Ribeiro, F.R., Ridgway, K.D., Romero, O.E., Slagle, A.L., Stoner, J.S., St-Onge, G., Suto, I., Walczak, M.D., Worthington, L.L., Bailey, I., Enkelmann, E., Reece, R., Swartz, J.M., 2015. Mid-Pleistocene climate transition drives net mass loss from rapidly uplifting St. Elias Mountains, Alaska. Proceedings of the National Academy of Sciences 112, 15042-15047.

Haflidason, H., Aarseth, I., Haugen, J.-E., Sejrup, H.P., Løvlieb, R., Reither, E., 1991. Quaternary stratigraphy of the Draugen area, mid-Norwegian shelf. Mar Geol 101, 125-146.

Haflidason, H., Iversen, M., Løvlie, R., 1998. Møre and Vøring Basin Geological Investigation: lithological and chronological analyses of the geotechnical borings. Unpublished Report, Department of Geology, University of Bergen, Norway, 50pp.

Haflidason, H., Lien, R., Sejrup, H.P., Forsberg, C.F., Bryn, P., 2005. The dating and morphometry of the Storegga Slide. Mar Petrol Geol 22, 123-136.

Haflidason, H., Sejrup, H.P., Berstad, I.M., Nygård, A., Richter, T.O., Bryn, P., Lien, R., Berg, K., 2003. A weak layer feature on the Northern Storegga Slide escarpment, European Margin Sediment Dynamics. Springer, pp. 55-62.

Haflidason, H., Sejrup, H.P., Nygard, A., Mienert, J., Bryn, P., Lien, R., Forsberg, C.F., Berg, K., Masson, D., 2004. The Storegga Slide: architecture, geometry and slide development. Mar Geol 213, 201-234.

Håkansson, L., Alexanderson, H., Hjort, C., Möller, P., Briner, J.P., Aldahan, A., Possnert, G., 2009. Late Pleistocene glacial history of Jameson Land, central East Greenland, derived from cosmogenic 10Be and 26Al exposure dating. Boreas 38, 244-260.

Håkansson, L., Briner, J., Alexanderson, H., Aldahan, A., Possnert, G., 2007. 10 Be ages from central east Greenland constrain the extent of the Greenland ice sheet during the Last Glacial Maximum. Quaternary Sci Rev 26, 2316-2321.

Hallam, A., 1989. Great geological controversies. Oxford University Press.

Hallet, B., Hunter, L., Bogen, J., 1996. Rates of erosion and sediment evacuation by glaciers: A review of field data and their implications. Global and Planetary Change 12, 213-235.

Hansen, L., Funder, S., Murray, A.S., Mejdahl, V., 1999. Luminescence dating of the last Weichselian glacier advance in East Greenland. Quaternary Sci Rev 18, 179-190.

Harbitz, C.B., Løvholt, F., Bungum, H., 2014. Submarine landslide tsunamis: how extreme and how likely? Nat Hazards 72, 1341-1374.

Harbitz, C.B., Løvholt, F., Pedersen, G., Masson, D.G., 2006. Mechanisms of tsunami generation by submarine landslides: a short review. Norsk Geologisk Tidsskrift 86, 255.

Hart, J.K., Rose, K.C., Martinez, K., 2011. Subglacial till behaviour derived from in situ wireless multi-sensor subglacial probes: Rheology, hydro-mechanical interactions and till formation. Quaternary Sci Rev 30, 234-247.

Heezen, B.C., Ewing, M., 1955. Orleansville earthquake and turbidity currents. AAPG Bulletin 39, 2505-2514.

Heezen, B.C., Ewing, W.M., 1952. Turbidity currents and submarine slumps, and the 1929 Grand Banks [Newfoundland] earthquake. American Journal of Science 250, 849-873.

Heezen, B.C., Menzies, R.J., Schneider, E.D., Ewing, W.M., Granelli, N.C.L., 1964. Congo submarine canyon. AAPG Bulletin 48, 1126-1149.

Helmke, J.P., Bauch, H.A., 2003. Comparison of glacial and interglacial conditions between the polar and subpolar North Atlantic region over the last five climatic cycles. Paleoceanography 18.

Helmke, J.P., Bauch, H.A., Erlenkeuser, H., 2003a. Development of glacial and interglacial conditions in the Nordic seas between 1.5 and 0.35 Ma. Quaternary Sci Rev 22, 1717-1728.

Helmke, J.P., Bauch, H.A., Mazaud, A., 2003b. Evidence for a mid-Pleistocene shift of ice-drift pattern in the Nordic seas. Journal of Quaternary Science 18, 183-191.

Helmke, J.P., Bauch, H.A., Röhl, U., Mazaud, A., 2005. Changes in sedimentation patterns of the Nordic seas region across the mid-Pleistocene. Mar Geol 215, 107-122.

Henrich, R., 1989. Glacial/interglacial cycles in the Norwegian Sea: sedimentology, paleoceanography, and evolution of Late Pliocene to Quaternary northern hemisphere climate, Proceedings of the Ocean Drilling Program, scientific results, pp. 189-232.

Henrich, R., Baumann, K.-H., 1994. Evolution of the Norwegian Current and the Scandinavian Ice Sheets during the past 2.6 my: evidence from ODP Leg 104 biogenic carbonate and terrigenous records. Palaeogeography, Palaeoclimatology, Palaeoecology 108, 75-94.

Henriksen, S., Fichler, C., Grønlie, A., Henningsen, T., Laursen, I., Løseth, H., Ottesen, D., Prince, I., 2005. The Norwegian Sea during the Cenozoic, in: Wandås, B.T.G., Nystuen, J.P., Eide, E., Gradstein, F. (Eds.), Norwegian Petroleum Society Special Publications. Elsevier, pp. 111-133.

Henriksen, S., Vorren, T.O., 1996. Late Cenozoic sedimentation and uplift history on the mid-Norwegian continental shelf. Global and Planetary Change 12, 171-199.

Herman, F., Beaud, F., Champagnac, J.-D., Lemieux, J.-M., Sternai, P., 2011. Glacial hydrology and erosion patterns: a mechanism for carving glacial valleys. Earth and Planetary Science Letters 310, 498-508.

Heroy, D.C., Anderson, J.B., 2005. Ice-sheet extent of the Antarctic Peninsula region during the Last Glacial Maximum (LGM)—Insights from glacial geomorphology. Geological Society of America Bulletin 117, 1497-1512.

Hesse, R., Klauck, I., Khodabakhsh, S., Piper, D., 1999. Continental slope sedimentation adjacent to an ice margin. III. The upper Labrador Slope. Mar Geol 155, 249-276.

Hesse, R., Klaucke, I., Khodabakhsh, S., Piper, D.J.W., Ryan, W.B.F., Group, N.S., 2001. Sandy submarine braid plains: potential deep-water reservoirs. AAPG bulletin 85, 1499-1521.

Hesse, R., Klaucke, I., Khodabakhsh, S., Ryan, W.B.F., 1997. Glacimarine Drainage Systems in Deep-sea: The NAMOC System of the Labrador Sea and its Sibling, in: Davies, T.A., al., e. (Eds.), Glaciated Continental Margins. Springer, pp. 286-289.

Hesse, R., Rashid, H., Khodabakhsh, S., 2004. Fine-grained sediment lofting from meltwater-generated turbidity currents during Heinrich events. Geology 32, 449-452.

Hibbert, F.D., Austin, W.E.N., Leng, M.J., Gatliff, R.W., 2010. British Ice Sheet dynamics inferred from North Atlantic ice-rafted debris records spanning the last 175 000 years. Journal of Quaternary Science 25, 461-482.

Hillenbrand, C.-D., Camerlenghi, A., Cowan, E.A., Hernández-Molina, F.J., Lucchi, R.G., Rebesco, M., Uenzelmann-Neben, G., 2008. The present and past bottom-current flow regime around the sediment drifts on the continental rise west of the Antarctic Peninsula. Mar Geol 255, 55-63.

Hillenbrand, C.-D., Larter, R.D., Dowdeswell, J.A., Ehrmann, W., Ó Cofaigh, C., Benetti, S., Graham, A.G.C., Grobe, H., 2010. The sedimentary legacy of a palaeo-ice stream on the shelf of the southern Bellingshausen Sea: Clues to West Antarctic glacial history during the Late Quaternary. Quaternary Sci Rev 29, 2741-2763.

Hjelstuen, B.O., Andreassen, E.V., 2015. North Atlantic Ocean deep-water processes and depositional environments: A study of the Cenozoic Norway Basin. Mar Petrol Geol 59, 429-441.

Hjelstuen, B.O., Eldholm, O., Faleide, J.I., 2007. Recurrent Pleistocene mega-failures on the SW Barents Sea margin. Earth and Planetary Science Letters 258, 605-618.

Hjelstuen, B.O., Elverhøi, A., Faleide, J.I., 1996. Cenozoic erosion and sediment yield in the drainage area of the Storfjorden Fan. Global and Planetary Change 12, 95-117.

Hjelstuen, B.O., Sejrup, H.P., Haflidason, H., Nygård, A., Berstad, I.M., Knorr, G., 2004. Late Quaternary seismic stratigraphy and geological development of the south Vøring margin, Norwegian Sea. Quaternary Sci Rev 23, 1847-1865.

Hjelstuen, B.O., Sejrup, H.P., Haflidason, H., Nygard, A., Ceramicola, S., Bryn, P., 2005. Late Cenozoic glacial history and evolution of the Storegga Slide area and adjacent slide flank regions, Norwegian continental margin. Mar Petrol Geol 22, 57-69.

Hogan, K.A., Dowdeswell, J.A., Mienert, J., 2013. New insights into slide processes and seafloor geology revealed by side-scan imagery of the massive Hinlopen Slide, Arctic Ocean margin. Geo-Mar Lett 33, 325-343.

Hogan, K.A., Ó Cofaigh, C., Jennings, A.E., Dowdeswell, J.A., Hiemstra, J.F., 2016. Deglaciation of a major palaeo-ice stream in Disko Trough, West Greenland. Quaternary Sci Rev 147, 5-26.

2632 Hornbach, M.J., Lavier, L.L., Ruppel, C.D., 2007. Triggering mechanism and tsunamogenic potential of
2633 the Cape Fear Slide complex, US Atlantic margin. Geochemistry, Geophysics, Geosystems 8.
2634
2635 Houmark-Nielsen, M., Demidov, I., Funder, S., Grøsfjeld, K., Kjær, K.H., Larsen, E., Lavrova, N., Lyså,
2636 A., Nielsen, J.K., 2001. Early and Middle Valdaian glaciations, ice-dammed lakes and periglacial
2637 interstadials in northwest Russia: new evidence from the Pyoza River area. Global and Planetary
2638 Change 31, 215-237.
2639
2640 Hovland, M., Svensen, H., Forsberg, C.F., Johansen, H., Fichler, C., Fosså, J.H., Jonsson, R., Rueslåtten,
2641 H., 2005. Complex pockmarks with carbonate-ridges off mid-Norway: products of sediment
2642 degassing. Mar Geol 218, 191-206.
2643
2644 Hsu, S.K., Kuo, J., Lo, C.L., Tsai, C.H., Doo, W.B., Ku, C.Y., Sibuet, J.C., 2008. Turbidity Currents,
2645 Submarine Landslides and the 2006 Pingtung Earthquake off SW Taiwan. Terr Atmos Ocean Sci 19,
2646 767-772.
2647
2648 Hughes, A.L.C., Gyllencreutz, R., Lohne, Ø.S., Mangerud, J., Svendsen, J.I., 2016. The last Eurasian ice
2649 sheets–a chronological database and time-slice reconstruction, DATED-1. Boreas 45, 1-45.
2650
2651 Hughes Clarke, J.E., O'Leary, D., Piper, D.J.W., 1992. The relative importance of mass wasting and
2652 deep boundary current activity on the continental rise off western Nova Scotia, in: W., P.C., de
2653 Graniansky, P.C. (Eds.), Geologic evolution of Atlantic continental rises. Edited by CW Poag and PC de
2654 Graciansky. van Nostrand Reinhold, New York. van Nostrand Reinhold, New York, pp. 266-281.
2655
2656 Hughes Clarke, J.E., Shor, A.N., Piper, D.J.W., Mayer, L.A., 1990. Large-scale current-induced erosion
2657 and deposition in the path of the 1929 Grand Banks turbidity current. Sedimentology 37, 613-629.
2658
2659 Hunt, J.E., Wynn, R.B., Masson, D.G., Talling, P.J., Teagle, D.A.H., 2011. Sedimentological and
2660 geochemical evidence for multistage failure of volcanic island landslides: A case study from Icod
2661 landslide on north Tenerife, Canary Islands. Geochemistry, Geophysics, Geosystems 12, n/a-n/a.
2662
2663 Hunt, J.E., Wynn, R.B., Talling, P.J., Masson, D.G., 2013. Multistage collapse of eight western Canary
2664 Island landslides in the last 1.5 Ma: Sedimentological and geochemical evidence from subunits in
2665 submarine flow deposits. Geochemistry, Geophysics, Geosystems 14, 2159-2181.
2666
2667 Huppertz, T.J., Piper, D.J.W., 2009. The influence of shelf-crossing glaciation on continental slope
2668 sedimentation, Flemish Pass, eastern Canadian continental margin. Mar Geol 265, 67-85.
2669
2670 Ikehara, K., 2012. Offshore earthquake-and/or tsunami-induced sediment transports and their
2671 deposits: Importance of marine sediment study for understanding past earthquakes and tsunami.
2672 Journal of the Sedimentological Society of Japan 71, 141-147.
2673
2674 Imbo, Y., De Batist, M., Canals, M., Prieto, M.J., Baraza, J., 2003. The Gebra slide: a submarine slide
2675 on the Trinity Peninsula Margin, Antarctica. Mar Geol 193, 235-252.
2676
2677 Ingólfsson, Ó., Landvik, J.Y., 2013. The Svalbard–Barents Sea ice-sheet–Historical, current and future
2678 perspectives. Quaternary Sci Rev 64, 33-60.
2679 Ingólfsson, Ó., Lyså, A., Funder, S., Møller, P., Björck, S., 1994. Late Quaternary glacial history of the
2680 central west coast of Jameson Land, East Greenland. Boreas 23, 447-458.
2681

Ivanov, V.V., Shapiro, G.I., Huthnance, J.M., Aleynik, D.L., Golovin, P.N., 2004. Cascades of dense water around the world ocean. Progress in Oceanography 60, 47-98.

Jakobsson, M., Andreassen, K., Bjarnadóttir, L.R., Dove, D., Dowdeswell, J.A., England, J.H., Funder, S., Hogan, K.A., Ingólfsson, Ó., Jennings, A., 2014. Arctic Ocean glacial history. Quaternary Sci Rev 92, 40-67.

Jansen, E., Bleil, U., Henrich, R., Kringstad, L., Slettemark, B., 1988. Paleoenvironmental changes in the Norwegian Sea and the northeast Atlantic during the last 2.8 my: Deep Sea Drilling Project/Ocean Drilling Program sites 610, 642, 643 and 644. Paleoceanography 3, 563-581.

Jansen, E., et al., 1996. 8. Site 985, Proc. Ocean Drill. Program Initial Rep, pp. 253-283.

Jansen, E., Fronval, T., Rack, F., Channell, J.E.T., 2000. Pliocene-Pleistocene ice rafting history and cyclicity in the Nordic Seas during the last 3.5 Myr. Paleoceanography 15, 709-721.

Jansen, E., Raymo, M.E., 1996. 1. Leg 162: New Frontiers on Past Climates, in: Jansen, E., Raymo, M.E., Blum, P., et al. (Eds.), Proceedings Ocean Drilling Program Initial Reports, vol. 162.

Jansen, E., Sjøholm, J., 1991. Reconstruction of glaciation over the past 6 Myr from ice-borne deposits in the Norwegian Sea. Nature 349, 600-603.

Jenner, K.A., Piper, D.J.W., Campbell, D.C., Mosher, D.C., 2007. Lithofacies and origin of late Quaternary mass transport deposits in submarine canyons, central Scotian Slope, Canada. Sedimentology 54, 19-38.

Jennings, A.E., Grönvold, K., Hilberman, R., Smith, M., Hald, M., 2002. High-resolution study of Icelandic tephras in the Kangerlussuaq Trough, southeast Greenland, during the last deglaciation. Journal of Quaternary Science 17, 747-757.

Jennings, A.E., Hald, M., Smith, M., Andrews, J.T., 2006. Freshwater forcing from the Greenland Ice Sheet during the Younger Dryas: evidence from southeastern Greenland shelf cores. Quaternary Sci Rev 25, 282-298.

Jessen, S.P., Rasmussen, T.L., Nielsen, T., Solheim, A., 2010. A new Late Weichselian and Holocene marine chronology for the western Svalbard slope 30,000–0 cal years BP. Quaternary Sci Rev 29, 1301-1312.

Kandiano, E.S., Bauch, H.A., 2003. Surface ocean temperatures in the north-east Atlantic during the last 500 000 years: evidence from foraminiferal census data. Terra Nova 15, 265-271.

Kandiano, E.S., Bauch, H.A., 2007. Phase relationship and surface water mass change in the Northeast Atlantic during Marine Isotope Stage 11 (MIS 11). Quaternary Res 68, 445-455.

Kayen, R.E., Lee, H.J., 1991. Pleistocene slope instability of gas hydrate-laden sediment on the Beaufort sea margin. Marine Georesources & Geotechnology 10, 125-141.

Kennett, J.P., Cannariato, K.G., Hendy, I.L., Behl, R.J., 2003. Methane hydrates in Quaternary climate change: The clathrate gun hypothesis. American Geophysical Union.

King, E.L., Haflidason, H., Sejrup, H.P., Løvlie, R., 1998. Glacigenic debris flows on the North Sea Trough Mouth Fan during ice stream maxima. Mar Geol 152, 217-246.

King, E.L., Sejrup, H.P., Haflidason, H., Elverhøi, A., Aarseth, I., 1996. Quaternary seismic stratigraphy of the North Sea Fan: glacially-fed gravity flow aprons, hemipelagic sediments, and large submarine slides. Mar Geol 130, 293-315.

Kjemperud, A.T., Fjeldskaar, W., 1992. Pleistocene glacial isostasy—implications for petroleum geology. Tectonic modelling and its application to petroleum geology. Norwegian Petroleum Society Spec Publ 1, 187-195.

Kleiven, H.F., Jansen, E., Fronval, T., Smith, T.M., 2002. Intensification of Northern Hemisphere glaciations in the circum Atlantic region (3.5–2.4 Ma)–ice-rafted detritus evidence. Palaeogeography, Palaeoclimatology, Palaeoecology 184, 213-223.

Kleman, J., Hättestrand, C., Borgström, I., Stroeven, A., 1997. Fennoscandian palaeoglaciology reconstructed using a glacial geological inversion model. J Glaciol 43, 283-299.

Knies, J., Kleiber, H.-P., Matthiessen, J., Müller, C., Nowaczyk, N., 2001. Marine ice-rafted debris records constrain maximum extent of Saalian and Weichselian ice-sheets along the northern Eurasian margin. Global and Planetary Change 31, 45-64.

Knies, J., Matthiessen, J., Mackensen, A., Stein, R., Vogt, C., Frederichs, T., Nam, S.-I., 2007. Effects of Arctic freshwater forcing on thermohaline circulation during the Pleistocene. Geology 35, 1075-1078.

Knies, J., Matthiessen, J., Vogt, C., Laberg, J.S., Hjelstuen, B.O., Smelror, M., Larsen, E., Andreassen, K., Eidvin, T., Vorren, T.O., 2009. The Plio-Pleistocene glaciation of the Barents Sea–Svalbard region: a new model based on revised chronostratigraphy. Quaternary Sci Rev 28, 812-829.

Knies, J., Nowaczyk, N., Müller, C., Vogt, C., Stein, R., 2000. A multiproxy approach to reconstruct the environmental changes along the Eurasian continental margin over the last 150 000 years. Mar Geol 163, 317-344.

Knies, J., Vogt, C., Stein, R., 1998. Late Quaternary growth and decay of the Svalbard/Barents Sea ice sheet and paleoceanographic evolution in the adjacent Arctic Ocean. Geo-Mar Lett 18, 195-202.

Koppes, M., Hallet, B., Rignot, E., Mouginot, J., Wellner, J.S., Boldt, K., 2015. Observed latitudinal variations in erosion as a function of glacier dynamics. Nature 526, 100-103.

Krissek, L.A., 1989. Late Cenozoic records of ice-rafting at ODP Sites 642, 643, and 644, Norwegian Sea: onset, chronology, and characteristics of glacial/interglacial fluctuations, Proceedings of the Ocean Drilling Project. Scientific Results. Texas A&M University College Station, TX, pp. 61-69.

Kristoffersen, Y., Coakley, B., Jokat, W., Edwards, M., Brekke, H., Gjengedal, J., 2004. Seabed erosion on the Lomonosov Ridge, central Arctic Ocean: A tale of deep draft icebergs in the Eurasia Basin and the influence of Atlantic water inflow on iceberg motion? Paleoceanography 19, n/a-n/a.

Kuvaas, B., Kristoffersen, Y., 1991. The Crary Fan: a trough-mouth fan on the Weddell Sea continental margin, Antarctica. Mar Geol 97, 345-362.

Kuvaas, B., Kristoffersen, Y., 1996. Mass movements in glaciomarine sediments on the Barents Sea continental slope. Global and Planetary Change 12, 287-307.

Kuvaas, B., Kristoffersen, Y., Guseva, J., Leitchenkov, G., Gandjukhin, V., Løvås, O., Sand, M., Brekke, H., 2005. Interplay of turbidite and contourite deposition along the Cosmonaut Sea/Enderby Land margin, East Antarctica. Mar Geol 217, 143-159.

Kuvaas, B., Leitchenkov, G., 1992. Glaciomarine turbidite and current controlled deposits in Prydz Bay, Antarctica. Mar Geol 108, 365-381.

Kvalstad, T.J., Andresen, L., Forsberg, C.F., Berg, K., Bryn, P., Wangen, M., 2005. The Storegga slide: evaluation of triggering sources and slide mechanics. Mar Petrol Geol 22, 245-256.

L'Heureux, J.S., Vanneste, M., Rise, L., Brendryen, J., Forsberg, C.F., Nadim, F., Longva, O., Chand, S., Kvalstad, T.J., Haflidason, H., 2013. Stability, mobility and failure mechanism for landslides at the upper continental slope off Vesterålen, Norway. Mar Geol 346, 192-207.

Laberg, J.S., Andreassen, K., Knies, J., Vorren, T.O., Winsborrow, M., 2010. Late Pliocene–Pleistocene development of the Barents Sea ice sheet. Geology 38, 107-110.

Laberg, J.S., Dowdeswell, J.A., 2016. Glacigenic debris-flows on the Bear Island Trough-Mouth Fan, Barents Sea margin, in: Dowdeswell, J.A., Canals, M., Jakobsson, M., Todd, B.J., Dowdeswell, E.K., Hogan, K.A. (Eds.), Atlas of Submarine Glacial Landforms: Modern, Quaternary and Ancient. Geological Society, Geological Society, London, Memoirs, v. 46.

Laberg, J.S., Forwick, M., Husum, K., Nielsen, T., 2013. A re-evaluation of the Pleistocene behavior of the Scoresby Sund sector of the Greenland Ice Sheet. Geology 41, 1231-1234.

Laberg, J.S., Vorren, T.O., 1995. Late Weichselian submarine debris flow deposits on the Bear Island Trough mouth fan. Mar Geol 127, 45-72.

Laberg, J.S., Vorren, T.O., 1996. The Middle and Late Pleistocence evolution and the Bear Island Trough Mouth Fan. Global and Planetary Change 12, 309-330.

Laberg, J.S., Vorren, T.O., 2000. The Trænadjupet Slide, offshore Norway—morphology, evacuation and triggering mechanisms. Mar Geol 171, 95-114.

Laberg, J.S., Vorren, T.O., Dowdeswell, J.A., Kenyon, N.H., Taylor, J., 2000. The Andoya Slide and the Andoya Canyon, north-eastern Norwegian-Greenland Sea. Mar Geol 162, 259-275.

Laberg, J.S., Vorren, T.O., Mienert, J., Bryn, P., Lien, R., 2002a. The Trænadjupet Slide: a large slope failure affecting the continental margin of Norway 4,000 years ago. Geo-Mar Lett 22, 19-24.

Laberg, J.S., Vorren, T.O., Mienert, J., Evans, D., Lindberg, B., Ottesen, D., Kenyon, N.H., Henriksen, S., 2002b. Late Quaternary palaeoenvironment and chronology in the Trænadjupet Slide area offshore Norway. Mar Geol 188, 35-60.

Laberg, J.S., Vorren, T.O., Mienert, J., Haflidason, H., Bryn, P., Lien, R., 2003. Preconditions Leading to the Holocene Trænadjupet Slide Offshore Norway, in: Locat, J., Mienert, J., Boisvert, L. (Eds.), Adv Nat Tech Haz Res. Springer Netherlands, pp. 247-254.

Lambeck, K., Purcell, A., Zhao, J., Svensson, N.O., 2010. The Scandinavian ice sheet: from MIS 4 to the end of the Last Glacial Maximum. Boreas 39, 410-435.

Landvik, J.Y., 1994. The last glaciation of Germania Land and adjacent areas, northeast Greenland. Journal of Quaternary Science 9, 81-92.

Landvik, J.Y., Bolstad, M., Lycke, A.K., Mangerud, J., Sejrup, H.P., 1992. Weichselian stratigraphy and palaeoenvironments at Bellsund, western Svalbard. Boreas 21, 335-358.

Landvik, J.Y., Ingolfsson, O., Mienert, J., Lehman, S.J., Solheim, A., Elverhøi, A., Ottesen, D., 2005. Rethinking Late Weichselian ice-sheet dynamics in coastal NW Svalbard. Boreas 34, 7-24.

Landvik, J.Y., Lysså, A., Funder, S., Kelly, M., 1994. The Eemian and Weichselian stratigraphy of the Langelandselv area, Jameson Land, East Greenland. Boreas 23, 412-423.

Larsen, H., Saunders, A., Clift, P., Beget, J., Wei, W., Spezzaferri, S., Party, a.O.L.S., 1994. Seven million years of glaciation in Greenland. Science 264, 952 - 955.

Larsen, H.C., 1990. The East Greenland shelf. The Geology of North America 50, 185-210.

Larsen, N.K., Knudsen, K.L., Krohn, C.F., Kronborg, C., Murray, A.S., Nielsen, O.B., 2009. Late Quaternary ice sheet, lake and sea history of southwest Scandinavia–a synthesis. Boreas 38, 732-761.

Lebreiro, S.M., Voelker, A.H.L., Vizcaino, A., Abrantes, F.G., Alt-Epping, U., Jung, S., Thouveny, N., Gracia, E., 2009. Sediment instability on the Portuguese continental margin under abrupt glacial climate changes (last 60 kyr). Quaternary Sci Rev 28, 3211-3223.

Lee, H.J., 2009. Timing of occurrence of large submarine landslides on the Atlantic Ocean margin. Mar Geol 264, 53-64.

Lee, H.J., Chough, S.K., Yoon, S.H., 1996. Slope-stability change from late pleistocene to holocene in the Ulleung Basin, East Sea (Japan Sea). Sediment Geol 104, 39-51.

Lee, J.R., Busschers, F.S., Sejrup, H.P., 2012. Pre-Weichselian Quaternary glaciations of the British Isles, The Netherlands, Norway and adjacent marine areas south of 68 N: implications for long-term ice sheet development in northern Europe. Quaternary Sci Rev 44, 213-228.

Lekens, W.A.H., Haflidason, H., Sejrup, H.P., Nygård, A., Richter, T., Vogt, C., Frederichs, T., 2009. Sedimentation history of the northern North Sea Margin during the last 150 ka. Quaternary Sci Rev 28, 469-483.

Lekens, W.A.H., Sejrup, H.P., Haflidason, H., Knies, J., Richter, T., 2006. Meltwater and ice rafting in the southern Norwegian Sea between 20 and 40 calendar kyr BP: Implications for Fennoscandian Heinrich events. Paleoceanography 21.

Lekens, W.A.H., Sejrup, H.P., Haflidason, H., Petersen, G.Ø., Hjelstuen, B.O., Knorr, G., 2005. Laminated sediments preceding Heinrich event 1 in the Northern North Sea and Southern Norwegian Sea: origin, processes and regional linkage. Mar Geol 216, 27-50.

Leynaud, D., Mienert, J., Vanneste, M., 2009. Submarine mass movements on glaciated and non-glaciated European continental margins: A review of triggering mechanisms and preconditions to failure. Mar Petrol Geol 26, 618-632.

Leynaud, D., Sultan, N., Mienert, J., 2007. The role of sedimentation rate and permeability in the slope stability of the formerly glaciated Norwegian continental margin: the Storegga slide model. Landslides 4, 297-309.

Li, G., Piper, D.J.W., Calvin Campbell, D., 2011. The Quaternary Lancaster Sound trough-mouth fan, NW Baffin Bay. Journal of Quaternary Science 26, 511-522.

Lindberg, B., Laberg, J.S., Vorren, T.O., 2004. The Nyk Slide—morphology, progression, and age of a partly buried submarine slide offshore northern Norway. Mar Geol 213, 277-289.

Lisiecki, L.E., Raymo, M.E., 2007. Plio–Pleistocene climate evolution: trends and transitions in glacial cycle dynamics. Quaternary Sci Rev 26, 56-69.

Liu, J.T., Wang, Y.H., Yang, R.J., Hsu, R.T., Kao, S.J., Lin, H.L., Kuo, F.H., 2012. Cyclone-induced hyperpycnal turbidity currents in a submarine canyon. Journal of Geophysical Research: Oceans 117.

Llopart, J., Urgeles, R., Camerlenghi, A., Lucchi, R.G., Mol, B., Rebesco, M., Pedrosa, M.T., 2014. Slope Instability of Glaciated Continental Margins: Constraints from Permeability-Compressibility Tests and Hydrogeological Modeling Off Storfjorden, NW Barents Sea, in: Krastel, S., Behrmann, J.-H., Völker, D., Stipp, M., Berndt, C., Urgeles, R., Chaytor, J., Huhn, K., Strasser, M., Harbitz, C.B. (Eds.), Adv Nat Tech Haz Res. Springer International Publishing, pp. 95-104.

Llopart, J., Urgeles, R., Camerlenghi, A., Lucchi, R.G., Rebesco, M., De Mol, B., 2015. Late Quaternary development of the Storfjorden and Kveithola Trough Mouth Fans, northwestern Barents Sea. Quaternary Sci Rev 129, 68-84.

Locat, A., Leroueil, S., Bernander, S., Demers, D., Locat, J., Ouehb, L., 2008. Study of a lateral spread failure in an eastern Canada clay deposit in relation with progressive failure: the Saint-Barnabé-Nord slide, Proceedings of the 4th Canadian conference on geohazards: from causes to management, pp. 20-24.

Long, D., Smith, D.E., Dawson, A.G., 1989. A Holocene tsunami deposit in eastern Scotland. Journal of Quaternary Science 4, 61-66.

Long, D., Stevenson, A.G., Wilson, C.K., Bulat, J., 2003. Slope Failures in the Faroe — Shetland Channel, in: Locat, J., Mienert, J., Boisvert, L. (Eds.), Submarine Mass Movements and Their Consequences: 1st International Symposium. Springer Netherlands, Dordrecht, pp. 281-289.

Løvholt, F., Bondevik, S., Laberg, J.S., Kim, J., Boylan, N., 2017. Some giant submarine landslides do not produce large tsunamis. Geophys Res Lett 44, 8463-8472.

Løvholt, F., Harbitz, C.B., Haugen, K.B., 2005. A parametric study of tsunamis generated by submarine slides in the Ormen Lange/Storegga area off western Norway. Mar Petrol Geol 22, 219-231.

Løvholt, F., Pedersen, G., Harbitz, C.B., 2016. Tsunami-Genesis Due to Retrogressive Landslides on an Inclined Seabed, in: Lamarche, G., Mountjoy, J., Bull, S., Hubble, T., Krastel, S., Lane, E., Micallef, A., Moscardelli, L., Mueller, C., Pecher, I., Woelz, S. (Eds.), Adv Nat Tech Haz Res. Springer, pp. 569-578.

Lowe, A.L., Anderson, J.B., 2002. Reconstruction of the West Antarctic ice sheet in Pine Island Bay during the Last Glacial Maximum and its subsequent retreat history. Quaternary Sci Rev 21, 1879-1897.

Lucchi, R.G., Camerlenghi, A., Rebesco, M., Colmenero-Hidalgo, E., Sierro, F.J., Sagnotti, L., Urgeles, R., Melis, R., Morigi, C., Bárcena, M.-A., 2013. Postglacial sedimentary processes on the Storfjorden and Kveithola trough mouth fans: Significance of extreme glacimarine sedimentation. Global and planetary change 111, 309-326.

Lucchi, R.G., Pedrosa, M.T., Camerlenghi, A., Urgeles, R., De Mol, B., Rebesco, M., 2012. Recent submarine landslides on the continental slope of Storfjorden and Kveithola Trough-Mouth Fans (north west Barents Sea), Adv Nat Tech Haz Res. Springer, pp. 735-745.

Lykke-Andersen, H., 1998. Neogene-Quaternary depositional history of the East Greenland shelf in the vicinity of the Leg 152 shelf sites, in: Larsen, H.C., Saunders, A.D., Clift, P.D. (Eds.), Proceedings, Ocean Drilling Program, Scientific Results. National Science Foundation, Texas, pp. 29-38.

Madhusudhan, B.N., Clare, M.A., Clayton, C.R.I., Hunt, J.E., 2017. Geotechnical profiling of deep-ocean sediments at the AFEN submarine slide complex. Quarterly Journal of Engineering Geology and Hydrogeology 50, 148-157.

Mangerud, J., 1991. The last interglacial/glacial cycle in northern Europe. Quaternary landscapes 38, 75.

Mangerud, J., 2004. Ice sheet limits in Norway and on the Norwegian continental shelf. Developments in Quaternary Sciences 2, 271-294.

Mangerud, J., Astakhov, V.I., Murray, A., Svendsen, J.I., 2001. The chronology of a large ice-dammed lake and the Barents–Kara Ice Sheet advances, Northern Russia. Global and Planetary Change 31, 321-336.

Mangerud, J., Dokken, T., Hebbeln, D., Heggen, B., Ingolfsson, O., Landvik, J.Y., Mejdahl, V., Svendsen, J.I., Vorren, T.O., 1998. Fluctuations of the Svalbard–Barents Sea Ice Sheet during the last 150 000 years. Quaternary Sci Rev 17, 11-42.

Mangerud, J., Jakobsson, M., Alexanderson, H., Astakhov, V., Clarke, G.K.C., Henriksen, M., Hjort, C., Krinner, G., Lunkka, J.-P., Möller, P., 2004. Ice-dammed lakes and rerouting of the drainage of northern Eurasia during the Last Glaciation. Quaternary Sci Rev 23, 1313-1332.

Mangerud, J., Jansen, E., Landvik, J.Y., 1996. Late Cenozoic history of the Scandinavian and Barents Sea ice sheets. Global and Planetary Change 12, 11-26.

Mangerud, J., Løvlie, R., Gulliksen, S., Hufthammer, A.-K., Larsen, E., Valen, V., 2003. Paleomagnetic correlations between scandinavian ice-sheet fluctuations and greenland dansgaard–oeschger events, 45,000–25,000 yr BP. Quaternary Res 59, 213-222.

Mangerud, J., Svendsen, J.I., 1992. The last interglacial-glacial period on Spitsbergen, Svalbard. Quaternary Sci Rev 11, 633-664.

Maslin, M., Mikkelsen, N., Vilela, C., Haq, B., 1998. Sea-level- and gas-hydrate-controlled catastrophic sediment failures of the Amazon Fan. Geology 26, 1107-1110.

Maslin, M., Owen, M., Day, S., Long, D., 2004. Linking continental-slope failures and climate change: Testing the clathrate gun hypothesis. Geology 32, 53-56.

Masson, D.G., Arzola, R.G., Wynn, R.B., Hunt, J.E., Weaver, P.P.E., 2011. Seismic triggering of landslides and turbidity currents offshore Portugal. Geochem Geophy Geosy 12.

Masson, D.G., Harbitz, C.B., Wynn, R.B., Pedersen, G., Lovholt, F., 2006. Submarine landslides: processes, triggers and hazard prediction. Philos T R Soc A 364, 2009-2039.

Melles, M., Kuhn, G., 1993. Sub-bottom profiling and sedimentological studies in the southern Weddell Sea, Antarctica: evidence for large-scale erosional/depositional processes. Deep Sea Research Part I: Oceanographic Research Papers 40, 739-760.

Mienert, J., Posewang, J., Baumann, M., 1998. Gas hydrates along the northeastern Atlantic margin: possible hydrate-bound margin instabilities and possible release of methane. Geological Society, London, Special Publications 137, 275-291.

Mienert, J., Vanneste, M., Bunz, S., Andreassen, K., Haflidason, H., Sejrup, H.P., 2005. Ocean warming and gas hydrate stability on the mid-Norwegian margin at the Storegga Slide. Mar Petrol Geol 22, 233-244.

Milliman, J.D., Meade, R.H., 1983. World-wide delivery of river sediment to the oceans. The Journal of Geology, 1-21.

Montelli, A., Dowdeswell, J.A., Ottesen, D., Johansen, S.E., 2017a. Ice-sheet dynamics through the Quaternary on the mid-Norwegian continental margin inferred from 3D seismic data. Mar Petrol Geol 80, 228-242.

Montelli, A., Gulick, S.P.S., Worthington, L.L., Mix, A., Davies-Walczak, M., Zellers, S.D., Jaeger, J.M., 2017b. Late Quaternary glacial dynamics and sedimentation variability in the Bering Trough, Gulf of Alaska. Geology, G38836. 38831.

Mosher, D.C., Campbell, D.C., Gardner, J.V., Piper, D.J.W., Chaytor, J.D., Rebesco, M., 2017. The role of deep-water sedimentary processes in shaping a continental margin: The Northwest Atlantic. Mar Geol 393, 245-259.

Mosher, D.C., Moran, K., Hiscott, R.N., 1994. Late Quaternary Sediment, Sediment Mass-Flow Processes and Slope Stability on the Scotian Slope, Canada. Sedimentology 41, 1039-1061.

Mosher, D.C., Piper, D.J.W., Campbell, D.C., Jenner, K.A., 2004. Near-surface geology and sediment-failure geohazards of the central Scotian Slope. AAPG bulletin 88, 703-723.

Mosher, D.C., Piper, D.J.W., Vilks, G.V., Aksu, A.E., Fader, G.B., 1989. Evidence for Wisconsinan glaciations in the Verrill Canyon area, Scotian Slope. Quaternary Res 31, 27-40.

Mudelsee, M., Schulz, M., 1997. The Mid-Pleistocene climate transition: onset of 100 ka cycle lags ice volume build-up by 280 ka. Earth and Planetary Science Letters 151, 117-123.

Mudelsee, M., Stattegger, K., 1997. Exploring the structure of the mid-Pleistocene revolution with advanced methods of time-series analysis. Geologische Rundschau 86, 499-511.

Mugford, R.I., Dowdeswell, J.A., 2010. Modeling iceberg-rafted sedimentation in high-latitude fjord environments. Journal of Geophysical Research: Earth Surface 115.

Mulder, T., Moran, K., 1995. Relationship among Submarine Instabilities, Sea-Level Variations, and the Presence of an Ice-Sheet on the Continental-Shelf - an Example from the Verrill Canyon Area, Scotian Shelf. Paleoceanography 10, 137-154.

Mulder, T., Syvitski, J.P.M., Migeon, S., Faugeres, J.-C., Savoye, B., 2003. Marine hyperpycnal flows: initiation, behavior and related deposits. A review. Mar Petrol Geol 20, 861-882.

Myhre, A.M., Thiede, J., Firth, J.V., 1995. 1. North Atlantic-Arctic Gateways, in: Myhre, A.M., Thiede, J., Firth, J.V., et al. (Eds.), Proceedings Ocean Drilling Program Initial Reports, vol. 151.

Nam, S.-I., Stein, R., Grobe, H., Hubberten, H., 1995. Late Quaternary glacial-interglacial changes in sediment composition at the East Greenland continental margin and their paleoceanographic implications. Mar Geol 122, 243-262.

Nam, S.I., Stein, R.A., 1999. Late Quaternary variations in sediment accumulation rates and their paleoenvironmental implications: a case study from the East Greenland continental margin, Retrospective Collection. Trans Tech Publ, p. 223.

Newton, A.M.W., Huuse, M., Brocklehurst, S.H., 2016. Buried iceberg scours reveal reduced North Atlantic Current during the stage 12 deglacial. Nature communications 7, 10927.

Nitsche, F.O., Gohl, K., Vanneste, K., Miller, H., 1997. Seismic expression of glacially deposited sequences in the Bellingshausen and Amundsen Seas, West Antarctica, in: Barker, P.F., Cooper, A.K. (Eds.), Geology and Seismic Stratigraphy of the Antarctic Margin, pp. 95-108.

Noormets, R., Dowdeswell, J.A., Larter, R.D., Ó Cofaigh, C., Evans, J., 2009. Morphology of the upper continental slope in the Bellingshausen and Amundsen Seas–Implications for sedimentary processes at the shelf edge of West Antarctica. Mar Geol 258, 100-114.

Nothold, H., 1998. Die Auswirkungen der" NorthEastWater"-Polynya auf die Sedimentation vor NO-Grönland und Untersuchungen zur Paläo-Ozeanographie seit dem Mittelweichsel= The implication of the" NorthEastWater"-Polynya on the sedimentation by NE-Greenland and Late Quaternary Paleo-oceanic investigations. Berichte zur Polarforschung (Reports on Polar Research) 275.

Nygård, A., Haflidason, H., Sejrup, H.P., 2003. Morphology of a non-glacigenic debris flow lobe in the Helland Hansen area investigated with 3D seismic data, European Margin Sediment Dynamics. Springer, pp. 63-65.

Nygård, A., Sejrup, H.P., Haflidason, H., Bryn, P., 2005. The glacial North Sea Fan, southern Norwegian Margin: architecture and evolution from the upper continental slope to the deep-sea basin. Mar Petrol Geol 22, 71-84.

Nygård, A., Sejrup, H.P., Haflidason, H., Lekens, W.A.H., Clark, C.D., Bigg, G.R., 2007. Extreme sediment and ice discharge from marine-based ice streams: New evidence from the North Sea. Geology 35, 395-398.

O'Brien, P.E., Cooper, A.K., Florindo, F., Handwerger, D.A., Lavelle, M., Passchier, S., Pospichal, J.J., Quilty, P.G., Richter, C., Theissen, K.M., 2004. Prydz Channel Fan and the history of extreme ice advances in Prydz Bay, Proceedings of the Ocean Drilling Program, Scientific Results, pp. 1-32.

O'Brien, P.E., Goodwin, I., Forsberg, C.-F., Cooper, A.K., Whitehead, J., 2007. Late Neogene ice drainage changes in Prydz Bay, East Antarctica and the interaction of Antarctic ice sheet evolution and climate. Palaeogeography, Palaeoclimatology, Palaeoecology 245, 390-410.

O'brien, P.E., Harris, P.T., 1996. Patterns of glacial erosion and deposition in Prydz Bay and the past behaviour of the Lambert Glacier, Papers and Proceedings of the Royal Society of Tasmania, pp. 79-85.

Ó Cofaigh, C., Hogan, K. A., Jennings, A. E., Callard, S. L., Dowdeswell, J. A., Noormets, R., Evans, J., in review. The role of meltwater in high-latitude trough-mouth fan development: the Disko Trough-Mouth Fan, West Greenland. Marine Geology.

Ó Cofaigh, C., Dowdeswell, J. A., Jennings, A. E., Hogan, K., Kilfeather, A., Hiemstra, J. F., Noormets, R., Evans, J., McCarthy, D. J., Andrews, J. T., Lloyd, J. M., Moros, M. (2013a). An extensive and dynamic ice sheet on the West Greenland shelf during the last glacial cycle. Geology 41, 219-222.

Ó Cofaigh, C., Andrews, J.T., Jennings, A.E., Dowdeswell, J.A., Hogan, K.A., Kilfeather, A.A., Sheldon, C., 2013b. Glacimarine lithofacies, provenance and depositional processes on a West Greenland trough-mouth fan. Journal of Quaternary Science 28, 13-26.

Ó Cofaigh, C., Dowdeswell, J.A., Evans, J., Kenyon, N.H., Taylor, J., Mienert, J., Wilken, M., 2004. Timing and significance of glacially influenced mass-wasting in the submarine channels of the Greenland Basin. Mar Geol 207, 39-54.

Ó Cofaigh, C., Dowdeswell, J.A., Evans, J., Larter, R.D., 2008. Geological constraints on Antarctic palaeo-ice-stream retreat. Earth Surf Proc Land 33, 513-525.

Ó Cofaigh, C., Dowdeswell, J.A., Kenyon, N.H., 2006. Geophysical investigations of a high-latitude submarine channel system and associated channel-mouth lobe in the Lofoten Basin, polar North Atlantic. Mar Geol 226, 41-50.

Ó Cofaigh, C., Larter, R.D., Dowdeswell, J.A., Hillenbrand, C.D., Pudsey, C.J., Evans, J., Morris, P., 2005. Flow of the West Antarctic Ice Sheet on the continental margin of the Bellingshausen Sea at the Last Glacial Maximum. Journal of Geophysical Research: Solid Earth 110.

Ó Cofaigh, C., Taylor, J., Dowdeswell, J.A., Pudsey, C.J., 2003. Palaeo-ice streams, trough mouth fans and high-latitude continental slope sedimentation. Boreas 32, 37-55.

Olsen, J., van der Borg, K., Bergstrøm, B., Sveian, H., Lauritzen, S.-E., Hansen, G., 2001a. AMS radiocarbon dating of glacigenic sediments with low organic carbon content - an important tool for reconstructing the glacial variations in Norway. Norwegian Journal of Geology 2, 59-92.

Olsen, L., Sveian, H., Bergstrøm, B., 2001b. Rapid adiustments of the western part of the Scandinavian lee Sheet during the Mid and late Weichselian. Norwegian Journal of Geology 2, 93-117.

Ottesen, D., Dowdeswell, J.A., 2006. Assemblages of submarine landforms produced by tidewater glaciers in Svalbard. Journal of Geophysical Research: Earth Surface (2003–2012) 111.

Ottesen, D., Dowdeswell, J.A., Bugge, T., 2014. Morphology, sedimentary infill and depositional environments of the Early Quaternary North Sea Basin (56°–62°N). Mar Petrol Geol 56, 123-146.

Ottesen, D., Dowdeswell, J.A., Rise, L., 2005. Submarine landforms and the reconstruction of fast-flowing ice streams within a large Quaternary ice sheet: The 2500-km-long Norwegian-Svalbard margin (57–80 N). Geological Society of America Bulletin 117, 1033-1050.

Ottesen, D., Dowdeswell, J.A., Rise, L., Bugge, T., 2012. Large-scale development of the mid-Norwegian shelf over the last three million years and potential for hydrocarbon reservoirs in glacial sediments. Geological Society, London, Special Publications 368, 53-73.

Ottesen, D., Rise, L., Rokoengen, K., 2001. Glacial processes and large-scale morphology on the mid-Norwegian continental shelf. Norwegian Petroleum Society Special Publications 10, 441-449.

Ottesen, D., Rise, L., Sletten Andersen, E., Bugge, T., Eidvin, T., 2009. Geological evolution of the Norwegian continental shelf between 61° N and 68° N during the last 3 million years. Norwegian Journal of Geology 89, 251-265.

Øverland, I., 2010. Russia's Arctic energy policy. International Journal 65, 865-878.

Owen, L.A., Kamp, U., Khattak, G.A., Harp, E.L., Keefer, D.K., Bauer, M.A., 2008. Landslides triggered by the 8 October 2005 Kashmir earthquake. Geomorphology 94, 1-9.

Owen, M., Day, S., Maslin, M., 2007. Late Pleistocene submarine mass movements: occurrence and causes. Quaternary Sci Rev 26, 958-978.

Özener, P.T., Özaydın, K., Berilgen, M.M., 2009. Investigation of liquefaction and pore water pressure development in layered sands. Bulletin of Earthquake Engineering 7, 199-219.

Parsons, J.D., Bush, J.W.M., Syvitski, J.P.M., 2001. Hyperpycnal plume formation from riverine outflows with small sediment concentrations. Sedimentology 48, 465-478.

Passchier, S., O'Brien, P.E., Damuth, J.E., Januszczak, N., Handwerger, D.A., Whitehead, J.M., 2003. Pliocene–Pleistocene glaciomarine sedimentation in eastern Prydz Bay and development of the Prydz trough-mouth fan, ODP Sites 1166 and 1167, East Antarctica. Mar Geol 199, 279-305.

Patton, H., Andreassen, K., Bjarnadóttir, L.R., Dowdeswell, J.A., Winsborrow, M.C.M., Noormets, R., Polyak, L., Auriac, A., Hubbard, A., 2015. Geophysical constraints on the dynamics and retreat of the Barents Sea Ice Sheet as a palaeo-benchmark for models of marine ice-sheet deglaciation. Rev Geophys 53, 1051-1098.

Patton, H., Hubbard, A., Andreassen, K., Winsborrow, M., Stroeven, A.P., 2016. The build-up, configuration, and dynamical sensitivity of the Eurasian ice-sheet complex to Late Weichselian climatic and oceanic forcing. Quaternary Sci Rev 153, 97-121.

Paull, C.K., Ussler, W., Holbrook, W.S., 2007. Assessing methane release from the colossal Storegga submarine landslide. Geophys Res Lett 34.

Pedrosa, M.T., Camerlenghi, A., De Mol, B., Urgeles, R., Rebesco, M., Lucchi, R.G., 2011. Seabed morphology and shallow sedimentary structure of the Storfjorden and Kveithola trough-mouth fans (north west Barents Sea). Mar Geol 286, 65-81.

Pickrill, R., Piper, D.J.W., Collins, J., Kleiner, A., Gee, L., 2001. Scotian Slope mapping project: the benefits of an integrated regional high-resolution multibeam survey, Offshore Technology Conference. Offshore Technology Conference.

Piper, D.J., Hundert, T., 2002. Provenance of distal Sohm Abyssal Plain sediments: history of supply from the Wisconsinan glaciation in eastern Canada. Geo-Mar Lett 22, 75-85.

Piper, D.J.W., 1988. Glaciomarine sedimentation on the continental slope off eastern Canada. Geoscience Canada 15.

Piper, D.J.W., 2005. Late Cenozoic evolution of the continental margin of eastern Canada. Norsk geologisk tidsskrift 85, 305.

Piper, D.J.W., Aksu, A.E., 1987. The source and origin of the 1929 grand banks turbidity current inferred from sediment budgets. Geo-Mar Lett 7, 177-182.

Piper, D.J.W., Campbell, D.C., 2005. Quaternary geology of Flemish Pass and its application to geohazard evaluation for hydrocarbon development. GAC Special Paper 43, 29-43.

Piper, D.J.W., Campbell, D.C., Mosher, D.C., 2016. Mid-latitude complex trough-mouth fans, Laurentian and Northeast fans, eastern Canada. Geological Society, London, Memoirs 46, 363-364.

Piper, D.J.W., Cochonat, P., Morrison, M.L., 1999. The sequence of events around the epicentre of the 1929 Grand Banks earthquake: initiation of debris flows and turbidity current inferred from sidescan sonar. Sedimentology 46, 79-97.

Piper, D.J.W., Deptuck, M.E., Mosher, D.C., Hughes Clarke, J.E., Migeon, S., 2012. Erosional and depositional features of glacial meltwater discharges on the eastern Canadian continental margin. Applications of the Principles of Seismic Geomorphology to Continental Slope and Base-of-slope Systems: Case Studies from Seafloor and Near-Seafloor Analogues. Edited by BE Prather, ME Deptuck, D. Mohrig, B. van Hoorn, and R. Wynn. Society for Sedimentary Geology (SEPM), Special Publications 99, 61-80.

Piper, D.J.W., Farre, J.A., Shor, A., 1985. Late Quaternary slumps and debris flows on the Scotian Slope. Geological Society of America Bulletin 96, 1508-1517.

Piper, D.J.W., Ingram, S., 2003. Major Quaternary sediment failures on the east Scotian Rise, eastern Canada. Natural Resources Canada, Geological Survey of Canada.

Piper, D.J.W., McCall, C., 2003. A Synthesis of the Distribution of Submarine Mass Movements on the Eastern Canadian Margin, in: Locat, J., Mienert, J., Boisvert, L. (Eds.), Submarine Mass Movements and Their Consequences: 1st International Symposium. Springer Netherlands, Dordrecht, pp. 291-298.

Piper, D.J.W., Mosher, D.C., Gauley, B.-J., Jenner, K., Campbell, D.C., 2003. The chronology and recurrence of submarine mass movements on the continental slope off southeastern Canada, Adv Nat Tech Haz Res. Springer, pp. 299-306.

Piper, D.J.W., Mudie, P.J., Aksu, A.E., Skene, K.I., 1994. A 1 Ma record of sediment flux south of the Grand Banks used to infer the development of glaciation in southeastern Canada. Quaternary Sci Rev 13, 23-37.

Piper, D.J.W., Normark, W.R., 2009. Processes that initiate turbidity currents and their influence on turbidites: a marine geology perspective. Journal of Sedimentary Research 79, 347-362.

Piper, D.J.W., Savoye, B., 1993. Processes of late Quaternary turbidity current flow and deposition on the Var deep-sea fan, north-west Mediterranean Sea. Sedimentology 40, 557-582.

Piper, D.J.W., Shaw, J., Skene, K.I., 2007. Stratigraphic and sedimentological evidence for late Wisconsinan sub-glacial outburst floods to Laurentian Fan. Palaeogeography, Palaeoclimatology, Palaeoecology 246, 101-119.

Pope, E.L., Talling, P.J., Carter, L., 2017a. Which earthquakes trigger damaging submarine mass movements: Insights from a global record of submarine cable breaks? Mar Geol 348, 131-146.

Pope, E.L., Talling, P.J., Carter, L., Clare, M.A., Hunt, J.E., 2017b. Damaging sediment density flows triggered by tropical cyclones. Earth and Planetary Science Letters 458, 161-169.

Pope, E.L., Talling, P.J., Hunt, J.E., Dowdeswell, J.A., Allin, J.R., Cartigny, M.J.B., Long, D., Mozzato, A., Stanford, J.D., Tappin, D.R., Watts, M., 2016. Long-term record of Barents Sea Ice Sheet advance to the shelf edge from a 140,000 year record. Quaternary Sci Rev 150, 55-66.

Pope, E.L., Talling, P.J., Urlaub, M., Hunt, J.E., Clare, M.A., Challenor, P., 2015. Are large submarine landslides temporally random or do uncertainties in available age constraints make it impossible to tell? Mar Geol 369, 19-33.

Powell, R.D., Alley, R.B., 1997. Grounding-Line Systems: Processes, Glaciological Inferences and the Stratigraphic Record. Geology and seismic stratigraphy of the Antarctic Margin, 2, 169-187.

Powell, R.D., Domack, E., 1995. Modern glaciomarine environments. Glacial environments 1, 445-486.

Prior, D.B., Coleman, J.M., Bornhold, B.D., 1982. Results of a known seafloor instability event. Geo-Mar Lett 2, 117-122.

Pudsey, C.J., Camerlenghi, A., 1998. Glacial–interglacial deposition on a sediment drift on the Pacific margin of the Antarctic Peninsula. Antarctic Science 10, 286-308.

Quinn, P.E., Diederichs, M.S., Rowe, R.K., Hutchinson, D.J., 2012. Development of progressive failure in sensitive clay slopes. Canadian Geotechnical Journal 49, 782-795.

Rasmussen, E., Fjeldskaar, W., 1996. Quantification of the Pliocene-Pleistocene erosion of the Barents Sea from present-day bathymetry. Global and Planetary Change 12, 119-133.

Rasmussen, T.L., Thomsen, E., Kuijpers, A., Wastegård, S., 2003. Late warming and early cooling of the sea surface in the Nordic seas during MIS 5e (Eemian Interglacial). Quaternary Sci Rev 22, 809-821.

Rasmussen, T.L., Thomsen, E., Ślubowska, M.A., Jessen, S., Solheim, A., Koç, N., 2007. Paleoceanographic evolution of the SW Svalbard margin (76 N) since 20,000 14 C yr BP. Quaternary Res 67, 100-114.

Rasmussen, T.L., Van Weering, T.C.E., Labeyrie, L., 1997. Climatic instability, ice sheets and ocean dynamics at high northern latitudes during the last glacial period (58-10 KA BP). Quaternary Sci Rev 16, 71-80.

Rauscher, K.F., 2010. The Reliability of Global Undersea Communications Cable Infrastructure (ROGUCCI) Report. IEEE.

Raymo, M.E., Nisancioglu, K.H., 2003. The 41 kyr world: Milankovitch's other unsolved mystery. Paleoceanography 18.

Raymo, M.E., Ruddiman, W.F., 1992. Tectonic forcing of late Cenozoic climate. Nature 359, 117-122.

Rebesco, M., Camerlenghi, A., 2008. Late Pliocene margin development and mega debris flow deposits on the Antarctic continental margins: Evidence of the onset of the modern Antarctic Ice Sheet? Palaeogeography, Palaeoclimatology, Palaeoecology 260, 149-167.

Rebesco, M., Larter, R.D., Camerlenghi, A., Barker, P.F., 1996. Giant sediment drifts on the continental rise west of the Antarctic Peninsula. Geo-Mar Lett 16, 65-75.

Rebesco, M., Liu, Y., Camerlenghi, A., Winsborrow, M., Laberg, J.S., Caburlotto, A., Diviacco, P., Accettella, D., Sauli, C., Wardell, N., 2011. Deglaciation of the western margin of the Barents Sea Ice Sheet—a swath bathymetric and sub-bottom seismic study from the Kveithola Trough. Mar Geol 279, 141-147.

Rebesco, M., Pedrosa, M.T., Camerlenghi, A., Lucchi, R.G., Sauli, C., De Mol, B., Madrussani, G., Urgeles, R., Rossi, G., Böhm, G., 2012. One million years of climatic generated landslide events on the northwestern Barents Sea continental margin, Adv Nat Tech Haz Res. Springer, pp. 747-756.

Rebesco, M., Pudsey, C.J., Canals, M., Camerlenghi, A., Barker, P.F., Estrada, F., Giorgetti, A., 2002. Sediment drifts and deep-sea channel systems, Antarctic Peninsula Pacific Margin. Geological Society, London, Memoirs 22, 353-371.

Rise, L., Bøe, R., Riis, F., Bellec, V.K., Laberg, J.S., Eidvin, T., Elvenes, S., Thorsnes, T., 2013. The Lofoten-Vesterålen continental margin, North Norway: Canyons and mass-movement activity. Mar Petrol Geol 45, 134-149.

Rise, L., Chand, S., Haflidason, H., L'Heureux, J.S., Hjelstuen, B.O., Bellec, V., Longva, O., Brendryen, J., Vanneste, M., Bøe, R., 2012. Investigations of Slides at the Upper Continental Slope Off Vesterålen, North Norway, in: Yamada, Y., Kawamura, K., Ikehara, K., Ogawa, Y., Urgeles, R., Mosher, D., Chaytor, J., Strasser, M. (Eds.), Adv Nat Tech Haz Res. Springer Netherlands, pp. 167-176.

Rise, L., Chand, S., Hjelstuen, B.O., Haflidason, H., Bøe, R., 2010. Late Cenozoic geological development of the south Vøring margin, mid-Norway. Mar Petrol Geol 27, 1789-1803.

Rise, L., Ottesen, D., Berg, K., Lundin, E., 2005. Large-scale development of the mid-Norwegian margin during the last 3 million years. Mar Petrol Geol 22, 33-44.

Rise, L., Ottesen, D., Longva, O., Solheim, A., Andersen, E.S., Ayers, S., 2006. The Sklinnadjupet slide and its relation to the Elsterian glaciation on the mid-Norwegian margin. Mar Petrol Geol 23, 569-583.

Rokoengen, K., Rise, L., Bryn, P., Frengstad, B., Gustavsen, B., Nygaard, E., Sættem, J., 1995. Upper Cenozoic stratigraphy on the mid-Norwegian continental shelf. Norsk Geologisk Tidsskrift 75, 88-104.

Rydningen, T.A., Laberg, J.S., Kolstad, V., 2016. Late Cenozoic evolution of high-gradient trough mouth fans and canyons on the glaciated continental margin offshore Troms, northern Norway—Paleoclimatic implications and sediment yield. Geological Society of America Bulletin 128, 576-596.

Sættem, J., Bugge, T., Fanavoll, S., Goll, R.M., Mørk, A., Mørk, M.B.E., Smelror, M., Verdenius, J.G., 1994. Cenozoic margin development and erosion of the Barents Sea: Core evidence from southwest of Bjørnøya. Mar Geol 118, 257-281.

Sættem, J., Poole, D.A.R., Ellingsen, L., Sejrup, H.P., 1992. Glacial geology of outer Bjørnøyrenna, southwestern Barents Sea. Mar Geol 103, 15-51.

Sawyer, D.E., DeVore, J.R., 2015. Elevated shear strength of sediments on active margins: Evidence for seismic strengthening. Geophys Res Lett 42.

Sawyer, D.E., Reece, R.S., Gulick, S.P.S., Lenz, B.L., 2017. Submarine landslide and tsunami hazards offshore southern Alaska: Seismic strengthening versus rapid sedimentation. Geophys Res Lett.

Scheuer, C., Gohl, K., Larter, R.D., Rebesco, M., Udintsev, G., 2006. Variability in Cenozoic sedimentation along the continental rise of the Bellingshausen Sea, West Antarctica. Mar Geol 227, 279-298.

Šeirienė, V., Karabanov, A., Rylova, T., Baltrūnas, V., Savchenko, I., 2015. The Pleistocene stratigraphy of the south-eastern sector of the Scandinavian glaciation (Belarus and Lithuania): a review. Baltica 28.

Sejrup, H.P., Aarseth, I., Haflidason, H., Løvlie, R., Bratten, Å., Tjøstheim, G., Forsberg, C.F., Ellingsen, K.L., 1995. Quaternary of the Norwegian Channel: glaciation history and palaeoceanography. Norwegian Journal of Geology 75, 65-87.

Sejrup, H.P., Haflidason, H., Aarseth, I., King, E.L., Forsberg, C.F., Long, D., Rokoengen, K., 1994. Late Weichselian glaciation history of the northern North Sea. Boreas-International Journal of Quaternary Research 23, 1-13.

Sejrup, H.P., Haflidason, H., Hjelstuen, B.I., Nygard, A., Bryn, P., Lien, R., 2004. Pleistocene development of the SE Nordic seas margin. Mar Geol 213, 169-200.

Sejrup, H.P., Hjelstuen, B.O., Dahlgren, K.I.T., Haflidason, H., Kuijpers, A., Nygård, A., Praeg, D., Stoker, M.S., Vorren, T.O., 2005. Pleistocene glacial history of the NW European continental margin. Mar Petrol Geol 22, 1111-1129.

Sejrup, H.P., King, E.L., Aarseth, I., Haflidason, H., Elverhøi, A., 1996. Quaternary erosion and depositional processes: western Norwegian fjords, Norwegian Channel and North Sea Fan. Geological Society, London, Special Publications 117, 187-202.

Sejrup, H.P., Larsen, E., Haflidason, H., Berstad, I.M., Hjelstuen, B.O., Jonsdottir, H.E., King, E.L., Landvik, J., Longva, O., Nygård, A., Ottesen, D., Raunholm, S., Rise, L., Stalsberg, K., 2003. Configuration, history and impact of the Norwegian Channel Ice Stream. Boreas 32, 18-36.

Sejrup, H.P., Larsen, E., Landvik, J., King, E.L., Haflidason, H., Nesje, A., 2000. Quaternary glaciations in southern Fennoscandia: evidence from southwestern Norway and the northern North Sea region. Quaternary Sci Rev 19, 667-685.

Sejrup, H.P., Nagy, J., Brigham-Grette, J., 1989. Foraminiferal stratigraphy and amino acid geochronology of Quaternary sediments in the Norwegian Channel, northern North Sea. Norsk geologisk tidsskrift 69, 111-124.

Shennan, I., Peltier, W.R., Drummond, R., Horton, B., 2002. Global to local scale parameters determining relative sea-level changes and the post-glacial isostatic adjustment of Great Britain. Quaternary Sci Rev 21, 397-408.

Shepard, F.P., Marshall, N.F., McLoughlin, P.A., Sullivan, G.G., 1979. Currents in submarine canyons and other seavalleys.

Siegert, M.J., Dowdeswell, J.A., Hald, M., Svendsen, J.-I., 2001. Modelling the Eurasian Ice Sheet through a full (Weichselian) glacial cycle. Global and Planetary Change 31, 367-385.

Smith, D.E., Harrison, S., Jordan, J.T., 2013. Sea level rise and submarine mass failures on open continental margins. Quaternary Sci Rev 82, 93-103.

Smith, D.E., Shi, S., Cullingford, R.A., Dawson, A.G., Dawson, S., Firth, C.R., Foster, I.D.L., Fretwell, P.T., Haggart, B.A., Holloway, L.K., 2004. The holocene storegga slide tsunami in the United Kingdom. Quaternary Sci Rev 23, 2291-2321.

Solheim, A., Andersen, E.S., Elverhøi, A., Fiedler, A., 1996. Late Cenozoic depositional history of the western Svalbard continental shelf, controlled by subsidence and climate. Global and Planetary Change 12, 135-148.

Solheim, A., Berg, K., Forsberg, C.F., Bryn, P., 2005a. The Storegga Slide complex: repetitive large scale sliding with similar cause and development. Mar Petrol Geol 22, 97-107.

Solheim, A., Bryn, P., Sejrup, H.P., Mienert, J., Berg, K., 2005b. Ormen Lange—an integrated study for the safe development of a deep-water gas field within the Storegga Slide Complex, NE Atlantic continental margin; executive summary. Mar Petrol Geol 22, 1-9.

Solheim, A., Elverhøi, A., 1985. A pockmark field in the Central Barents Sea; gas from a petrogenic source? Polar research 3, 11-19.

Solheim, A., Faleide, J.I., Andersen, E.S., Elverhøi, A., Forsberg, C.F., Vanneste, K., Uenzelmann-Neben, G., Channell, J.E.T., 1998. Late Cenozoic seismic stratigraphy and glacial geological development of the East Greenland and Svalbard–Barents Sea continental margins. Quaternary Sci Rev 17, 155-184.

Solheim, A., Kristoffersen, Y., 1984. Sediments above the upper regional unconformity: thickness, seismic stratigraphy and outline of the glacial history. Norsk Polarinstitutt.

Spiegler, D., Jansen, E., 1989. Planktonic foraminifer biostratigraphy of Norwegian Sea sediments: ODP Leg 104, Proceedings of the Ocean Drilling Program, Scientific Results. TX (Ocean Drilling Program) College Station, pp. 681-696.

Spielhagen, R.F., Baumann, K.-H., Erlenkeuser, H., Nowaczyk, N.R., Nørgaard-Pedersen, N., Vogt, C., Weiel, D., 2004. Arctic Ocean deep-sea record of northern Eurasian ice sheet history. Quaternary Sci Rev 23, 1455-1483.

St. John, K.E., Krissek, L.A., 2002. The late Miocene to Pleistocene ice-rafting history of southeast Greenland. Boreas 31, 28-35.

Steffen, H., Wu, P., 2011. Glacial isostatic adjustment in Fennoscandia—a review of data and modeling. J Geodyn 52, 169-204.

Stein, R., Grobe, H., Hubberten, H., Marienfeld, P., Nam, S., 1993. Latest Pleistocene to Holocene changes in glaciomarine sedimentation in Scoresby Sund and along the adjacent East Greenland Continental Margin: Preliminary results. Geo-Mar Lett 13, 9-16.

Stein, R., Nam, S.-I., Grobe, H., Hubberten, H., 1996. Late Quaternary glacial history and short-term ice-rafted debris fluctuations along the East Greenland continental margin. Geological Society, London, Special Publications 111, 135-151.

Stewart, I.S., Sauber, J., Rose, J., 2000. Glacio-seismotectonics: ice sheets, crustal deformation and seismicity. Quaternary Sci Rev 19, 1367-1389.

Stewart, M.A., Lonergan, L., Hampson, G., 2013. 3D seismic analysis of buried tunnel valleys in the central North Sea: morphology, cross-cutting generations and glacial history. Quaternary Sci Rev 72, 1-17.

Stigall, J., Dugan, B., 2010. Overpressure and earthquake initiated slope failure in the Ursa region, northern Gulf of Mexico. J Geophys Res-Sol Ea 115.

Stoker, M.S., Leslie, A.B., Scott, W.D., Briden, J.C., Hine, N.M., Harland, R., Wilkinson, I.P., Evans, D., Ardus, D.A., 1994. A record of late Cenozoic stratigraphy, sedimentation and climate change from the Hebrides Slope, NE Atlantic Ocean. Journal of the Geological Society 151, 235-249.

STRATAGEM, P., 2002. The Neogene stratigraphy of the glaciated European margin from Lofoten to Porcupine. A product of the EC-supported STRATAGEM project, p. 75.

Sultan, N., Cochonat, P., Canals, M., Cattaneo, A., Dennielou, B., Haflidason, H., Laberg, J.S., Long, D., Mienert, J., Trincardi, F., Urgeles, R., Vorren, T.O., Wilson, C., 2004a. Triggering mechanisms of slope instability processes and sediment failures on continental margins: a geotechnical approach. Mar Geol 213, 291-321.

Sultan, N., Cochonat, P., Foucher, J.-P., Mienert, J., 2004b. Effect of gas hydrates melting on seafloor slope instability. Mar Geol 213, 379-401.

Svendsen, J.I., Alexanderson, H., Astakhov, V.I., Demidov, I., Dowdeswell, J.A., Funder, S., Gataullin, V., Henriksen, M., Hjort, C., Houmark-Nielsen, M., 2004a. Late Quaternary ice sheet history of northern Eurasia. Quaternary Sci Rev 23, 1229-1271.

Svendsen, J.I., Astakhov, V.I., Bolshiyanov, D.Y., Demidov, I., Dowdeswell, J.A., Gataullin, V., Hjort, C., Hubberten, H.W., Larsen, E., Mangerud, J., 1999. Maximum extent of the Eurasian ice sheets in the Barents and Kara Sea region during the Weichselian. Boreas 28, 234-242.

Svendsen, J.I., Briner, J.P., Mangerud, J., Young, N.E., 2015. Early break-up of the norwegian channel ice stream during the last glacial maximum. Quaternary Sci Rev 107, 231-242.

Svendsen, J.I., Gataullin, V., Mangerud, J., Polyak, L., 2004b. The glacial history of the Barents and Kara Sea region. Developments in Quaternary Sciences 2, 369-378.

Talling, P.J., Clare, M.A., Urlaub, M., Pope, E., Hunt, J.E., Watt, S.F.L., 2014. Large Submarine Landslides on Continental Slopes. Oceanography 27, 32.

Talwani, M., Udintsev, G.B., White, S.M., 1976. Introduction and explanatory notes, leg 38, deep sea drilling project. Initial Reports DSDP 38.

Tappin, D.R., Watts, P., McMurtry, G.M., Lafoy, Y., Matsumoto, T., 2001. The Sissano, Papua New Guinea tsunami of July 1998 - offshore evidence on the source mechanism. Mar Geol 175, 1-23.

Tasianas, A., Martens, I., Bünz, S., Mienert, J., 2016. Mechanisms initiating fluid migration at Snøhvit and Albatross fields, Barents Sea. arktos 2, 26.

Taylor, J., Dowdeswell, J.A., Kenyon, N.H., Ó Cofaigh, C., 2002a. Late Quaternary architecture of trough-mouth fans: debris flows and suspended sediments on the Norwegian margin. Geological Society, London, Special Publications 203, 55-71.

Taylor, J., Dowdeswell, J.A., Siegert, M.J., 2002b. Late Weichselian depositional processes, fluxes, and sediment volumes on the margins of the Norwegian Sea (62–75 N). Mar Geol 188, 61-77.

ten Brink, U.S., Lee, H.J., Geist, E.L., Twichell, D., 2009. Assessment of tsunami hazard to the US East Coast using relationships between submarine landslides and earthquakes. Mar Geol 264, 65-73.

ten Brink, U.S., Schneider, C., Johnson, A.H., 1995. Morphology and Stratal Geometry of the Antarctic Continental Shelf: Insights from Models, in: Cooper, A.K., Barker, P.F., Brancolini, G. (Eds.), Geology and Seismic Stratigraphy of the Antarctic Margin. American Geophysical Union, pp. 1-24.

Thiede, J., Eldholm, O., Taylor, E., 1989. Variability of Cenozoic Norwegian-Greenland Sea paleoceanography and northern hemisphere paleoclimate, Proceedings of the Ocean Drilling Program, Scientific Results, pp. 1067-1118.

Thiede, J., Winkler, A., Wolf-Welling, T.C.W., Eldholm, O., Myhre, A.M., Baumann, K.-H., Henrich, R., Stein, R., 1998. Late Cenozoic history of the polar North Atlantic: results from ocean drilling. Quaternary Sci Rev 17, 185-208.

Thierens, M., Pirlet, H., Colin, C., Latruwe, K., Vanhaecke, F., Lee, J.R., Stuut, J.-B., Titschack, J., Huvenne, V.A.I., Dorschel, B., 2012. Ice-rafting from the British–Irish ice sheet since the earliest

Pleistocene (2.6 million years ago): implications for long-term mid-latitudinal ice-sheet growth in the North Atlantic region. Quaternary Sci Rev 44, 229-240.

Thomas, S., Hooper, J., Clare, M.A., 2010. Constraining geohazards to the past: Impact assessment of submarine mass movements on seabed developments, Adv Nat Tech Haz Res. Springer, pp. 387-398.

Tripsanas, E.K., Piper, D.J.W., 2008a. Glaciogenic debris-flow deposits of Orphan Basin, offshore eastern Canada: sedimentological and rheological properties, origin, and relationship to meltwater discharge. Journal of Sedimentary Research 78, 724-744.

Tripsanas, E.K., Piper, D.J.W., 2008b. Late Quaternary stratigraphy and sedimentology of Orphan Basin: implications for meltwater dispersal in the southern Labrador Sea. Palaeogeography, Palaeoclimatology, Palaeoecology 260, 521-539.

Trofimuk, A., Cherskiy, N., Tsarev, V., 1977. The role of continental glaciation and hydrate formation on petroleum occurrences, Future supply of nature made petroleum and gas. Pergamon, New York, pp. 919-926.

Tveranger, J., Houmark-Nielsen, M., Løvberg, K., Mangerud, J., 1994. Eemian-Weichselian stratigraphy of the Flakkerhuk ridge, southern Jameson Land, East Greenland. Boreas 23, 359-384.

Tziperman, E., Gildor, H., 2003. On the mid-Pleistocene transition to 100-kyr glacial cycles and the asymmetry between glaciation and deglaciation times. Paleoceanography 18.

Urciuoli, G., Picarelli, L., Leroueil, S., 2007. Local soil failure before general slope failure. Geotechnical and Geological Engineering 25, 103-122.

Urlaub, M., Talling, P.J., Clare, M.A., 2014. Sea-level-induced seismicity and submarine landslide occurrence: Comment. Geology 42, e337.

Urlaub, M., Zervos, A., Talling, P.J., Masson, D.G., Clayton, C.I., 2012. How Do ~2° Slopes Fail in Areas of Slow Sedimentation? A Sensitivity Study on the Influence of Accumulation Rate and Permeability on Submarine Slope Stability, in: Yamada, Y., Kawamura, K., Ikehara, K., Ogawa, Y., Urgeles, R., Mosher, D., Chaytor, J., Strasser, M. (Eds.), Adv Nat Tech Haz Res. Springer Netherlands, pp. 277-287.

Vadakkepuliyambatta, S., Bünz, S., Mienert, J., Chand, S., 2013. Distribution of subsurface fluid-flow systems in the SW Barents Sea. Mar Petrol Geol 43, 208-221.

Vail, P.R., Mitchum Jr, R.M., Thompson III, S., 1977. Seismic stratigraphy and global changes of sea level: Part 4. Global cycles of relative sea level change., in: Payton, C.E. (Ed.), Seismic stratigraphy - Applications to hydrocarbon exploration: American Association of Petroleum Geologists Memoir 26, pp. 83-97.

Vanneste, K., Uenzelmann-Neben, G., Miller, H., 1995. Seismic evidence for long-term history of glaciation on central East Greenland shelf south of Scoresby Sund. Geo-Mar Lett 15, 63-70.

Vanoudheusden, E., Sultan, N., Cochonat, P., 2004. Mechanical behaviour of unsaturated marine sediments: experimental and theoretical approaches. Mar Geol 213, 323-342.

Velichko, A.A., Pisareva, V.V., Faustova, M.A., 2005. Glaciations and interglacials of East European plain in the Early and Middle Pleistocene. Stratigr. Geol. Correl 13, 195-211.

Vogt, C., Knies, J., 2008. Sediment dynamics in the Eurasian Arctic Ocean during the last deglaciation—the clay mineral group smectite perspective. Mar Geol 250, 211-222.

Vogt, C., Knies, J., Spielhagen, R.F., Stein, R., 2001. Detailed mineralogical evidence for two nearly identical glacial/deglacial cycles and Atlantic water advection to the Arctic Ocean during the last 90,000 years. Global and Planetary Change 31, 23-44.

Völker, D., Scholz, F., Geersen, J., 2011. Analysis of submarine landsliding in the rupture area of the 27 February 2010 Maule earthquake, Central Chile. Mar Geol 288, 79-89.

Vorren, T.O., Laberg, J.S., 1997. Trough mouth fans—palaeoclimate and ice-sheet monitors. Quaternary Sci Rev 16, 865-881.

Vorren, T.O., Laberg, J.S., Blaume, F., Dowdeswell, J.A., Kenyon, N.H., Mienert, J., Rumohr, J., Werner, F., 1998. The Norwegian Greenland Sea continental margins: Morphology and late Quaternary sedimentary processes and environment. Quaternary Sci Rev 17, 273-302.

Vorren, T.O., Landvik, J.Y., Andreassen, K., Laberg, J.S., 2011. Glacial history of the Barents Sea region. Quaternary Glaciations—Extent and Chronology—A Closer Look, Dev. in Quat. Sci, 361-372.

Vorren, T.O., Lebesbye, E., Andreassen, K., Larsen, K.-B., 1989. Glacigenic sediments on a passive continental margin as exemplified by the Barents Sea. Mar Geol 85, 251-272.

Vorren, T.O., Lebesbye, E., Larsen, K.B., 1990. Geometry and genesis of the glacigenic sediments in the southern Barents Sea. Geological Society, London, Special Publications 53, 269-288.

Vorren, T.O., Plassen, L.I.V., 2002. Deglaciation and palaeoclimate of the Andfjord-Vågsfjord area, North Norway. Boreas 31, 97-125.

Waddington, C., Wicks, K., 2017. Resilience or wipe out? Evaluating the convergent impacts of the 8.2 ka event and Storegga tsunami on the Mesolithic of northeast Britain. Journal of Archaeological Science: Reports 14, 692-714.

Waythomas, C.F., Watts, P., 2003. Numerical simulation of tsunami generation by pryoclastic flow at Aniakchak Volcano, Alaska. Geophys Res Lett 30.

Waythomas, C.F., Watts, P., Walder, J.S., 2006. Numerical simulation of tsunami generation by cold volcanic mass flows at Augustine Volcano, Alaska. Natural Hazards & Earth System Sciences 6.

Weaver, A.J., Saenko, O.A., Clark, P.U., Mitrovica, J.X., 2003. Meltwater pulse 1A from Antarctica as a trigger of the Bølling-Allerød warm interval. Science 299, 1709-1713.

Weaver, P.P.E., Kuijpers, A., 1983. Climatic control of turbidite deposition on the Madeira Abyssal Plain.

Weber, M.E., Bonani, G., Fütterer, K.D., 1994. Sedimentation processes within channel-ridge systems, southeastern Weddell Sea, Antarctica. Paleoceanography 9, 1027-1048.

Weber, M.E., Clark, P.U., Ricken, W., Mitrovica, J.X., Hostetler, S.W., Kuhn, G., 2011. Interhemispheric ice-sheet synchronicity during the Last Glacial Maximum. Science 334, 1265-1269.

Wellner, J.S., Heroy, D.C., Anderson, J.B., 2006. The death mask of the Antarctic ice sheet: comparison of glacial geomorphic features across the continental shelf. Geomorphology 75, 157-171.

Wellner, J.S., Lowe, A.L., Shipp, S.S., Anderson, J.B., 2001. Distribution of glacial geomorphic features on the Antarctic continental shelf and correlation with substrate: implications for ice behavior. J Glaciol 47, 397-411.

Weninger, B., Schulting, R., Bradtmöller, M., Lee, C., Collard, M., Edinborough, K., Hilpert, J., Jöris, O., Niekus, M., Rohling, E.J., 2008. The catastrophic final flooding of Doggerland by the Storegga Slide tsunami. Documenta Praehistorica 35, 1.

Wicks, K., Mithen, S., 2014. The impact of the abrupt 8.2 ka cold event on the Mesolithic population of western Scotland: a Bayesian chronological analysis using 'activity events' as a population proxy. Journal of Archaeological Science 45, 240-269.

Wilken, M., Mienert, J., 2006. Submarine glacigenic debris flows, deep-sea channels and past ice-stream behaviour of the East Greenland continental margin. Quaternary Sci Rev 25, 784-810.

Winkelmann, D., Jokat, W., Jensen, L., Schenke, H.-W., 2010. Submarine end moraines on the continental shelf off NE Greenland–Implications for Lateglacial dynamics. Quaternary Sci Rev 29, 1069-1077.

Winkler, A., Wolf-Welling, T., Stattegger, K., Thiede, J., 2002. Clay mineral sedimentation in high northern latitude deep-sea basins since the Middle Miocene (ODP Leg 151, NAAG). International Journal of Earth Sciences 91, 133-148.

Winsborrow, M.C.M., Andreassen, K., Corner, G.D., Laberg, J.S., 2010. Deglaciation of a marine-based ice sheet: Late Weichselian palaeo-ice dynamics and retreat in the southern Barents Sea reconstructed from onshore and offshore glacial geomorphology. Quaternary Sci Rev 29, 424-442.

Winsborrow, M.C.M., Stokes, C.R., Andreassen, K., 2012. Ice-stream flow switching during deglaciation of the southwestern Barents Sea. Geological Society of America Bulletin 124, 275-290.

Wolf-Welling, T.C.W., Cremer, M., O'Connell, S., Winkler, A., Thiede, J., 1996. Cenozoic Arctic gateway paleoclimate variability: Indications from changes in coarse-fraction composition, Proceedings of the Ocean Drilling Program. Scientific Results. Ocean Drilling Program, pp. 515-567.

Zachos, J., Pagani, M., Sloan, L., Thomas, E., Billups, K., 2001. Trends, rhythms, and aberrations in global climate 65 Ma to present. Science 292, 686-693.

Zajaczkowski, M., 2008. Sediment supply and fluxes in glacial and outwash fjords, Kongsfjorden and Adventfjorden, Svalbard. Polish Polar Research 29, 59-72.

Zieba, K.J., Grøver, A., 2016. Isostatic response to glacial erosion, deposition and ice loading. Impact on hydrocarbon traps of the southwestern Barents Sea. Mar Petrol Geol 78, 168-183.

Ziegler, P.A., 1990. Geological atlas of western and central Europe. Geological Society of London.

3694

Figures

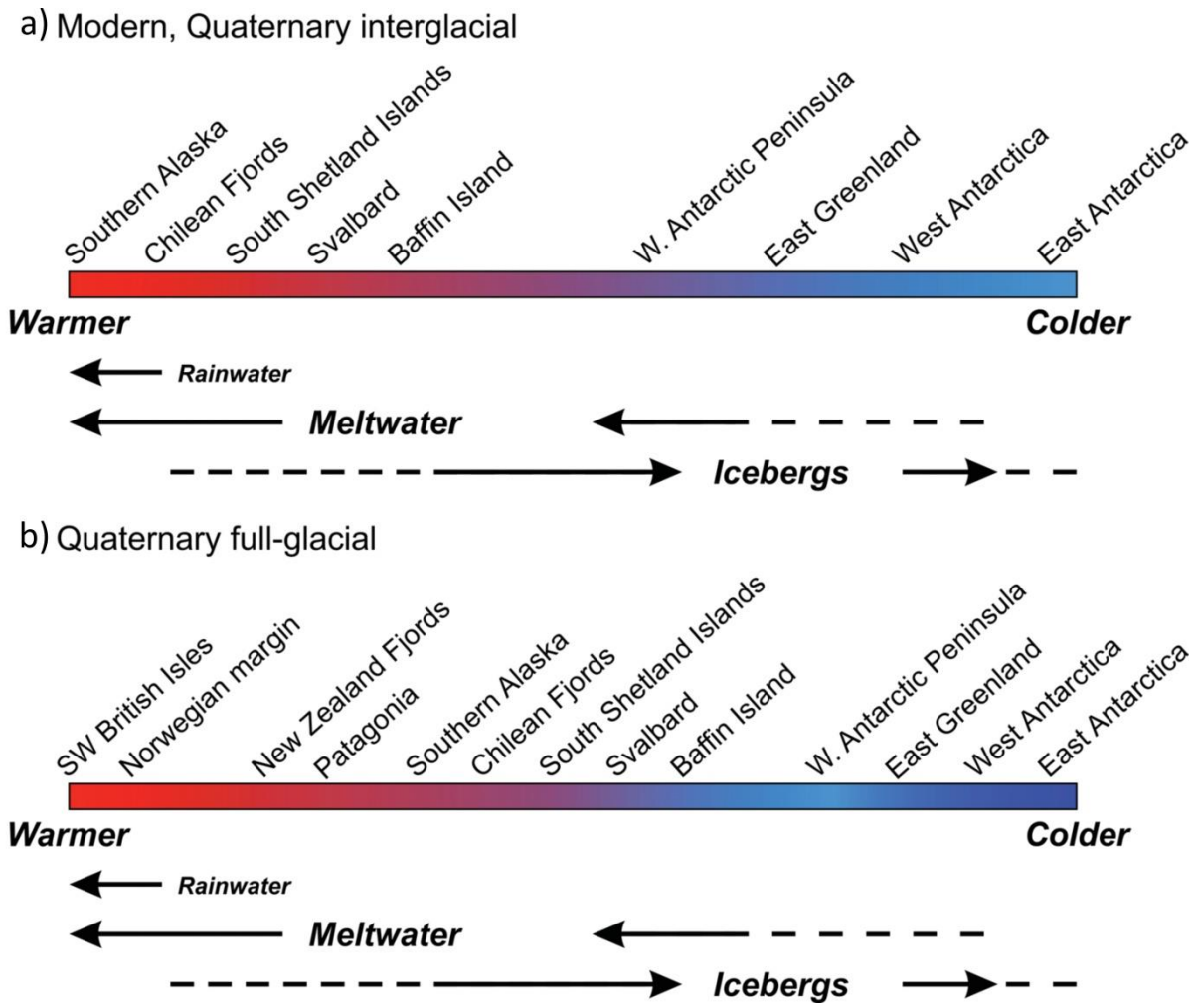

Fig. 1. The climatic continuum of glacier-influenced marine settings for (a) the modern, or Quaternary interglacial Earth, and (b) Quaternary full-glacial conditions. Adapted from Dowdeswell et al. (2006b).

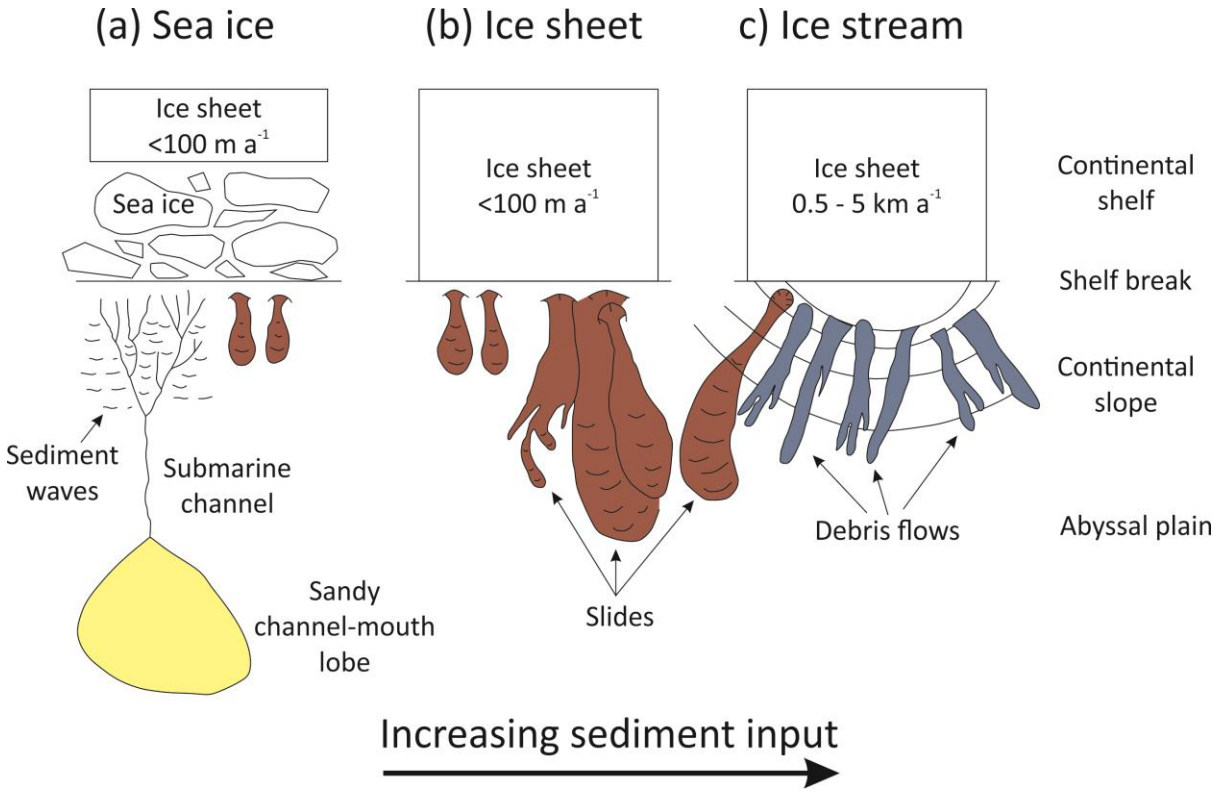

3701

3702 Fig. 2. Conceptual model of sedimentation on glacier-influenced continental margins. a) Sediment
3703 starved margin with an ice sheet terminating inshore of the shelf edge. b) Inter-ice stream areas with
3704 ice at the shelf edge. c) Continental margin dominated by ice stream delivery of sediment and the
3705 resulting formation of a trough-mouth fan (adapted from Dowdeswell et al., 1996).

3706

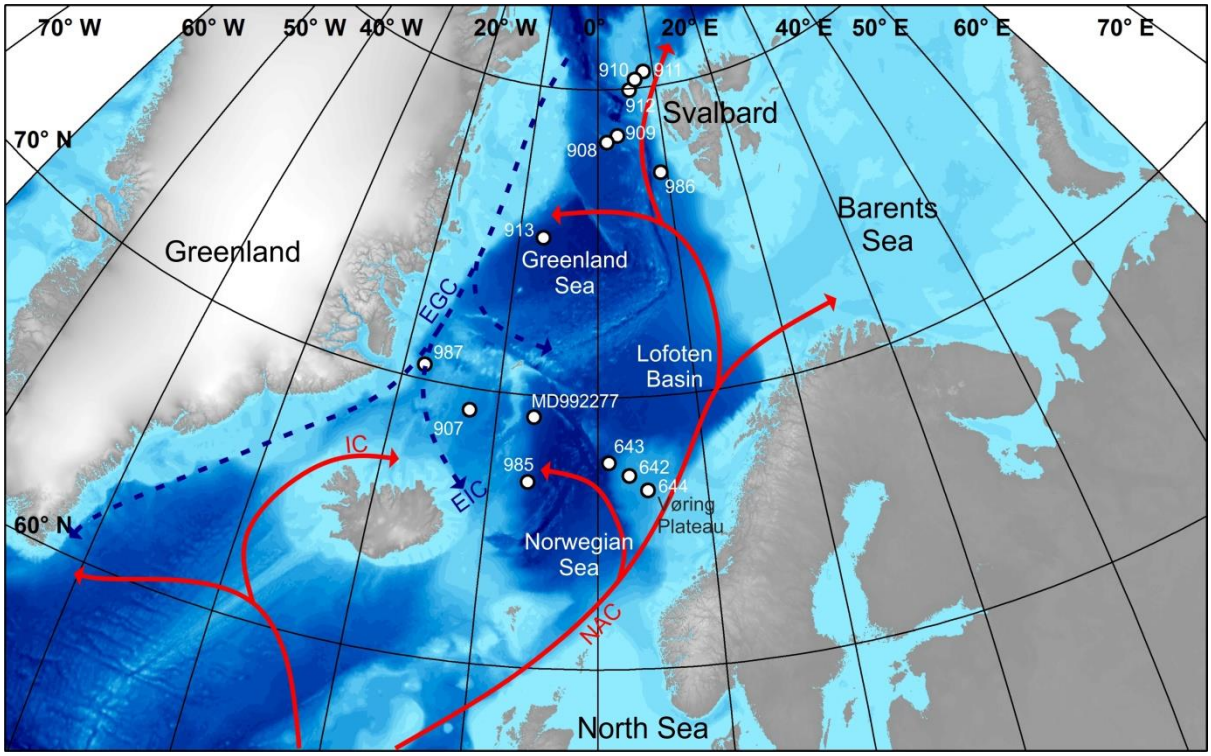

3707

3708 Fig. 3. Map of the Nordic Seas and the ODP sites used in this study. General ocean circulation during
3709 the present interglacial is also shown (red – warm; blue – cold). NAC – Norwegian Atlantic Current;
3710 EGC – East Greenland Current; EIC – East Iceland Current; IC – Irminger Current.

3711

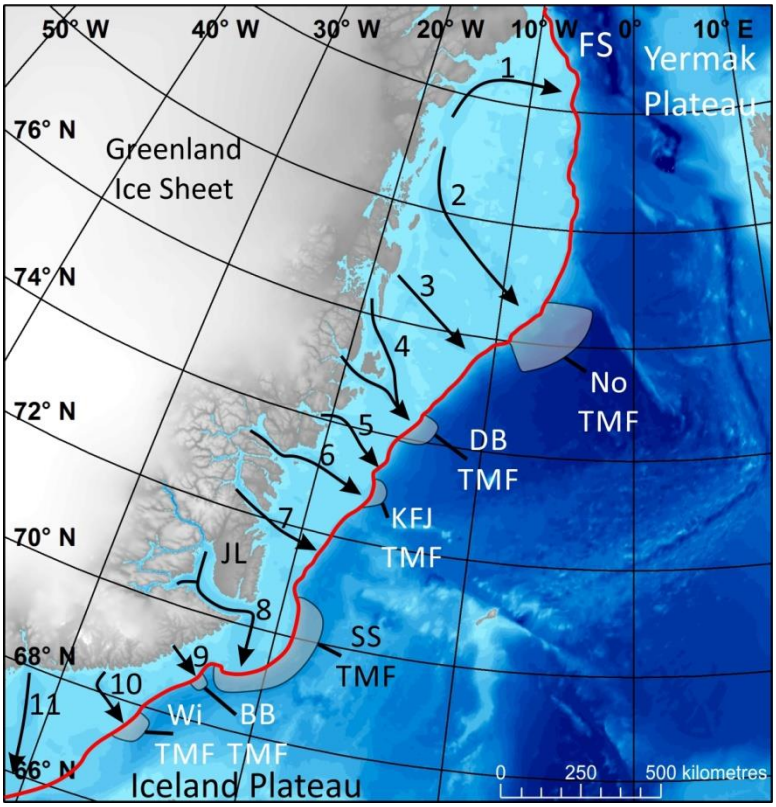

Fig. 4. Maximum Quaternary extent of the Greenland Ice Sheet in East Greenland (red line) with notable cross-shelf troughs and trough-mouth fans displayed on IBCAO bathymetric data (Jakobsson et al., 2012). Arrows indicate cross-shelf troughs thought to have previously contained ice streams. 1 = Westwind. 2 = Norske. 3 = Store Koldewey. 4 = Dove Bugt. 5 = Unnamed. 6 = Kaiser Franz Josef. 7 = Kong Oscar. 8 = Scorsby Sund. 9 = Barclay Bugt. 10 = Wiedemann. 11 = Kangerdlussuaq. Trough-mouth fans/bulges in bathymetry indicated by grey shading (Batchelor et al., 2014). No TMF = Norske Trough-Mouth Fan. DB TMF = Dove Bugt Trough-Mouth Fan. KFJ TMF = Kaiser Franz Josef Trough-Mouth Fan. SS TMF = Scorseby Sund Trough-Mouth Fan. BB TMF = Barclay Bugt Trough Mouth Fan. Wi TMF = Wiedemann Trough Mouth Fan. FS = Fram Strait. JL = Jameson Land.

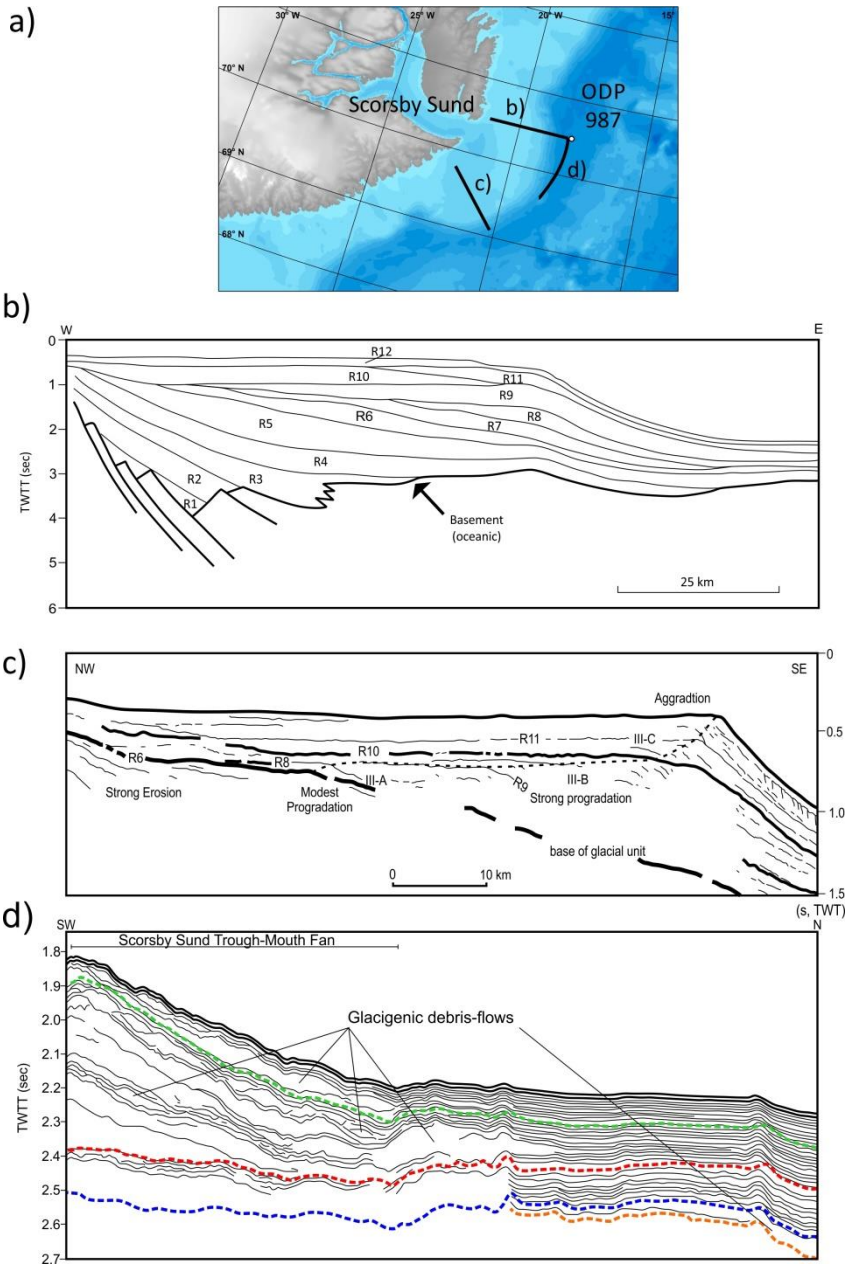

Fig. 5. Multichannel seismic lines on the Scoresby Sund Trough-Mouth Fan (modified from Vanneste et al., 1995; Solheim et al., 1998; Laberg et al., 2013). a) Location map showing seismic lines GGU 82-12 and 90600 and the line of Laberg et al. (2013), and the relative position of ODP Site 987. b) Seismic line GGU 82-12. According to Larson's (1990) original interpretation sequences 9 – 11 represent Late Miocene to Pliocene and 12 represents the Pleistocene. c) Interpretation of the stratal geometry in the continental shelf part of line 90600. Based on variations in the aggradation and progradation components, the glacial unit, Unit III, has been divided into subunits A (2.6 – 1.2 Ma), B (1.2 – 0.5 Ma), and C (0.5 – 0 Ma). d) Single channel seismic profile extending from ODP Site 987 southward. Lithological units, age model and seismic reflections according to Shipboard Scientific Party (1996) are reflected by dashed lines. Green – 0.78 Ma; Red – R1 reflector at 1.77 Ma; Blue – R2 reflector; Orange – 2.58 Ma.

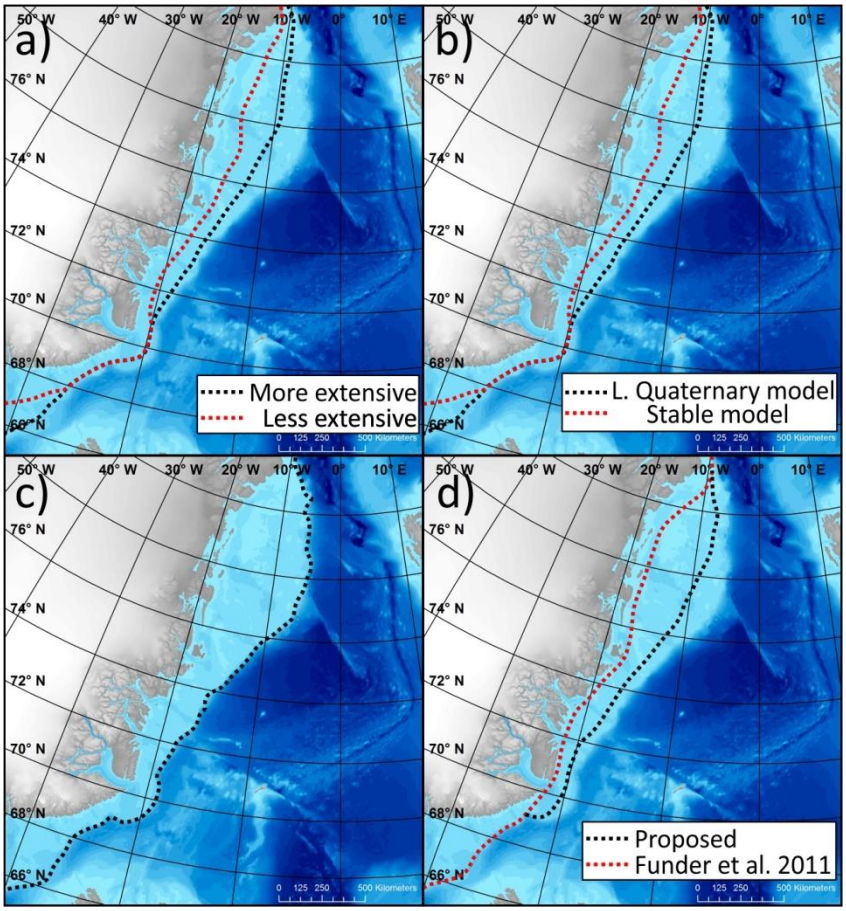

Fig. 6. Maximum extents of the Greenland Ice Sheet on the East Greenland Margin. a) 2.58 – 1.3 Ma. Two regimes of advance and retreat are envisaged for this period; an extensive advance regime (2.5 – 2.4 and ~2.1 Ma) and a less extensive advance regime. The ice sheet appears not to have undergone widespread collapses (Solheim et al., 1998). b) 1.3 – 0.7 Ma. Two regimes are again envisaged, a stable confined ice sheet or a dynamic ice sheet akin to the Late Quaternary Greenland Ice Sheet (Winkelmann et al., 2010). c) 0.7 – 0.13 Ma. Maximum extent of the Saalian Greenland Ice Sheet; the margin position of other advances between 0.7 and 0.13 are uncertain. d) 0.13 – 0 Ma. Maximum ice sheet extent according to Funder et al. (2011) and a revised limit based on shelf geomorphology. A large degree of uncertainty exists regarding the shown ice sheet margins. Even the Weichselian reconstruction is largely inferred.

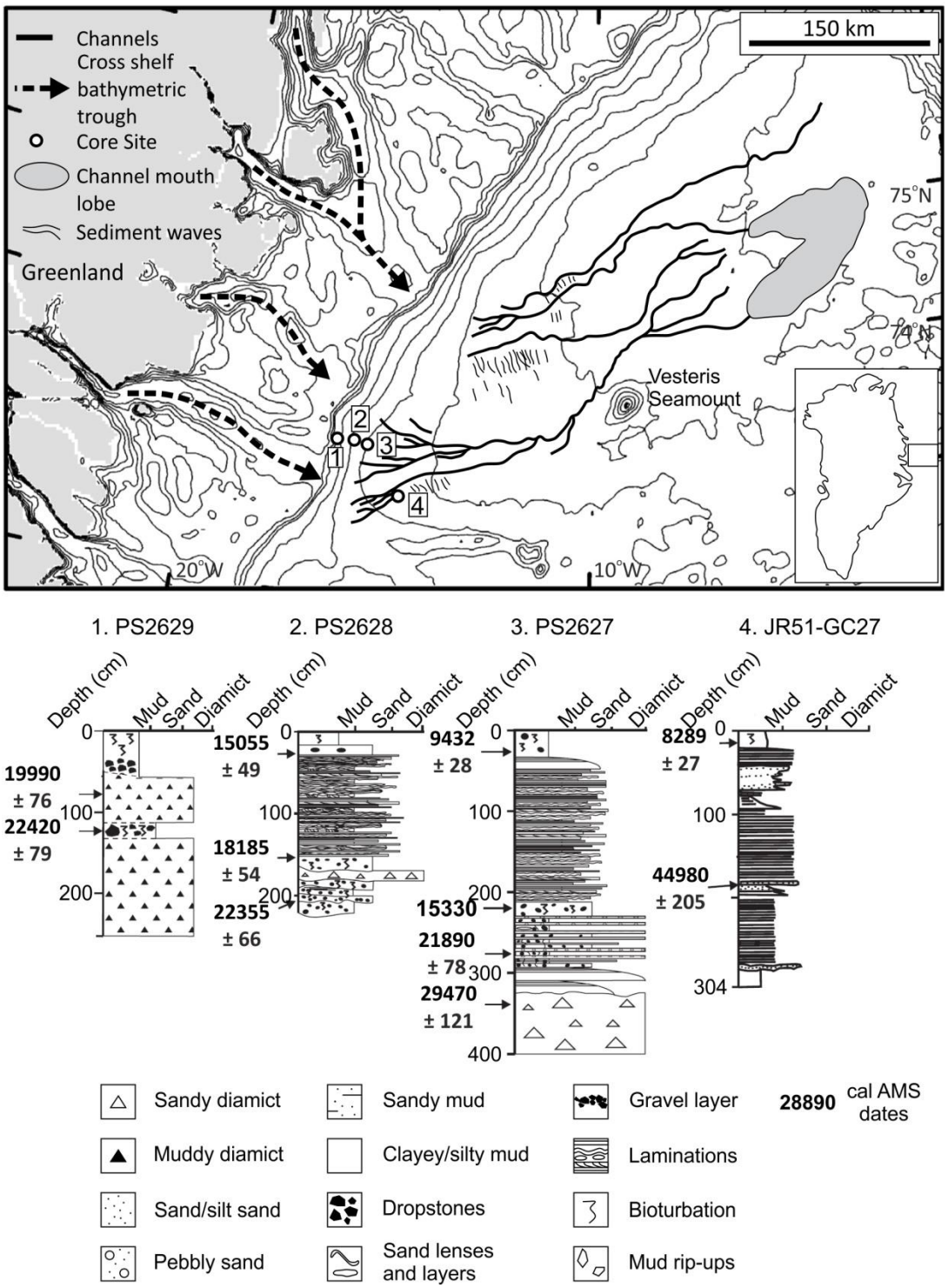

Fig. 7. Bathymetry of the Greenland Basin and the adjoining continental shelf, northeast Greenland and major submarine geological features (channel systems, sediment waves and channel-mouth lobes). Major cross-shelf troughs on the continental shelf are highlighted by arrows. Core sites are numbered 1 to 4. Sediment logs of gravity cores identified on the bathymetric map are included with calibrated AMS radiocarbon dates. Bathymetric data on continental shelf are derived from the IBCAO Arctic bathymetry database (Jakobsson et al., 2000). Figure is adapted from Ó Cofaigh et al. (2004).

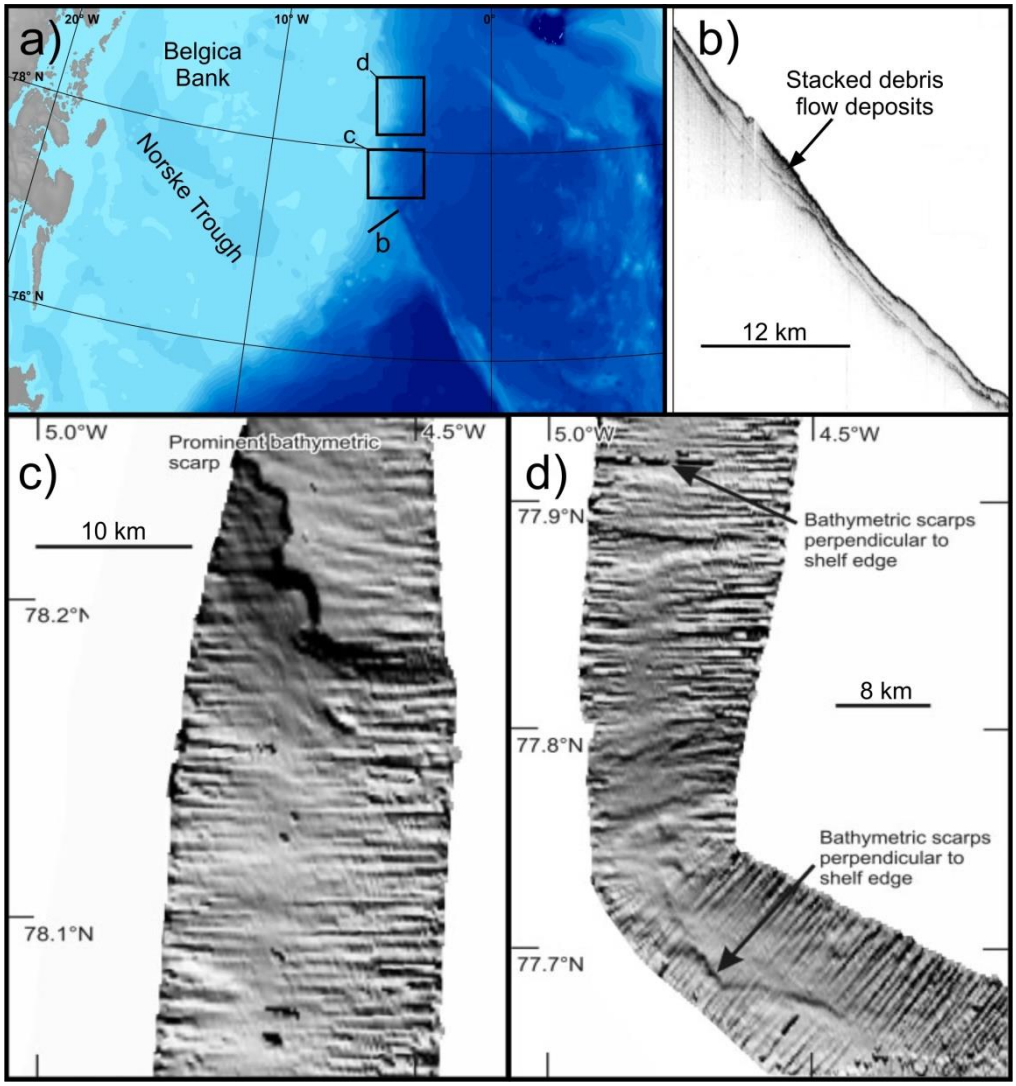

Fig. 8. a) Location map of the northeast Greenland continental margin. b) TOPAS sub-bottom acoustic profile. Along slope profile from the upper-middle slope showing acoustically transparent sediment lenses interpreted as stacked debris-flow deposits. c) and d) EM120 shaded swath bathymetry from the northeast Greenland continental slope showing prominent and sinuous bathymetric scarps consistent with slide scars produced during the process of sediment failure and sliding (adapted from Evans et al., 2009).

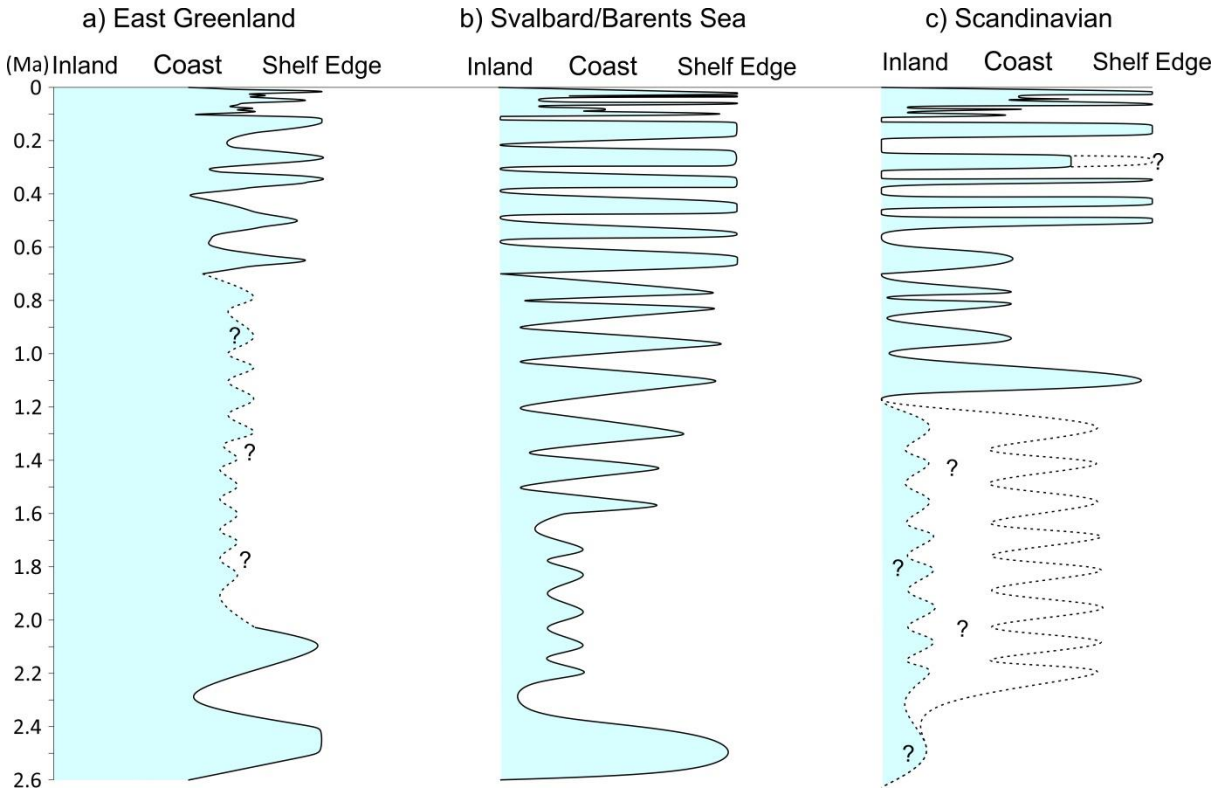

Fig. 9. Schematic glaciation curves for the general behaviour of the Greenland, Barents Sea and Scandinavian Ice Sheets. Dashed lines and question marks represent time periods where there is a lack of data from various margins or conflicting interpretations of ice sheet extent.

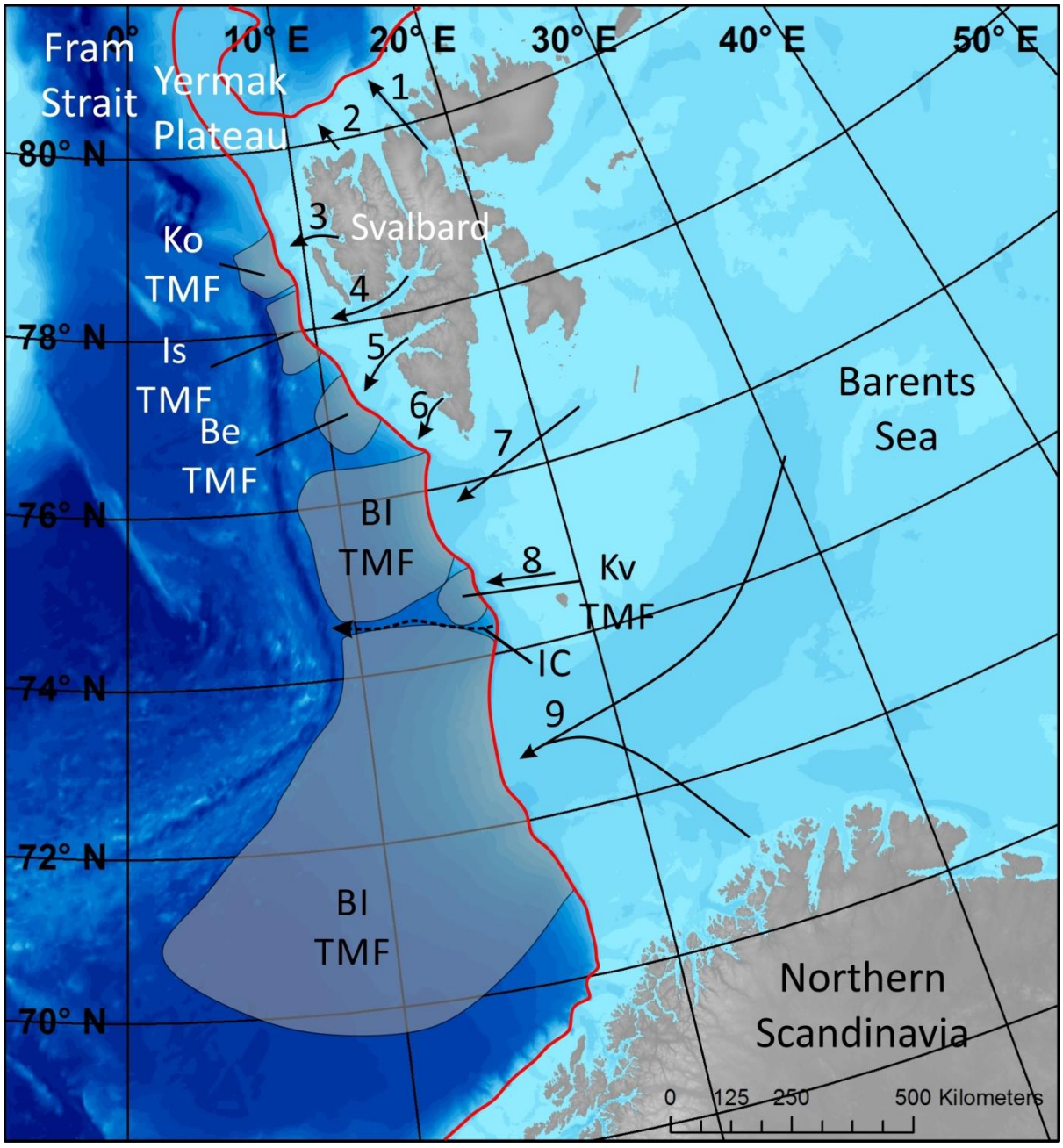

Fig. 10. Maximum westward Quaternary extent of the Barents Sea Ice Sheet (red line) with notable gross-shelf troughs and trough-mouth fans displayed on IBCAO bathymetric data (Jakobsson et al., 2012). Arrows indicate cross-shelf troughs thought to have previously contained ice streams. 1 = Hinlopen. 2 = Woodfjorden. 3 = Kongsfjorden. 4 = Isfjorden. 5 = Bellsund. 6 = Hornsund. 7 = Storfjorden. 8 = Kveithola. 9 = Bear Island. Trough-Mouth Fans on the Svalbard/Barents Sea southwest margin shown by grey shaded regions (Ottesen et al., 2006). Ko TMF = Kongsfjorden Trough-Mouth Fan. Is TMF = Trough-Mouth Fan. Be TMF = Bellsund Trough-Mouth Fan. Kv TMF = Kveithola Trough-Mouth Fan. BI TMF = Bear Island Trough-Mouth Fan. IC = INBIS Channel.

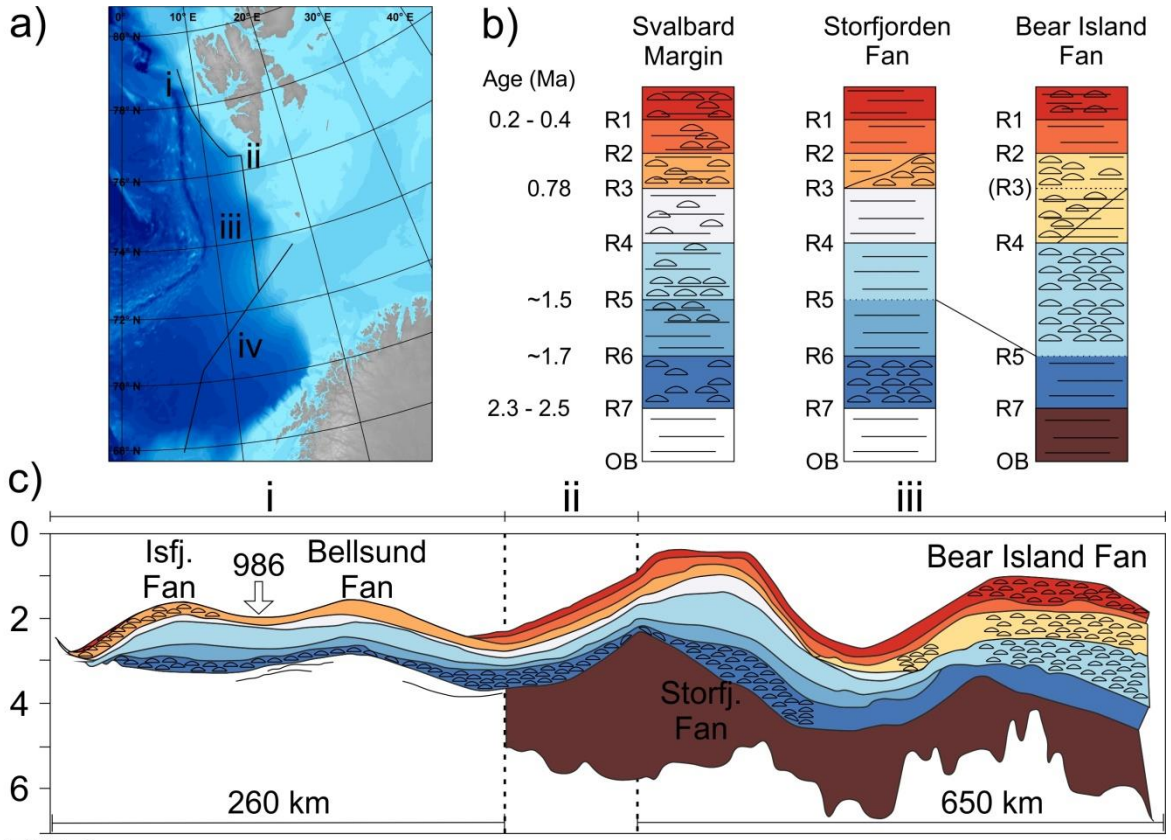

Fig. 11. a) Location map of seismic profiles along the Svalbard/Barents Sea continental margin. b) Seismic stratigraphic framework for the Svalbard/Barents Sea Margin, with correlation of the main sequence boundaries between the Svalbard Margin (Isfjorden), Storfjorden and Bear Island Trough-Mouth Fans. c) Composite regional seismic strike-line covering Isfjorden, Bellsund, Storfjorden and Bear Island Trough-Mouth Fans. Internal reflection pattern in b) and c) is indicated with changes between stratified (parallel lines) and chaotic with mass movement structures (half circle pattern). Regional reflectors based on chronology from ODP Site 986 are indicated. Modified from Faleide et al. (1996), Jansen et al. (1996) and Solheim et al. (1998).

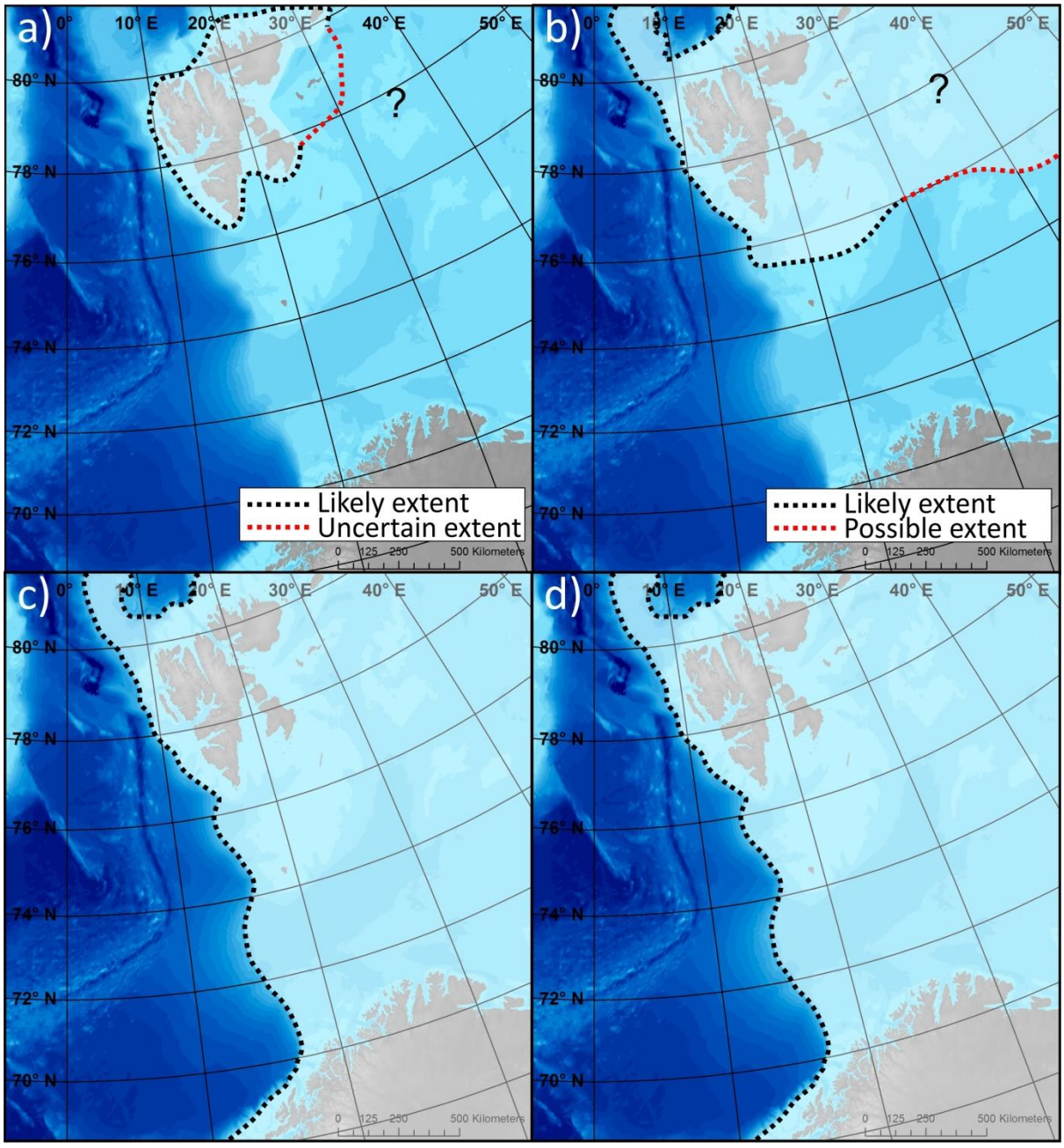

Fig. 12. Maximum extents of the Barents Sea Ice Sheet. a) 2.58 – 1.6 Ma. Limited advance and retreat of glaciers on Svalbard. The eastward extent of ice is uncertain (Knies et al., 2009). b) 1.6 – 1.3 Ma. Glaciers sourced from Svalbard expand sufficiently to reach the shelf edge. Ice masses are present in the Northern Barents Sea but southward expansion was limited (Solheim et al., 1998). c) 1.3 – 0.13 Ma. Glaciers on Svalbard continued to expand sufficiently to reach to shelf edge. Further south, the Barents Sea Ice Sheet expanded sufficiently to repeatedly reach the shelf edge along the southwestern margin of the Barents Sea (Andreassen et al., 2004; 2007). d) 0.13 – 0 Ma. Maximum ice extent of the Weichselian Ice Sheet (Svendsen et al., 2004).

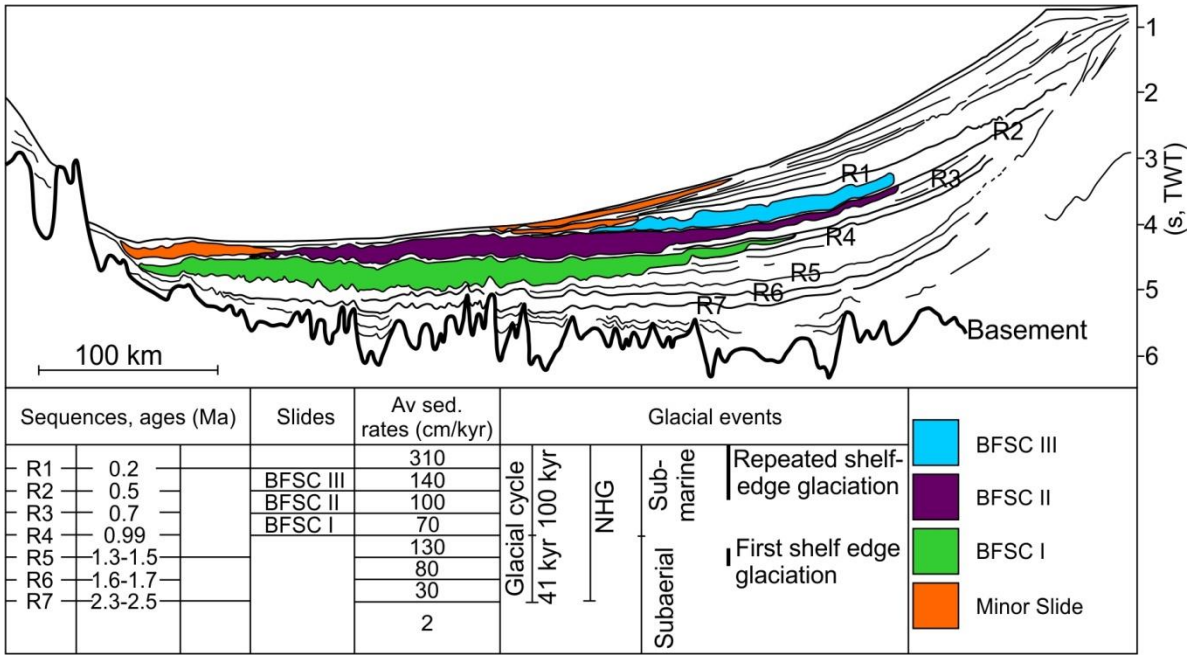

3799

3800 Fig. 13. Seismic transect across the Lofoten Basin from the Bear Island Trough-Mouth Fan to the
3801 Vøring Plateau (see Fig. 11a). Sequence boundaries (R1 – R7) and submarine landslide deposits (BFSC
3802 I – III) are indicated. GDF = Glacigenic Debris-Flow deposits. Summary of chronology, average
3803 depositional rates and main glacial events are shown in the lower panel. Modified from Hjelstuen et
3804 al. (2007).

3805

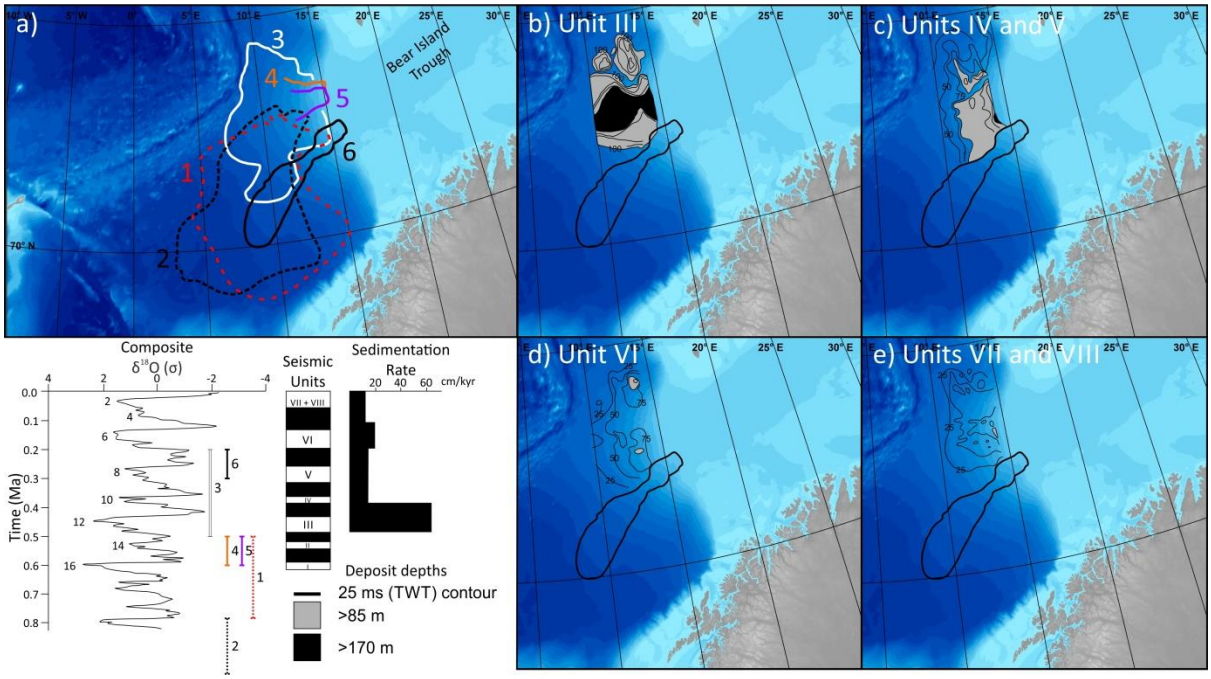

Fig. 14. a) Location of large submarine landslides sourced from the Bear Island Trough-Mouth Fan. 1) BFSC II; 2) BFSC I; 3) BFSC III; 4) Slide B; 5) Slide A; 6) Bjørnøya Slide. b) – e) Isopach maps of units deposited on the Bear Island Trough-Mouth Fan. Each isopach map is correlated to a given time period which can be compared to a composite $\delta^{18}O$ curve and the relative timings of the large submarine landslides outlined in a). b) = Unit III; c) = Unit IV and V; d = Unit VI; e) = Units VII and VIII. Contour interval 25 ms (TWT). For depth conversion an internal velocity of 1700 m/s was used. Modified from Laberg and Vorren (1996) and Hjelstuen et al. (2007).

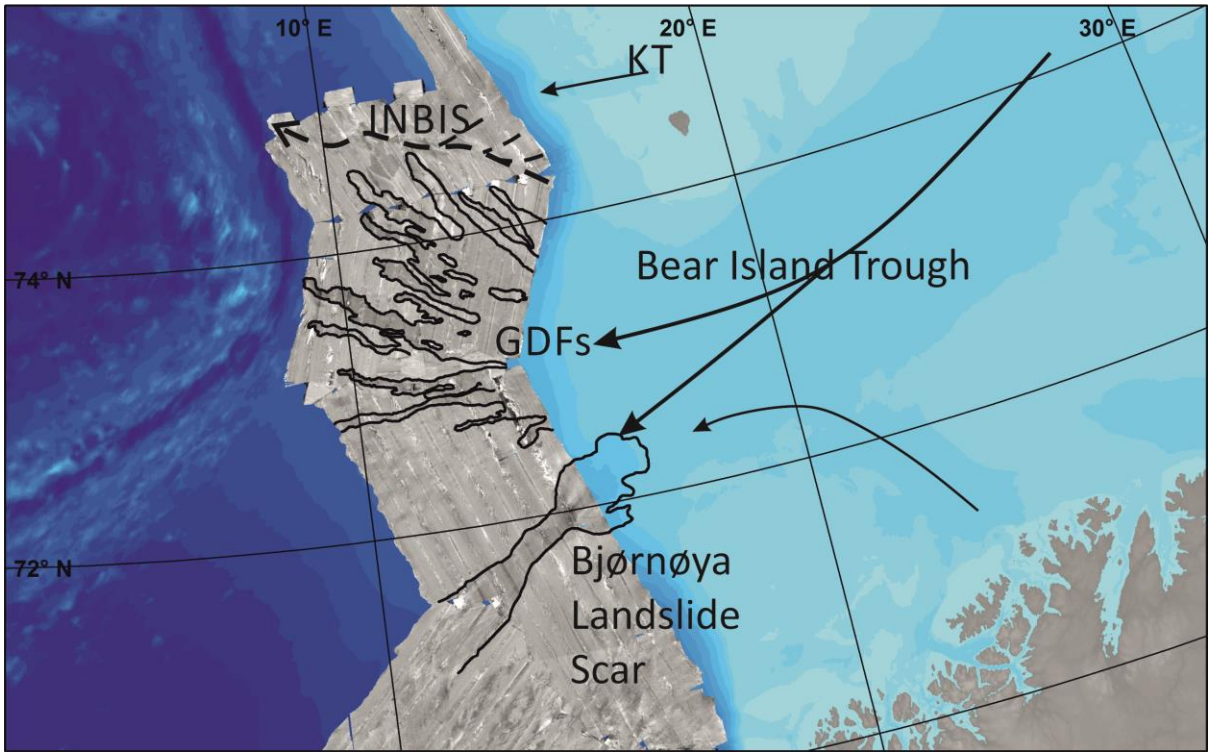

Fig. 15. GLORIA long range side-scan sonar imagery superimposed on the Bear Island Trough-Mouth Fan. Glacigenic Debris-Flows (GDF), the INBIS Submarine Channel system and the Bjørnøya submarine landslide are identified using the GLORIA imagery. Palaeo-ice flow directions are indicated by arrows. KT = Kveithola. Glacigenic debris-flows visible in the GLORIA imagery are thought to relate to the Late Weichselian (MIS 2) glacial advance.

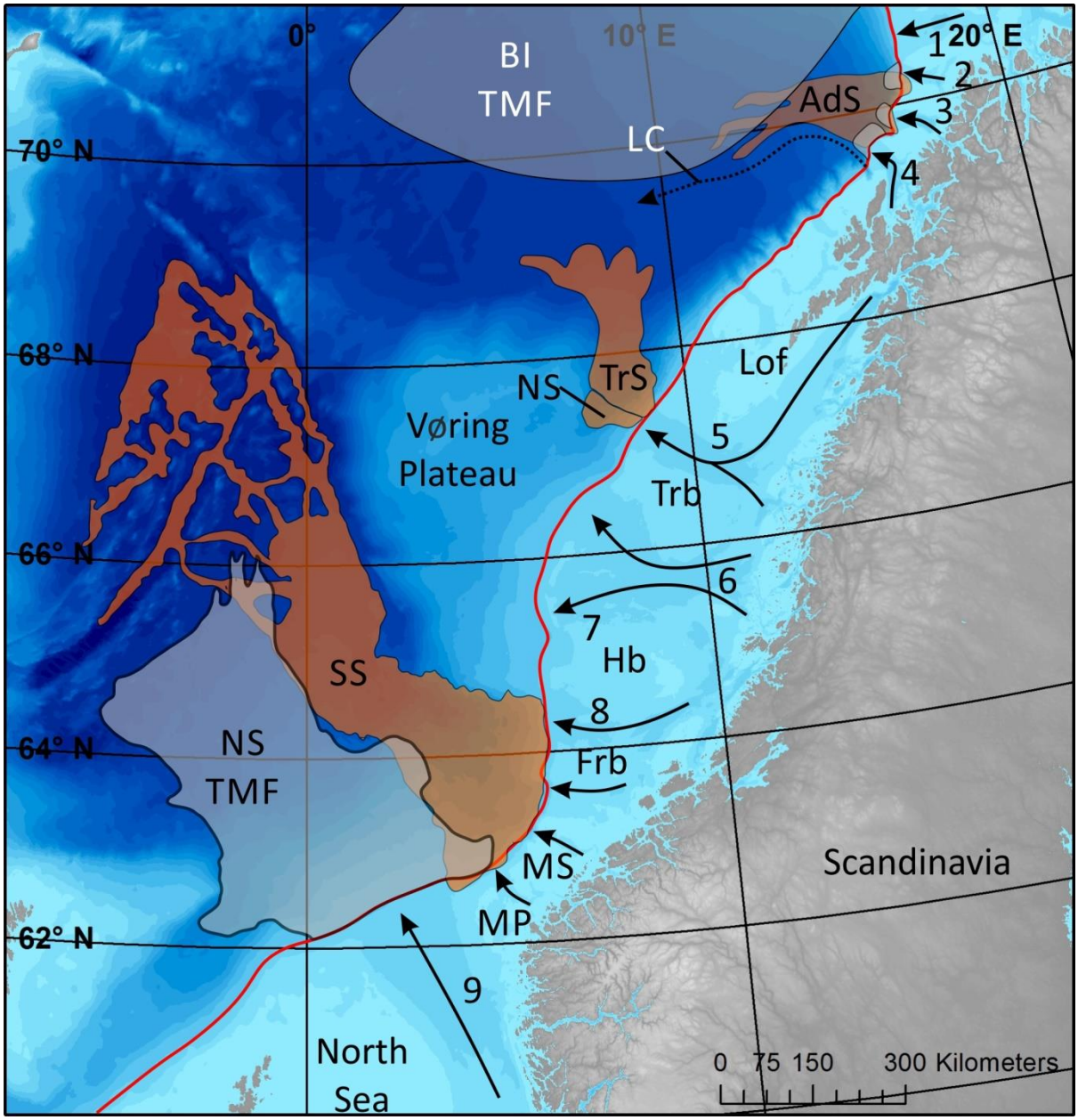

Fig. 16. Maximum westward Quaternary extent of the Scandinavian Ice Sheet (red line) with notable cross-shelf troughs, trough-mouth fans and landslides displayed on IBCAO bathymetric data (Jakobsson et al., 2012). Arrows indicate cross-shelf toughs thought to have previously contained ice streams. Grey shaded areas represent trough-mouth fans. 1 = Håkjerringdjupet 2 = Rebbenesdjupet. 3 = Malangsdjupet. 4 = Andfjord. 5 = Trænadjupet. 6 = Sklinnadjupet. 7 = Suladjupet. 8 = Buadjupet. 9 = Norwegian Channel. Lof = Lofoten. Trb = Trænabanken. Hb = Haltenbanken. Frb = Frøyabanken. MS = Møre Shelf. MP = Måløy Plateau. BI TMF = Bear Island Trough-Mouth Fan. NS = North Sea Trough-Mouth Fan. AdS = Andøya Slide. TrS = Trænadjupet Slide. NS = Nyk Slide. SS = Storegga Slide. LC = Lofoten Channel.

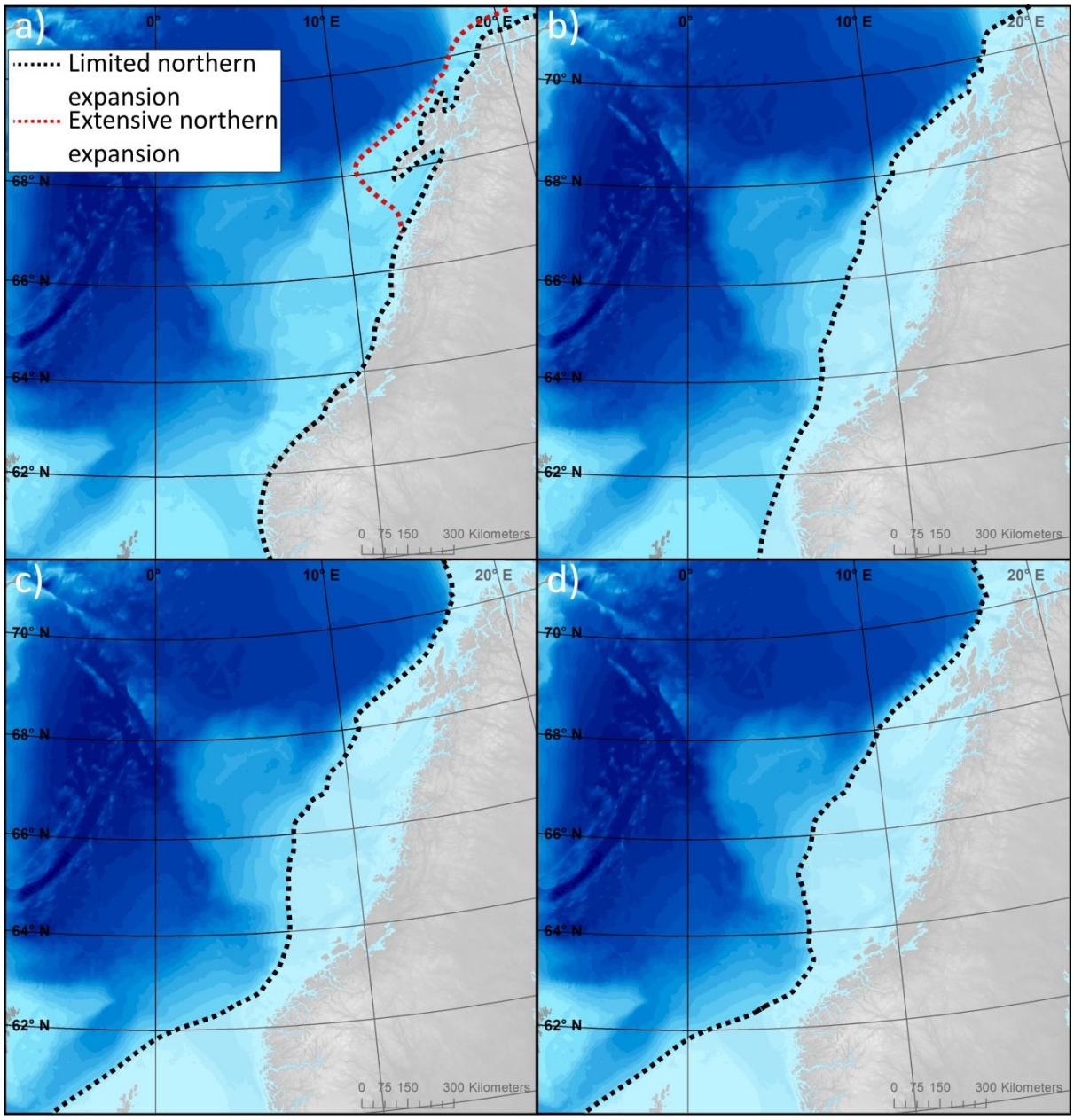

Fig. 17. Maximum extents of the Scandinavian Ice Sheet. a) 2.58 – 1.1 Ma. Two models of Scandinavian Ice Sheet extent during the Early Quaternary are envisaged. 1) Black-dashed line: An intermediate sized ice sheet rarely extending beyond the fjords of western Norway (Sejrup et al., 1996; Dowdeswell et al., 2013; Newton et al., 2016). 2) Red-dashed line: A limited southern extent but regular expansion to the shelf edge north of the Vøring Plateau (Rokoengen et al., 1995; Henriksen and Vorren, 1996). b) 1.1 – 0.7 Ma. Definitive first expansion of the ice sheet at 1.1 Ma followed by a retreat to dimensions more akin with outlined in a) (Helmke et al. 2005; Sejrup et al., 2005). c) 0.7 – 0.13 Ma. Extent of the Saalian Scandinavian Ice Sheet. Other glaciations have been reconstructed as delivering sediment to the mid-Norwegian Margin resulting in progressive westward movement of the shelf edge (Montelli et al., 2017a). d) 0.13 – 0 Ma. Maximum extent of the Weichelian ice sheet (Hughes et al., 2016).

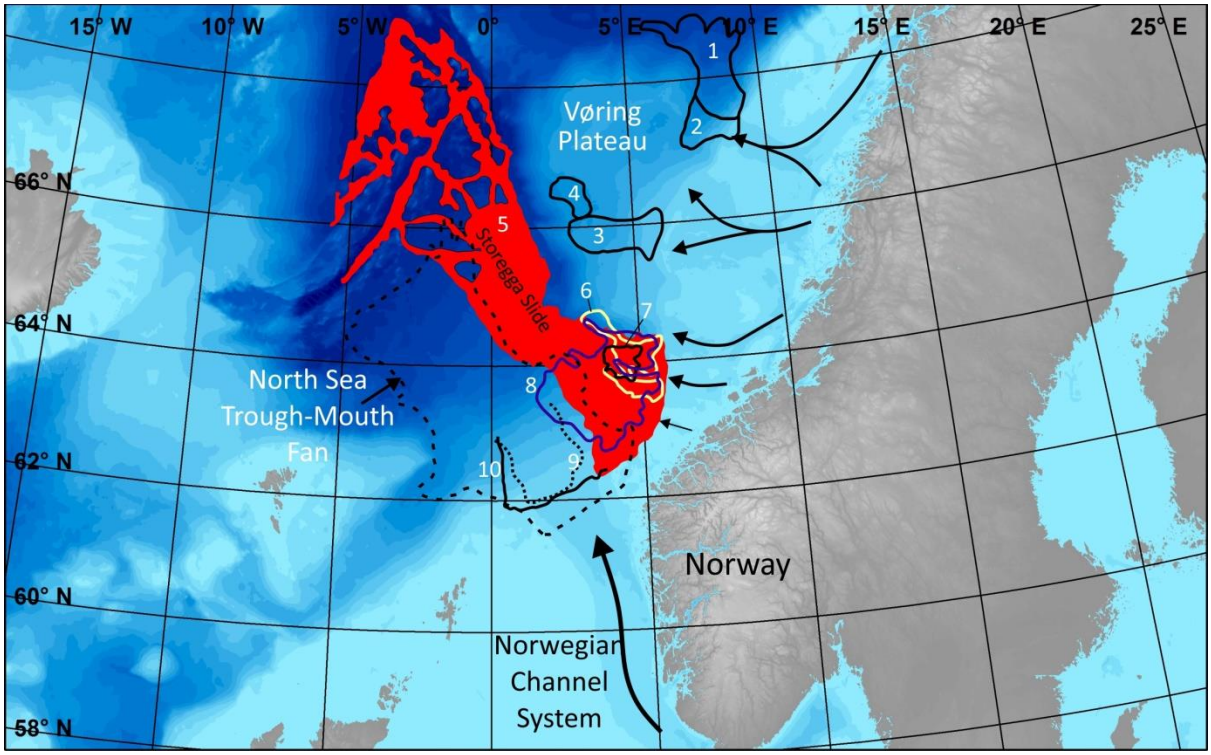

Fig. 18. Large submarine landslides identified on the Norwegian Continental Margin. 1) Trænadjupet Slide; 2) Nyk Slide; 3) Vigrid Slide; 4) Sklinnadjupet Slide; 5) Storegga Slide; 6) R Slide; 7) W Slide; 8) S Slide; 9) Tampen Slide; 10) Møre Slide. Palaeo-ice stream flow directions are indicated by arrows.

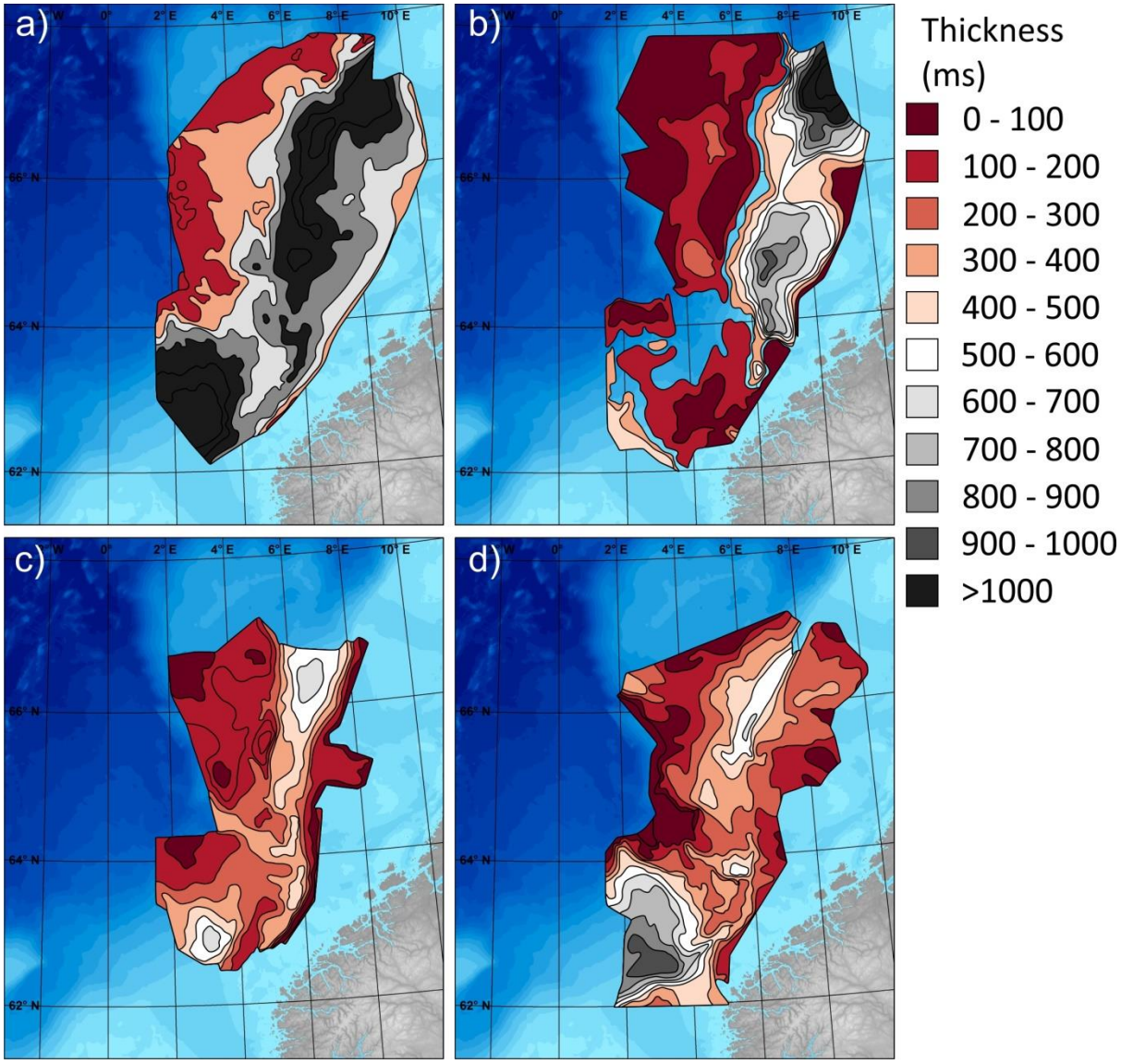

Fig. 19. Isopach maps of: a) Naust Formation; b) Naust W (deposited from 2.7 – 1.7 Ma); c) Naust U (deposited from 1.7 – 1.1 Ma) and Naust S (deposited from (1.1 – 0.4 Ma); d) Naust R (deposited from 0.4 – 0.2 Ma) and O (deposited from 0.2 – 0 Ma). Note that the thickness of the deposited material increases to the south with younger ages. Modified from Rise et al. (2005).

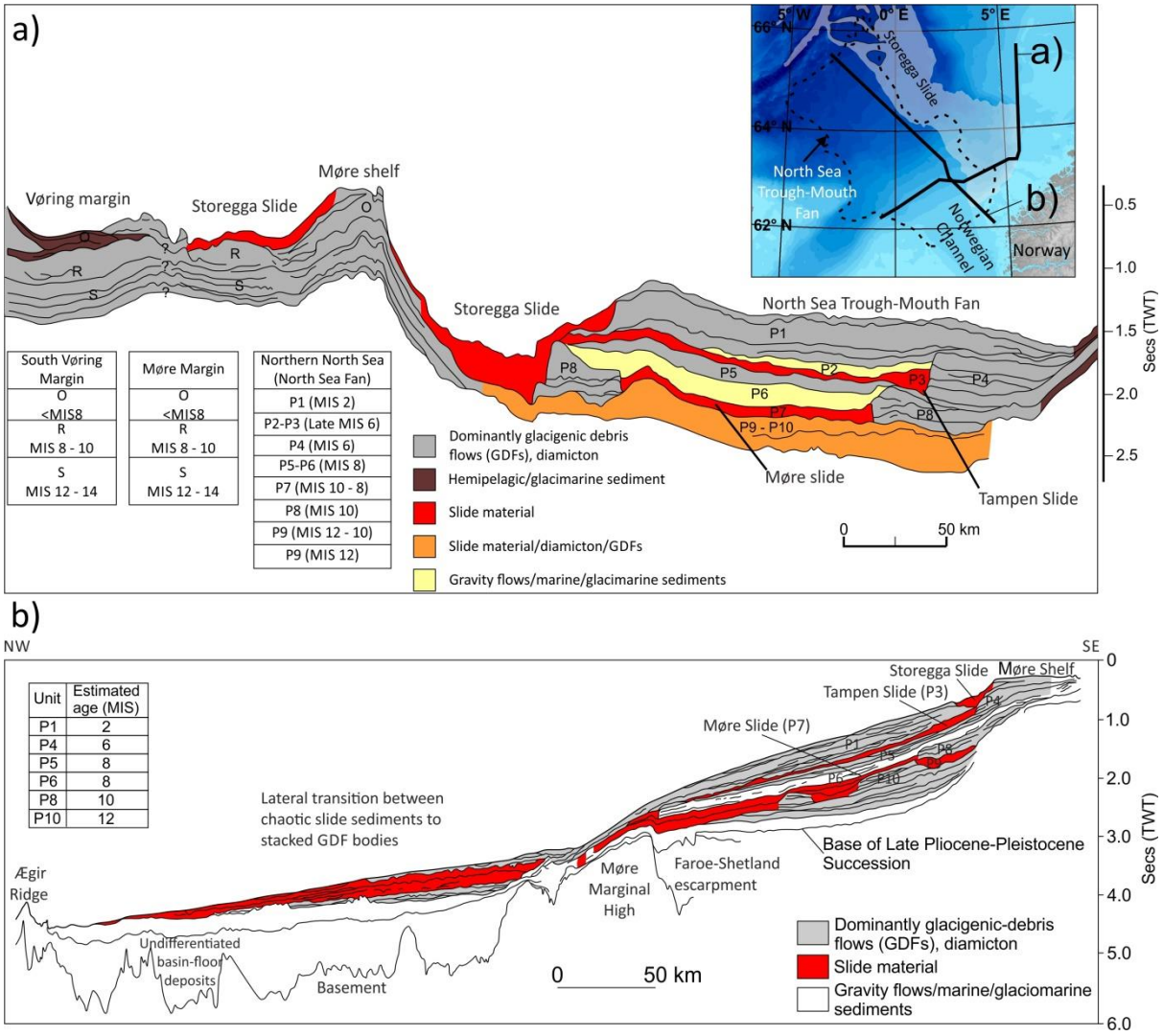

Fig. 20. Seismic profiles across the Storegga Slide and North Sea Trough-Mouth Fan; location of seismic lines shown in inset. a) Seismic profile crossing the southern Vøring Margin, the Storegga Slide and the North Sea Trough-Mouth Fan showing the distribution and correlation of identified Pleistocene units along the Norwegian Sea Margin. b) Seismic profile down the North Sea Trough-Mouth Fan. P1 – P10: identified Late Plio-Pleistocene seismic sequences on the proximal North Sea Trough-Mouth Fan. GDFs = glacigenic debris-flows. Adapted from Sejrup et al. 2004.

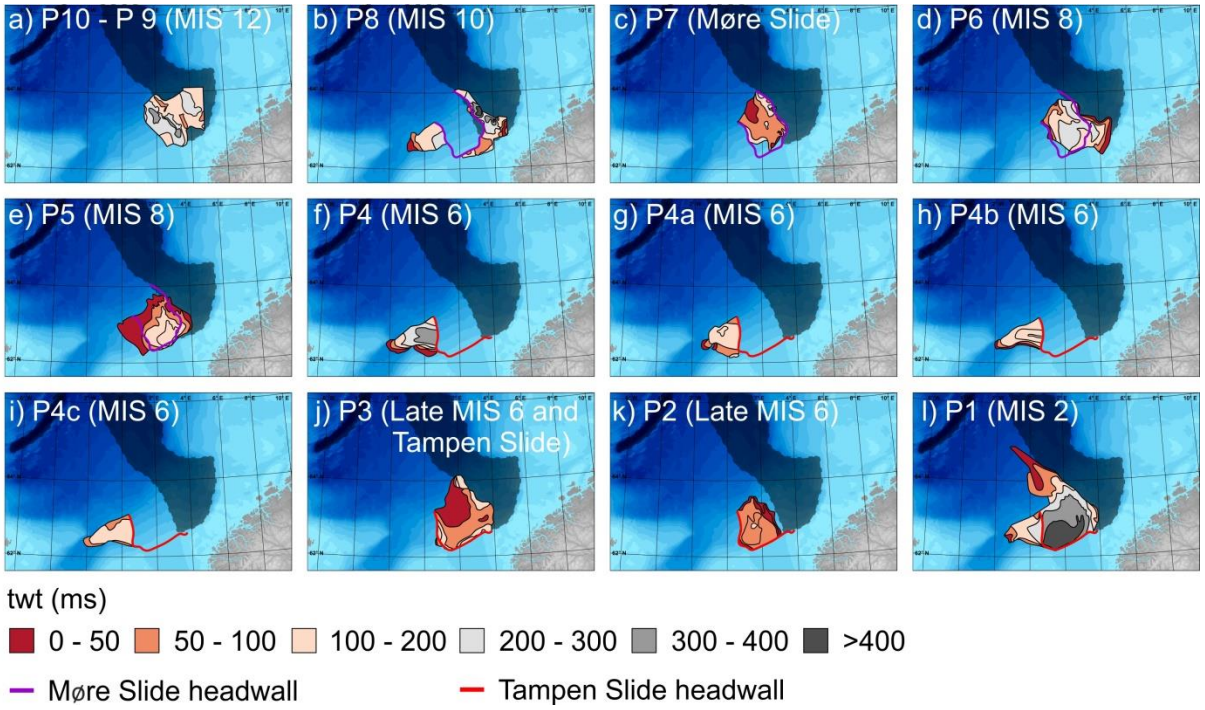

3859

3860 Fig. 21. Isopach maps for unis P1 – P10 identified in Fig. 20. a) P10 – P9; b) P8; c) P7; d) P6; e) P5; f)
3861 P4; g) P4a; h) P4b; i) P4c; j) P3 and Tampen Slide; k) P2; l) P1.

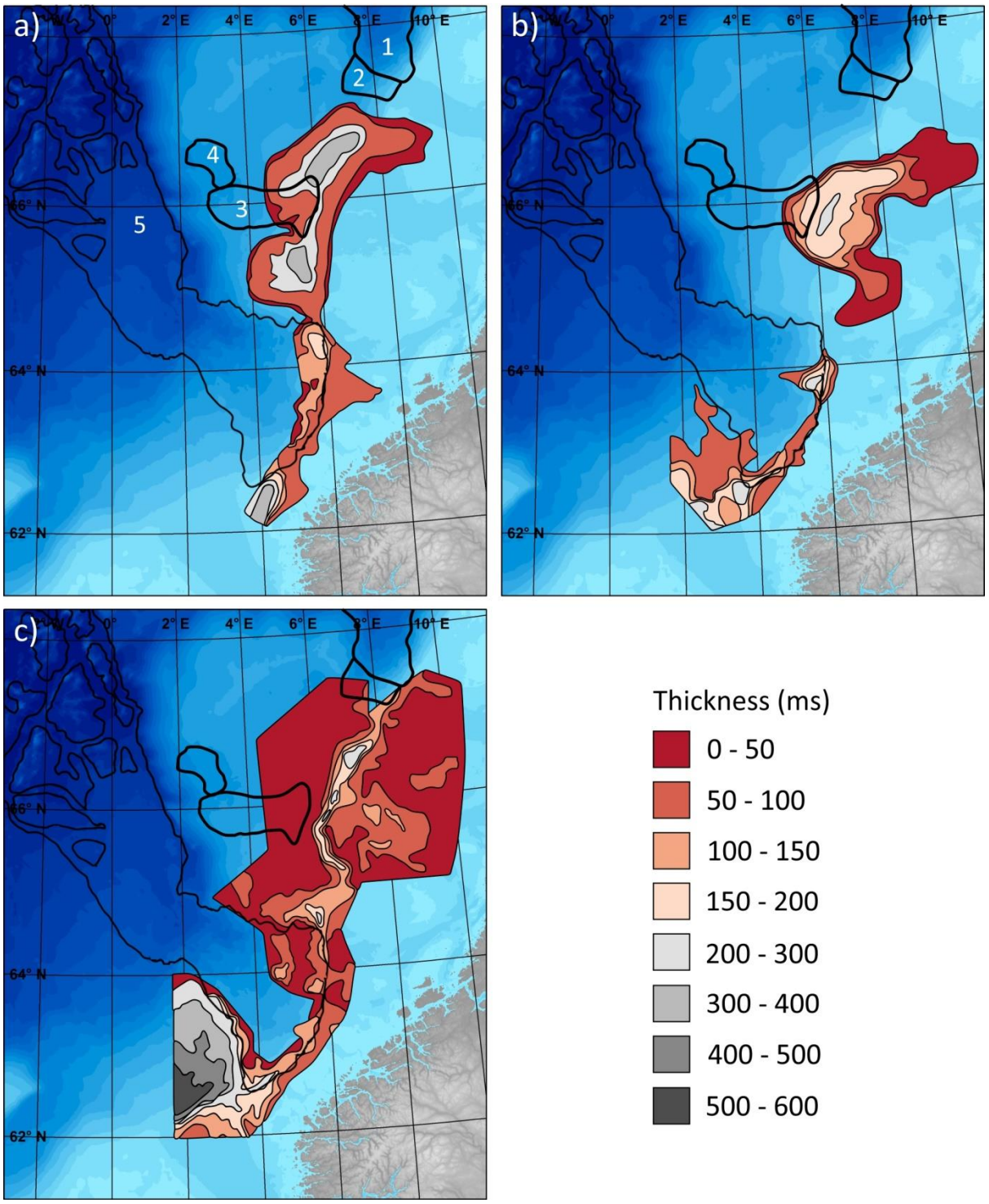

Fig. 22. Isopach maps of glacigenic deposits along the mid- and southern Norwegian margins from a) the Elsterian (MIS 10 – 8), b) the Saalian (MIS 6) and c) the Weichselian (MIS 5d – 2). 1 – 7: Submarine landslide outlines. 1) Trænadjupet Slide; 2) Nyk Slide; 3) Vigrid Slide; 4) Sklinnadjupet Slide; 5) Storegga Slide.

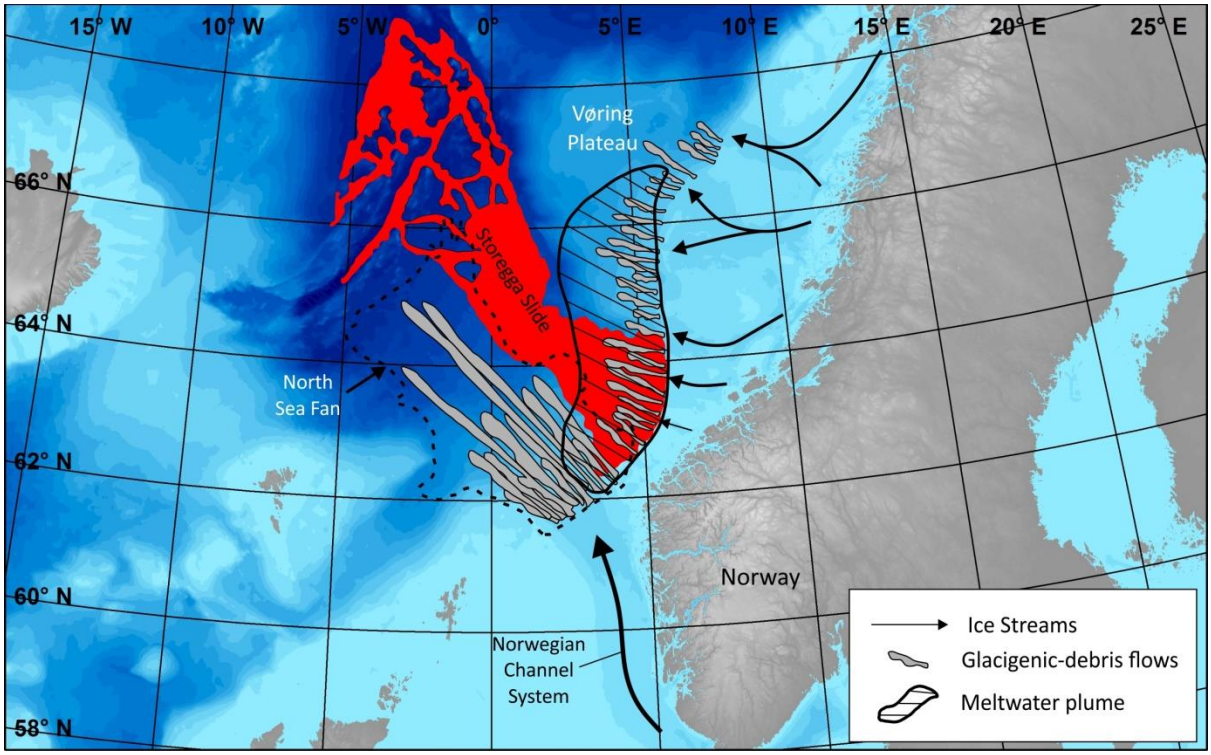

Fig. 23. Schematic model showing Late Weichselian ice sheet related deposition across the North Sea and South Vøring Margins. The continental slope is characterised by glacigenic debris-flow emplacement. The disintegration of the Norwegian Channel Ice Stream resulted in the release of a meltwater plume which transported fine-grained material to the Storegga Slide region and the south Voring margin. Palaeo-ice stream flow directions are indicated by arrows. Adapted from Lekens et al. (2005) and Hjelstuen et al. (2005).

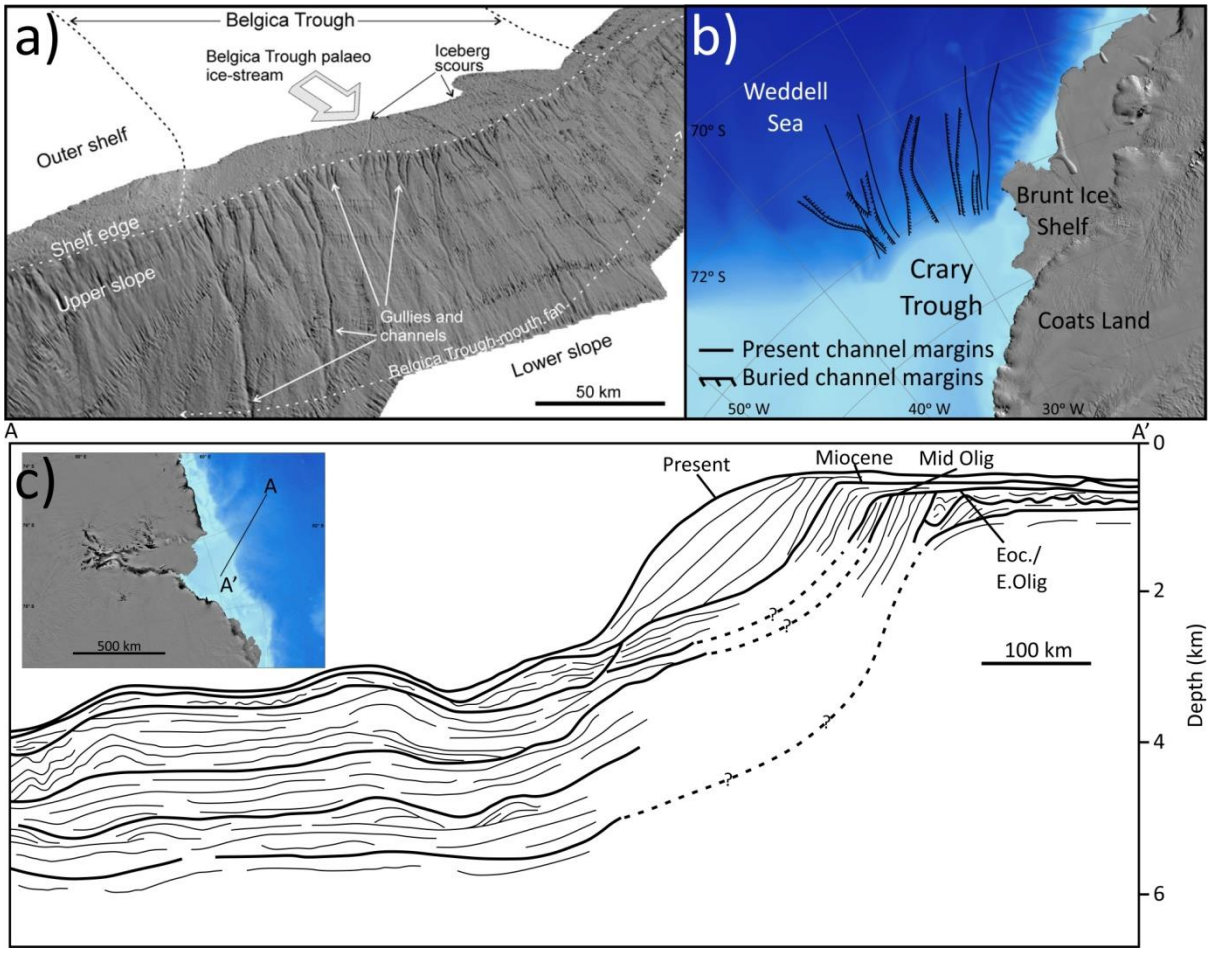

3874

3875 Fig. 24. Examples of trough-mouth fans from Antarctica with varying morphologies. a) Oblique view
3876 (from the North) of sun-illuminated swath bathymetry of the Belgica Trough-Mouth Fan and the
3877 major sedimentary features. b) Present and buried channels identified on the Crary Trough-Mouth
3878 Fan. c) Bathymetric map and seismic interpretation of the Prydz Bay Trough-Mouth Fan. Modified
3879 from Dowdeswell et al. (2008), Kuvaas and Kristoffersen (1991) and Passchier et al., (2003).

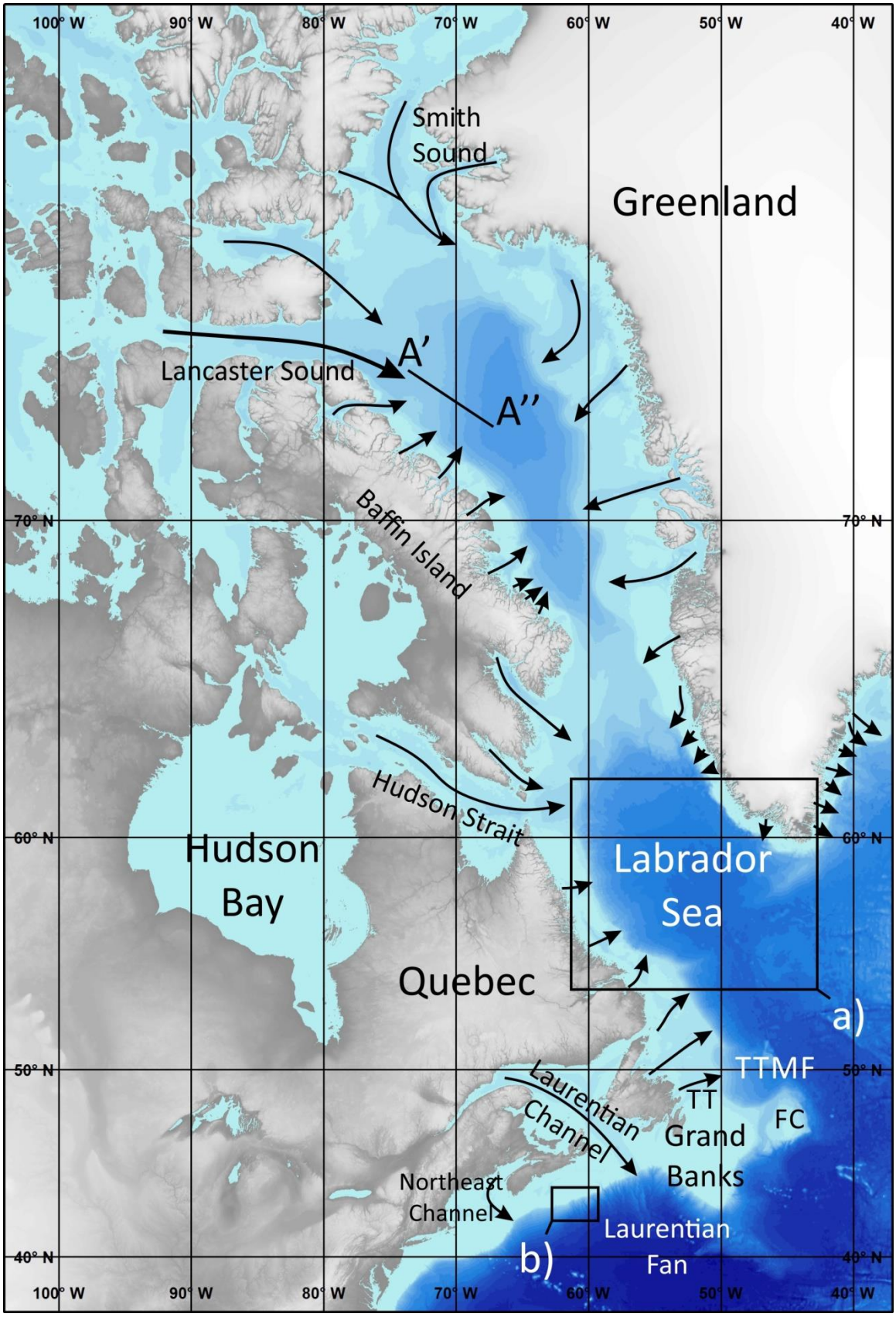

Fig. 25. Location map of the East Canadian Margin. Cross-shelf troughs inferred to have contained ice streams during the last glacial are illustrated with arrows.

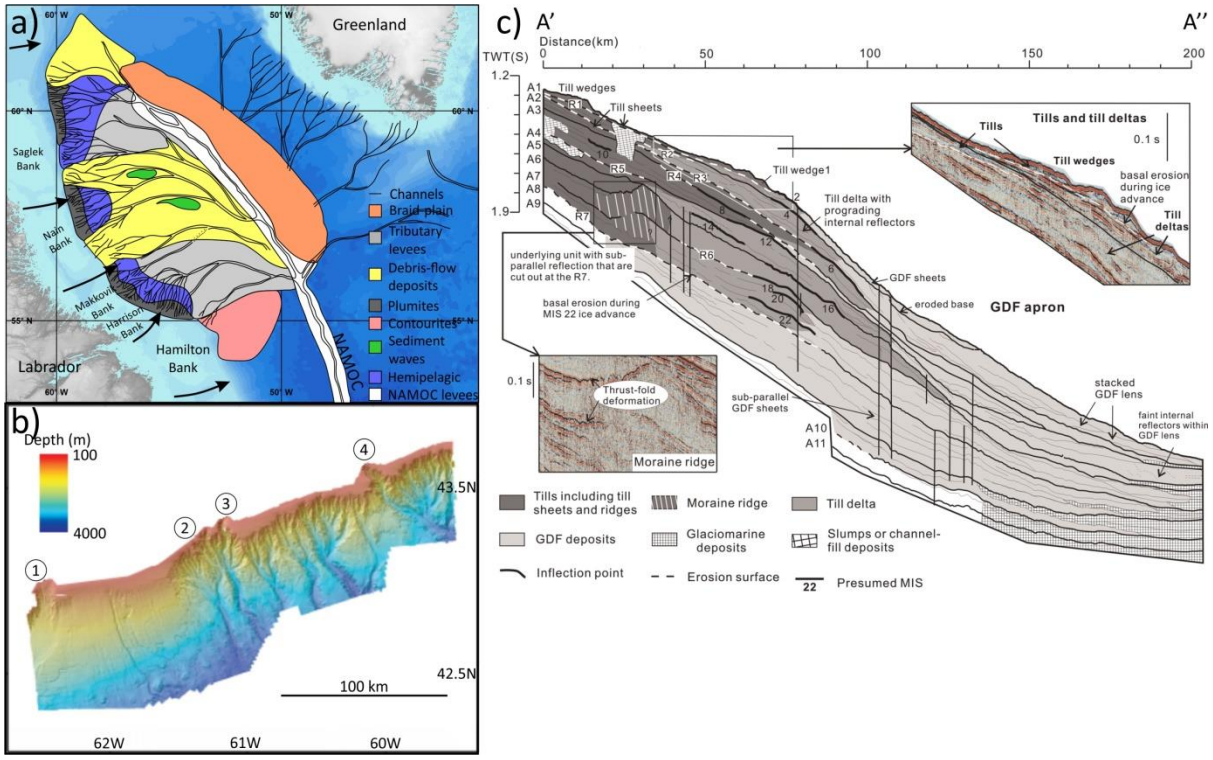

Fig. 26. Examples of ice sheet influenced sedimentary features on the East Canadian Margin. a) Map of the Labrador Sea showing the upslope branching of tributary channels on the slope and the distribution of major sediment facies (redrawn from Hesse et al. (1997) and Ó Cofaigh et al. (2003)). Inferred ice stream positions are marked with arrows. NAMOC = North Atlantic Mid-Ocean Channel. b) Multibeam bathymetry sonar data showing the morphology of the central Scotian Slope. 1 = Mohican Channel; 2) Verrill Canyon; 3) Dawson Canyon; 4) Logan Channel. Modified from Mosher et al. (2004). c) Seismic interpretation of the Lancaster Sound Trough-Mouth Fan from an airgun profile. Detail of stacked structure of till and till data are shown in the upper inset. A close-up of two moraine ridges is shown in the lower inset. Presumed MIS stages are labelled along their corresponding seismic reflector. Modified from Li et al. (2011).

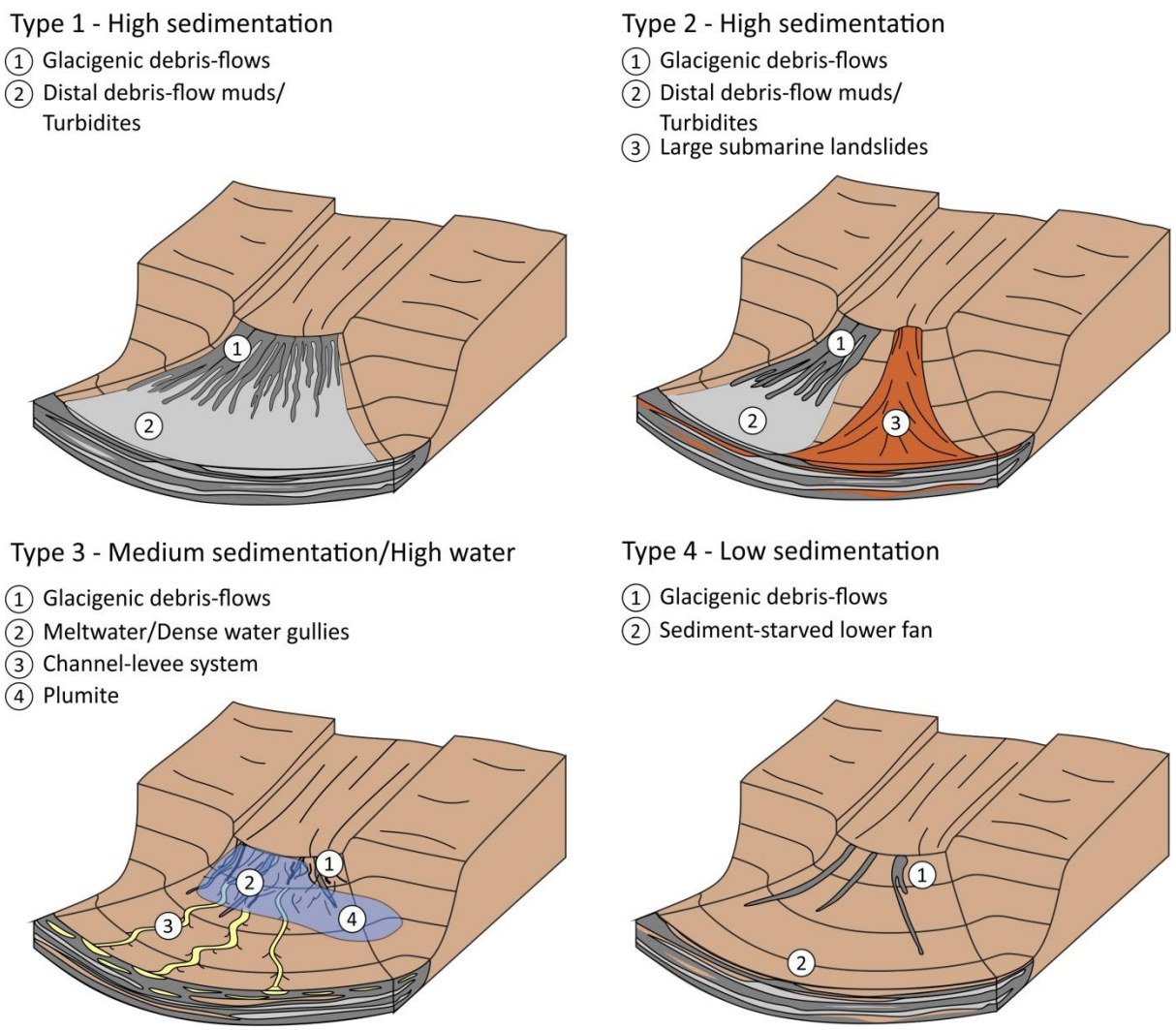

3894

3895 Fig. 27. Schematic model of trough-mouth fan classification from analysis of glaciated continental
3896 margins in this study.

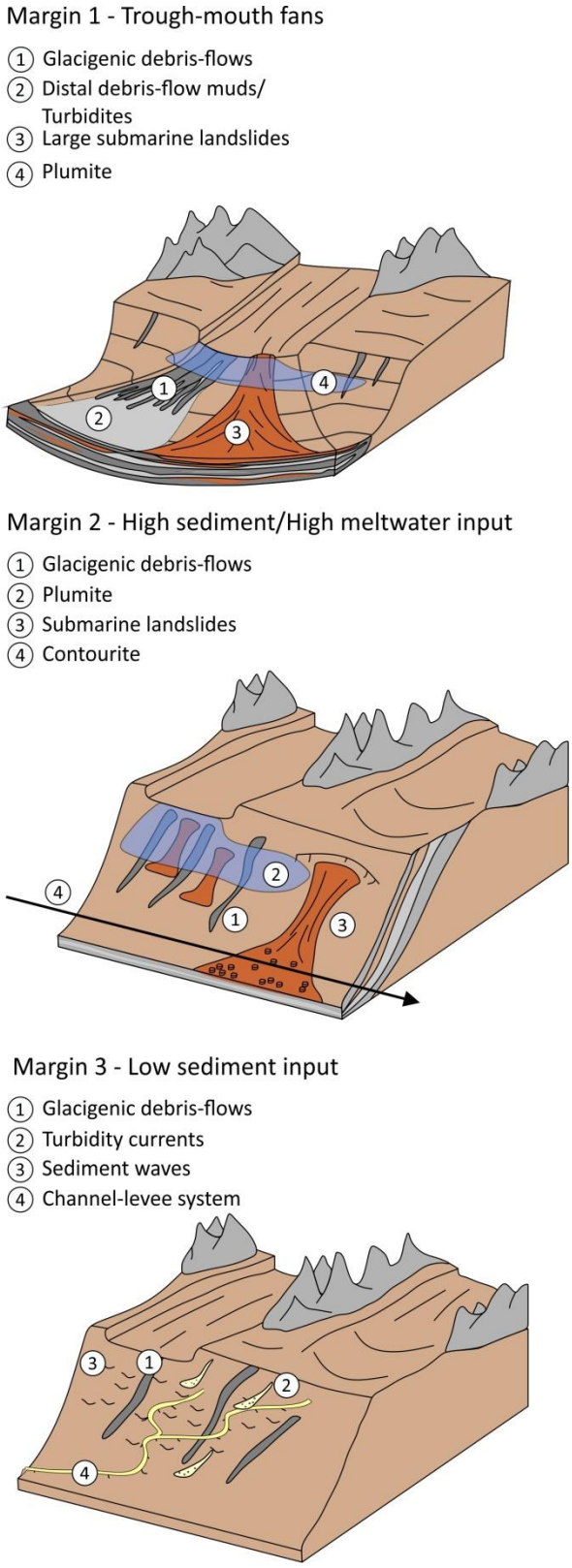

3897

3898 Fig. 28. Schematic model of glaciated margin classification from analysis of glaciated continental
3899 margins in this study.

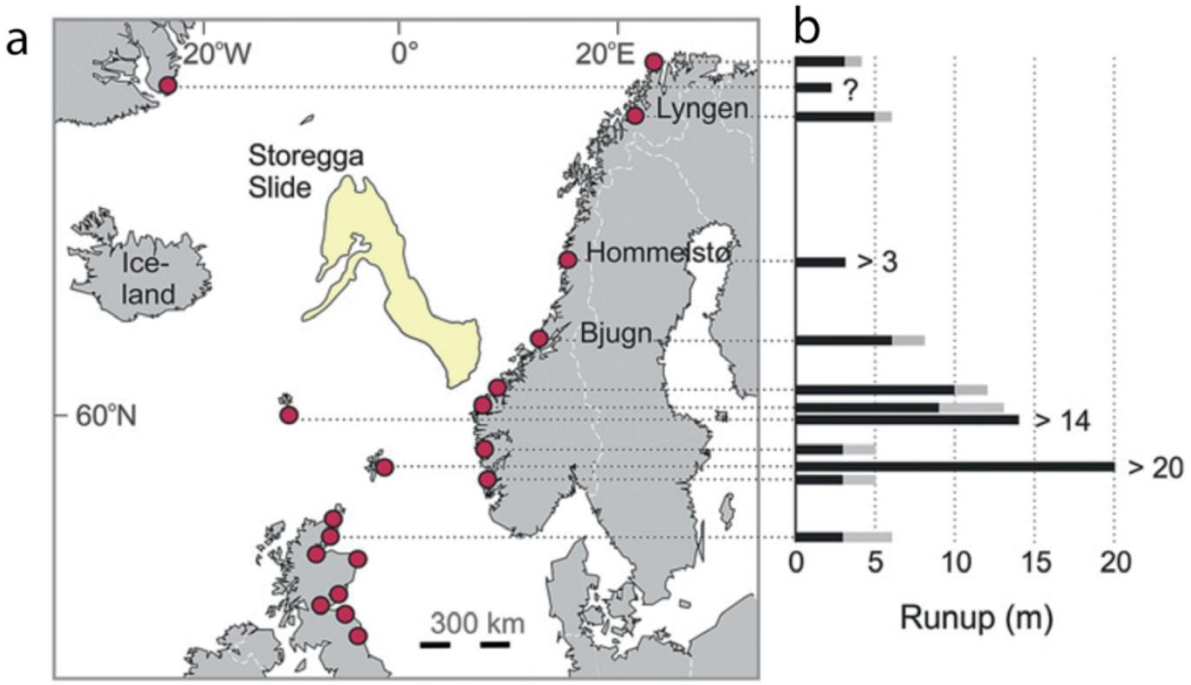

Fig. 29. Location of the Storegga Slide that comprises >3,000 km^3 of predominantly glacigenic material. Red dots indicate locations of tsunami deposits associated with the Storegga Slide. Tsunami runup heights above sea level are indicated in b). Black bars indicate minimum runup heights and grey bars maximum runup heights (Modified from Bondevik et al., 2005 and Talling et al., 2014).

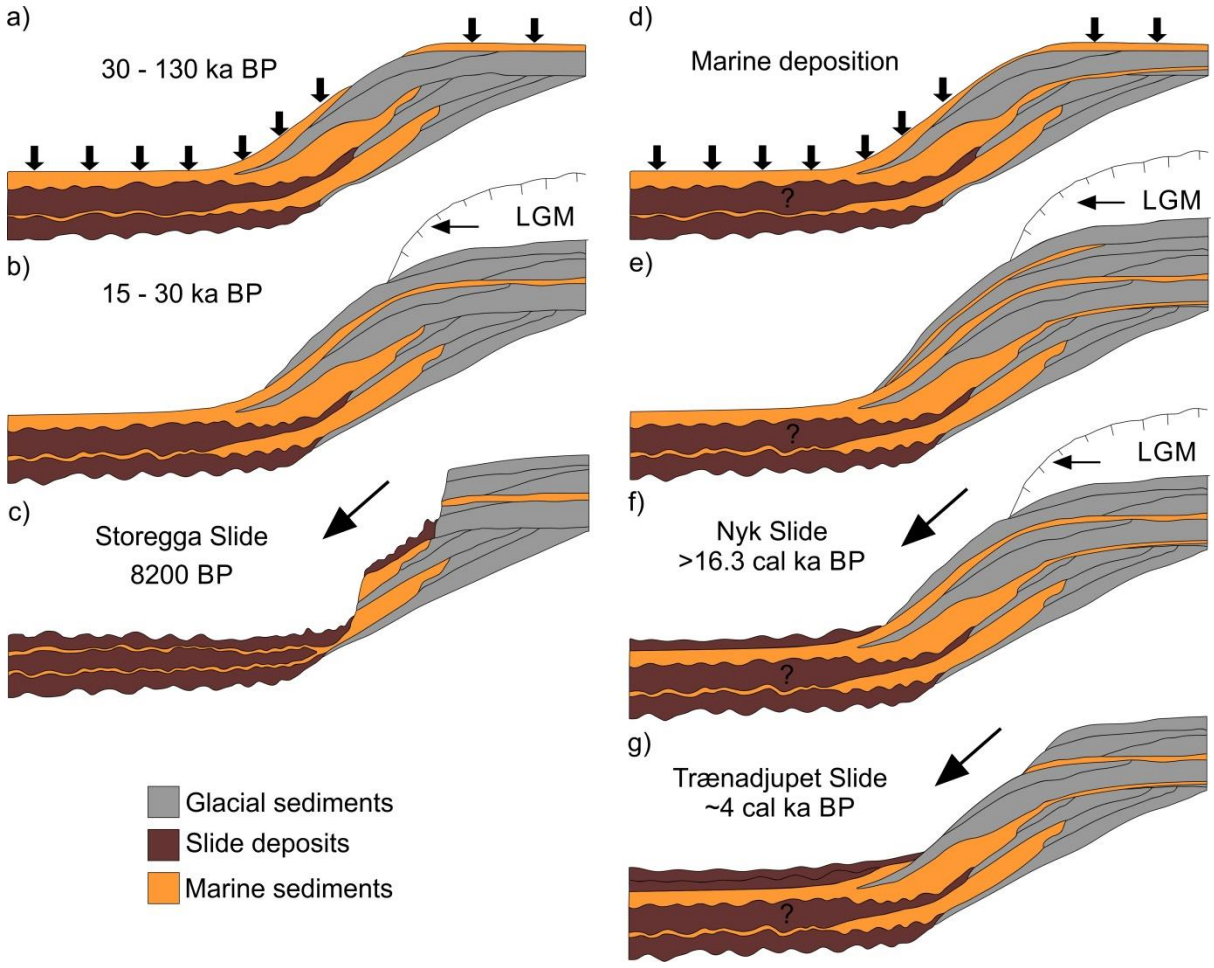

Fig. 30. Illustration of the proposed depositional and slide processes that occur in the Storegga Slide (a – c) and the Trænadjupet Slide (d – g) areas. a) Deposition of soft marine clays during the last interglacial. b) Ice at the shelf edge during the Last Glacial Maximum and the deposition of glacial sediments. c) The Storegga Slide. Two older slide scars are filled with marine clays below the Storegga Slide scar. Adapted from Bryn et al. (2005). d) Deposition of soft marine clays and contouritic sediments. e) Ice at the shelf edge and the deposition of glacial sediments. f) Nyk Slide occurs altering the properties of the sediment package on the continental slope. g) The Trænadjupet Slide.

Tables

Table 1. Summary of the important steps in glacial evolution of the East Greenland Margin and the resulting record of sedimentation.

Period (Ma)	Ice sheet history	Sedimentation record
2.58 - 1.3	Most extensive ice sheet surrounding the Nordic Seas Largest advances from 2.5 - 2.4 Ma and about 2.1 Ma Little evidence of widespread collapses during deglaciation	Dominates IRD signal in the Nordic Seas 2.5 - 2.4 Ma advance marked by regional reflector and glacigenic debris-flows on Scoresby Sund Trough-Mouth Fan Subsequent advances on Scoresby Sund sector characterised by silty clays with variable IRD content, turbidites and glacigenic debris-flows limited to the upper slope 5 km progradation of shelf edge
1.3 - 0.7	Hypothesis 1: relatively stable ice sheet remaining on/near to the continental shelf Hypothesis 2: repeated advances to and retreat from the shelf edge	Glacigenic debris-flows on the central and southern sides of Scoresby Sund Trough-Mouth Fan Enhanced glacimarine sedimentation through meltwater plumes and turbidity currents Submarine channel formation on east Greenland Margin 38 km progradation of the shelf edge 130 m vertical aggradation of the continental shelf
0.7 - 0.13	Expanded and more stable ice sheet Extent of advances relatively uncertain Saalian Greenland Ice Sheet represents the maximum ice extent reached during the Quaternary	Limited evidence of submarine mass movement occurrence beyond the continental shelf before the Saalian Saalian aged glacigenic debris-flows on the Scoresby Sund Trough-Mouth Fan and the east Greenland margin Submarina channel system was inactive during the Saalian <5 km progradation of the shelf edge >260 m vertical aggradation of the shelf
0.13 - 0	Advances during MIS 5d and 5b at least to the inner shelf Advance during MIS 4 (close to MIS 2 limit in Scorseby Sund sector) followed by a limited retreat MIS 3 limited advance and retreat cycles Maximum extent of Late Weichselian ice sheet between 21 - 16 ka BP Expansion to the shelf edge in Northeast and Scoresby Sund sectors; central east Greenland extent is uncertain	***Scoresby Sund:*** Glacigenic debris-flow emplacement ***East Greenland margin:*** Glacigenic debris-flow emplacement on the upper and mid- continental slope Below 2000 m sedimentological facies dominated by turbidites Laminated silt and mud layers on the upper continental slope and shelf Sedimentation rates peaked during deglaciation between 51 and 79 cm/kyr Channel system cross-cuts glacigenic debris-flow deposits ***Northeast sector:*** Glacigenic debris-flow emplacement on the upper and mid- continental slope Turbidite deposition on the lower continental slope Submarine landslide headscarps visible in bathymetry

Table 2. Areas, volumes and ages of known large submarine landslides in the Nordic Sea (adapted from Hjelstuen et al. (2007). The volumes reported for PLS-1, PLS-2 and PLS-3 represent minimum volumes (Llopart et al., 2015).

Slide	Area ($x 10^3$ km^2)	Volume ($x 10^3$ km^3)	Age (Ma)	Reference
LS-1.1	1338.4	46.84	0.061 - 0.2	Llopart et al. (2015)
LS-2.1	95.2	2.48	>0.0225	Llopart et al. (2015)
LS-2.2	35.5	1.06	>0.0225	Llopart et al. (2015)
LS-11.1	119.9	2.06		Llopart et al. (2015)
LS-11.2	52.9	1.11		Llopart et al. (2015)
LS-Kv	459.1	3.67		Llopart et al. (2015)
PLS-1	647.7	45.34	0.8 - 1.0	Llopart et al. (2015)
PLS-2	709	127.62	0.105 - 0.135	Llopart et al. (2015)
PLS-3	240	18	0.2 - 0.5	Llopart et al. (2015)
BFSC I	115	25.5	1.0 - 0.78	Hjelstuen et al. (2007)
BFSC II	120	24.5	0.78 - 0.5	Hjelstuen et al. (2007)
BFSC III	66	11.6	0.5 - 0.2	Hjelstuen et al. (2007)
Slide B			0.6 - 0.5	Laberg et al. (1996)
Slide A	12	5.1	0.6 - 0.5	Laberg et al. (1996)
Bjørnøya	12.5	1.1	0.2 - 0.3	Laberg et al. (1996) Lindberg et al. (2004)
Andøya	9.7		Holocene	Laberg et al. (2000)
Trænadjupet	4 - 5	0.4 - 0.9	0.004 - 0.0035	Laberg et al. (2002b)
Nyk	4 - 6	0.4 - 0.72	0.021- 0.016	Lindberg et al. (2004)
Vigrid	2.5		>0.2	Solheim et al. (2005)
Sklinnadjupet	7.7		0.3	Solheim et al. (2005)
Storegga	95	<3.2	0.0072	Haflidason et al. (2005)
R	6.8		0.3	Solheim et al. (2005)
W	63.7	24.6	2.7 - 1.7	Hjelstuen and Andreassen (2015)
S	72.3	15	0.5	Solheim et al. (2005)
Tampen			130	Nygård et al. (2005)
Møre		1.2	0.4 - 0.38	Nygård et al. (2005)
U	86.7	24.6	1.7 - 1.1	Evans et al. (2005) Hjelstuen and Andreassen (2015)

3927 Table 3. Summary of the important steps in glacial evolution of the Svalbard/Barents Sea margin and
3928 the resulting record of sedimentation.

Period (Ma)	Ice sheet history	Sedimentation record
2.58 - 1.6	Retreat of initially extensive ice sheet on Svalbard and the northern Barents Sea Subsequent limited advance and retreat of glaciers on Svalbard and in the Northern Barents Sea	Meltwater related increase in sedimentation on Svalbard continental slope Submarine mass movement deposits (not glacigenic debris-flows) on the Svalbard continental slope Meltwater sediment driven incision of channels into the continental slope Gradual aggradation and progradation of sedimentary wedges
1.6 - 1.3	Expansion to the shelf edge of glaciers sourced from Svalbard Limited southward expansion of Barents Sea Ice Sheet	***Svalbard margin:*** Period of major glacigenic debris-flow emplacement Acceleration of sedimentwary wedge progradation Deposits are thicker and seismically distinct from previous period
		Barents Sea margin: Glaciofluvial and glacimarine deposition
1.3 - 0.7	Advance to and retreat from the shelf edge of Svalbard glaciers First expansion to the shelf edge in the Bear Island Trough of the Barents Sea Ice Sheet	***Svalbard margin:*** Emplacement of glacigenic debris-flows on the continental shelf
		Barents Sea margin: 1.3 - 1.0 Ma ? emplacement of glacigenic debris-flow deposits; rate of sedimentation increased to 130 cm/kyr 1.0 - 0.78 Ma ? emplacement of glacigenic debris-flow deposits; rate of sedimentation drop to 70 cm/kyr; submarine landslide on Bear Island Trough-Mouth Fan (>25,000 km3) Change in sedimentation rate hypothesised to be a consequence of Barents Sea shelf submergence
0.7 - 0.13	Ice sheet expands to the shelf edge during MIS 16, 12, 8 and 6 MIS 14 advance believed to have reached shelf edge of Bear Island Trough but not around Svalbard	***Svalbard margin:*** Glacigenic debris-flow emplacement (decline in deposit thick with the adoption of 100 kyr climate cyclicity) Shift from net-erosion to net-accumulation of sediment on the continental shelf
		Storfjorden Trough-Mouth Fan: Each advance is associated with a package of glacigenic debris-flows
		Bear Island Trough-Mouth Fan: Upper and mid- slopes of the trough-mouth fan characterised by glacigenic debris-flow emplacement; lower slope is characterised by fine-grained turbidites and hemipelagic sediments MIS 12 advance ? 17,650 km3 of sediment deposited at a rate of 63 cm/ka across the fan MIS 10 and 8 advance ? 7266 km3 of sediment deposited at a rate of 14 cm/ka across the fan MIS 6 advance ? 4061 km3 of sediment deposited at a rate of 19 cm/ka Five large submarine landslides on the trough-mouth fan with volumes between 1.1 and 24.5 km3
0.13 - 0	MIS 5d (115 - 105 ka) advance to shelf edge limited to Svalbard MIS 5b (90 - 80 ka BP) advance on Svalbard is less extensive MIS 5b (90 - 80 ka BP) advance in Barents Sea limited to eastern Barents and Kara Seas MIS 4 (70 - 50 ka BP) advance to the shelf edge MIS 2 (32 - 20 cal ka BP) advance to the shelf edge Proposed advance to shelf edge of the Bear Island Trough during MIS 3 (40 - 35 cal ka BP)	***Svalbard margin:*** Deposition of turbidites on the continental slope during MIS 4 (rate of turbidite emplacement was especially high following the initial retreat of the ice) 32 - 24 cal ka BP ice expansion characterised by laminated and massive mud deposition and turbidite emplacement 24 - 20 cal ka BP advance characterised by glacigenic debris-flow emplacement 20 cal ka BP ? initial retreat of the ice sheet characterised by increased IRD and hemipelagic sedimentation 15.7 - 14.65 cal ka BP ? second phase of retreat characterised by increased IRD <14.65 cal ka BP ? accelerated retreat characterised by deposition of thick, fine-grained laminated mud deposits; rates of sedimentation 1 to 2 orders of magnitude greater than when ice was at the shelf edge
		Storfjorden Trough-Mouth Fan: Northern/Central Fan ? >50 m of glacigenic debris-flow deposits emplaced during MIS 2; gully incision into upper slope Southern Fan ? Multiple submarine landslide scars; interlaminated plumite deposits upto 50 m thick interbedded with discontinuous diamicts
		Bear Island Trough-Mouth Fan: Glacigenic debris-flow emplacement characterises each advance to the shelf edge Gullies are incised into the upper slope at the margins of the trough-mouth fan <1 m of glacimarine sediments recovered from the upper fan 2400 km3 of sediment accumulated at 13 cm/ka

3929
3930

3931 Table 4. Summary of the important steps in glacial evolution of the Norwegian Continental Margin
3932 and the resulting record of sedimentation.

Period (Ma)	Ice sheet history	Sedimentation record
2.58 - 1.1	***Reconstruction 1:*** Intermediate size ice sheet rarely expanding beyond fjords of western Norway ***Reconstruction 2:*** Glaciers regularly advanced to the shelf edge north of the Vøring Plateau Glaciers remained limited in size south of the Vøring Plateau	Slide W occurred between 2.7 and 1.7 Ma and is estimated to have rembolised 24,600 km3 ***Reconstruction 1:*** No evidence of ice sheet related submarine mass movements Limited delivery of IRD ***Reconstruction 2:*** Progradation of sediment wedges in the north where ice reached the shelf edge Little/no influence of ice along southern Norwegian margin
1.1 - 0.7	First expansion to the shelf edge after 1.1 Ma Subsequent reversion to limited ice sheet extent seen previously	1.1 Ma lacial advance marked by near continuous till layer Glacimarine sedimentation associated with 1.1 Ma advance beyond the shelf edge Retreat of ice sheet is marked by a return of marin sedimentation along the entire margin
0.7 - 0.13	Advances to the shelf edge during MIS 14, 12, 10 and 6 Uncertainty over whether MIS 8 advance reached the shelf edge or just the mid-continental shelf	***MIS 14:*** Till present on the outer shelf as far south as the Møre Shelf Glacigenic debris-flow emplacement on continental shelf beyond where till is present on the shelf Little/no sedimentary evidence of ice sheet advance south of the Møre Shelf
		MIS 12: Advance is marked by regional till layer Outer Møre Shelf and continental slope is characterised by marine/glacimarine deposition North Sea Trough-Mouth Fan underwent a major construction phase; 3000 km3 of sediment was deposited, mainly in the form of glacigenic debris-flow deposits Møre submarine landslide (400 - 380 ka BP) reworked 1200 km3 of sediment previously deposited on the North Sea Trough-Mouth Fan
		MIS 10 - 8: Mid-Nowegian margin ? MIS 10 and 8 cannot be clearly distinguished; sequence characterised by strong shelf erosion and glacigenic debris-flow emplacement on the continental slope South Norwegian margin? MIS 10 and 8 clearly distinguishable Two distinct glacigenic till units on the south Vøring and North Sea margin 2600 km3 of sediment emplaced as glacigenic debris-flow deposits on the North Sea Trough-Mouth Fan during MIS 10 3500 km3 of sediment emplaced on the North Sea Trough-Mouth Fan during MIS 8; 2100 km3 through glacimarine processes (ice not at the shelf edge), 1400 km3 by glacigenic debris-flows (ice at the shelf edge) Sklinnadjupet (300 ka BP) and R (300 ka BP) landslides occurred during MIS 8
		MIS 6: Mid-Norwegian margin ? deposition of stacked till tongues up to 200 m thick as a result of ice not reaching the shelf edge South Vøring to Northern North Sea margin ? extensive till layer deposited to the shelf edge; glacigenic debris-flow emplacement beyond teh shelf edge North Sea Trough-Mouth Fan ? 2600 km3 of sediment deposited, predominantly by glacigenic debris-flows
0.13 - 0	MIS 5d (109 - 96 ka BP) advance to coast and into fjords MIS 5b (87 - 82 ka BP) advance to the outer coastline MIS 4 (71 - 57 ka BP) advance to the shelf edge Minor readvance beyond the west Norwegian coastline around (42 cal ka BP) ***Northern Norway:*** Ice advanced from 34 cal ka BP, reaching the shelf edge from 24 - 23 cal ka BP Retreat of up to 100 km between 22 and 20 cal ka BP Readvance to the shelf edge from 16 - 14 cal ka BP ***Mid-Norway:*** Main expansion to shelf edge began at 23.5 cal ka BP	***North Norwegian Continental Shelf (MIS 3 - 1):*** Earliest dated glacigenic debris-flows emplaced around 34 cal ka BP Plumite deposition around 25,590 14C yr BP Additional glacigenic debris-flow sequences dated to 15.6 ka BP, 19.5 ka BP and 21.7 - 21.1 ka BP; laminated plumites interbed glacigenic debris flow deposits Large numbers of submarine landslides during the Holocene including the Andøya Slide
		Mid-Norwegian Continental Shelf (MIS 5 - 1): MIS 5 and 4 marine and glacimarine deposition on continental slope reflect withdrawn ice sheet position Two till layers associated with the MIS 2 advance from 22 - 16.5 c14 ka BP; glacigenic debris-flows associated with these advances are found on the continental slope Little/no evidence of plumites Two large submarine landslides (Nyk and Trænadjupet) occurred between 21.8 - 19.3 cal ka BP and 5.3 - 3.2 cal ka BP
		South Vøring Margin (MIS 2 - 1): Three glacigenic units interpreted as glacigenic debris-flows on the continental slope from MIS 2 (21,000, 16,200, 15,700 14C yr BP) Plumite deposits interbed the debris-flow units; deposition rates from Plumites during deglaciation as high as 1750 cm/kyr

3933